EUROPEAN ORGANIZATION FOR NUCLEAR RESEARCH

CERN–PH–EP/2009–009
3 April 2009

CROSS-SECTIONS OF LARGE-ANGLE HADRON PRODUCTION IN PROTON– AND PION–NUCLEUS INTERACTIONS III: TANTALUM NUCLEI AND BEAM MOMENTA FROM ± 3 GeV/c TO ± 15 GeV/c

Abstract

We report on double-differential inclusive cross-sections of the production of secondary protons, charged pions, and deuterons, in the interactions with a 5% $\lambda_{\rm abs}$ thick stationary tantalum target, of proton and pion beams with momentum from ± 3 GeV/c to ± 15 GeV/c. Results are given for secondary particles with production angles $20^\circ < \theta < 125^\circ$. They are of particular relevance for the optimization of the design parameters of the proton driver of a neutrino factory.

The HARP–CDP group

A. Bolshakova[1], I. Boyko[1], G. Chelkov[1a], D. Dedovitch[1], A. Elagin[1b], M. Gostkin[1], A. Guskov[1], Z. Kroumchtein[1], Yu. Nefedov[1], K. Nikolaev[1], A. Zhemchugov[1], F. Dydak[2], J. Wotschack[2*], A. De Min[3c], V. Ammosov[4], V. Gapienko[4], V. Koreshev[4], A. Semak[4], Yu. Sviridov[4], E. Usenko[4d], V. Zaets[4]

[1] **Joint Institute for Nuclear Research, Dubna, Russia**
[2] **CERN, Geneva, Switzerland**
[3] **Politecnico di Milano and INFN, Sezione di Milano-Bicocca, Milan, Italy**
[4] **Institute of High Energy Physics, Protvino, Russia**

(To be submitted to Eur. Phys. J. C)

---

[a] Also at the Moscow Institute of Physics and Technology, Moscow, Russia
[b] Now at Texas A&M University, College Station, USA
[c] On leave of absence at Ecole Polytechnique Fédérale, Lausanne, Switzerland
[d] Now at Institute for Nuclear Research RAS, Moscow, Russia

[*] Corresponding author; e-mail: joerg.wotschack@cern.ch

1 INTRODUCTION

The HARP experiment arose from the realization that the inclusive differential cross-sections of hadron production in the interactions of few GeV/c protons with nuclei were known only within a factor of two to three, while more precise cross-sections are in demand for several reasons. Pion production data on a variety of nuclei are required for (i) the understanding of the underlying physics and the modelling of Monte Carlo generators of hadron–nucleus collisions, (ii) the optimization of the design parameters of the proton driver of a neutrino factory, (iii) flux predictions for conventional neutrino beams, and (iv) the calculation of the atmospheric neutrino flux.

Consequently, the HARP detector was designed to carry out a programme of systematic and precise (i.e., at the few per cent level) measurements of hadron production by protons and pions with momenta from 1.5 to 15 GeV/c.

The detector combined a forward spectrometer with a large-angle spectrometer. The latter comprised a cylindrical Time Projection Chamber (TPC) around the target and an array of Resistive Plate Chambers (RPCs) that surrounded the TPC. The purpose of the TPC was track reconstruction and particle identification by $\mathrm{d}E/\mathrm{d}x$. The purpose of the RPCs was to complement the particle identification by time of flight.

The HARP experiment was performed at the CERN Proton Synchrotron in 2001 and 2002 with a set of stationary targets ranging from hydrogen to lead.

Here, we report on the large-angle production (polar angle θ in the range $20^\circ < \theta < 125^\circ$) of secondary protons and charged pions, and of deuterons, in the interactions with a 5% λ_{abs} Ta target of protons and pions with beam momenta of ± 3.0, ± 5.0, ± 8.0, ± 12.0, and ± 15.0 GeV/c.

The atomic number of tantalum ($A = 181.0$) is close to the one of mercury ($A = 200.6$) which is the preferred candidate for the pion production target of the proton driver of a neutrino factory. Therefore, the data presented here are of particular interest for (ii) in the list above, the design of a future neutrino factory.

This is the third of a series of cross-section papers with results from the HARP experiment. In the first two papers [1,2] we have reported on results from the interactions with a Be target and described the detector characteristics and our analysis algorithms. Our work involves only the HARP large-angle spectrometer, the characteristics of which are described in detail in Refs. [3] and [4].

2 THE T9 PROTON AND PION BEAMS, AND THE TARGET

The protons and pions were delivered by the T9 beam line in the East Hall of CERN's Proton Synchrotron. This beam line supports beam momenta between 1.5 and 15 GeV/c, with a momentum bite $\Delta p/p \sim 1\%$.

Beam particle identification was provided for by two threshold Cherenkov counters, BCA and BCB, filled with nitrogen, and by time of flight over a flight path of 24.3 m. Table 1 lists the beam instrumentation that was used at different beam momenta for p/π^+ and for π/e separation.

The pion beam had a contamination by muons from pion decays. It also had a contamination by electrons from converted photons from π^0 decays. Only for the beam momenta of 3 and 5 GeV/c were electrons identified by a beam Cherenkov counter and rejected.

The fractions of muon and electron contaminations of the pion beam were experimentally determined [5, 6] and are listed in Table 2 for all beam momenta. For the determination of interaction cross-sections of pions, the muon and electron contaminations must be subtracted from the incoming flux of pion-like particles (except electrons at the beam momenta of 3 and 5 GeV/c).

Table 1: Beam instrumentation for p/π^+ and π/e separation

Beam momentum [GeV/c]	p/π^+ separation	π/e separation
± 3.0	TOF	BCB (1.05 bar)
± 5.0	TOF BCB (2.50 bar)	BCA (0.60 bar)
± 8.0	BCA (1.25 bar) BCB (1.50 bar)	
± 12.0 and ± 15.0	BCA (3.50 bar) BCB (3.50 bar)	

Table 2: Contaminations of the pion beams by muons and electrons

Beam momentum [GeV/c]	Muon fraction	Electron fraction
± 3.0	$(4.1 \pm 0.4)\%$	rejected
± 5.0	$(5.1 \pm 0.4)\%$	rejected
± 8.0	$(1.9 \pm 0.5)\%$	$(1.2 \pm 0.5)\%$
± 12	$(0.6 \pm 0.6)\%$	$(0.5 \pm 0.5)\%$
± 15	$(0.0 \pm 0.5)\%$	$(0.0 \pm 0.5)\%$

There is also a kaon contamination of a few per cent in the proton and pion beams. Because the kaon interaction cross-sections are close to the proton and pion interaction cross-sections, this contamination is ignored.

The beam trajectory was determined by a set of three multiwire proportional chambers (MWPCs), located upstream of the target, several metres apart. The transverse error of the impact point on the target was 0.5 mm from the resolution of the MWPCs, plus a contribution from multiple scattering of the beam particles in various materials in the beam line. Excluding the target itself, the latter contribution is 0.2 mm for a 8 GeV/c beam particle.

We select 'good' beam particles by requiring the unambiguous reconstruction of the particle trajectory with good χ^2. In addition we require that the particle type is unambiguously identified. We select 'good' accelerator spills by requiring a minimal beam intensity and a 'smooth' variation of beam intensity across the 400 ms long spill[1)].

The target was a disc made of high-purity (99.95%) tantalum, with a density of 16.67 g/cm^3, a radius of 15 mm, and a thickness of 5.6 ± 0.05 mm (5% $\lambda_{\rm abs}$).

The finite thickness of the target leads to a small attenuation of the number of incident beam particles. The attenuation factor is $f_{\rm att} = 0.975$.

The size of the beam spot at the position of the target was several millimetres in diameter, determined by the setting of the beam optics and by multiple scattering. The nominal beam

[1)] A smooth variation of beam intensity eases corrections for dynamic TPC track distortions.

position[2)] was at $x_{\rm beam} = y_{\rm beam} = 0$, however, excursions by several millimetres could occur[3)]. A loose fiducial cut $\sqrt{x^2_{\rm beam} + y^2_{\rm beam}} < 12$ mm ensured full beam acceptance. The muon and electron contaminations of the pion beam, stated above, refer to this acceptance cut.

3 THE HARP LARGE-ANGLE DETECTORS

Our calibration work on the HARP TPC and RPCs is described in detail in Refs. [3] and [4], and in references cited therein. In particular, we recall that static and dynamic TPC track distortions up to 10 mm have been corrected to better than 300 μm. Therefore, TPC track distortions do not affect the precision of our cross-section measurements.

The resolution $\sigma(1/p_{\rm T})$ is typically 0.2 (GeV/c)$^{-1}$ and worsens towards small relative particle velocity β and small polar angle θ.

The absolute momentum scale is determined to be correct to better than 2%, both for positively and negatively charged particles.

The polar angle θ is measured in the TPC with a resolution of $\sim$9 mrad, for a representative angle of $\theta = 60^\circ$. To this a multiple scattering error has to be added which is on the average $\sim$8 mrad for a proton with $p_{\rm T} = 500$ MeV/c in the TPC gas and $\theta = 60^\circ$, and $\sim$5 mrad for a pion with the same characteristics. The polar-angle scale is correct to better than 2 mrad.

The TPC measures $\mathrm{d}E/\mathrm{d}x$ with a resolution of 16% for a track length of 300 mm.

The intrinsic efficiency of the RPCs that surround the TPC is better than 98%.

The intrinsic time resolution of the RPCs is 127 ps and the system time-of-flight resolution (that includes the jitter of the arrival time of the beam particle at the target) is 175 ps.

To separate measured particles into species, we assign on the basis of $\mathrm{d}E/\mathrm{d}x$ and β to each particle a probability of being a proton, a pion (muon), or an electron, respectively. The probabilities add up to unity, so that the number of particles is conserved. These probabilities are used for weighting when entering tracks into plots or tables.

4 MONTE CARLO SIMULATION

We used the Geant4 tool kit [7] for the simulation of the HARP large-angle spectrometer.

We had expected that Geant4 would provide us with reasonably realistic spectra of secondary hadrons. We found this expectation met by Geant4's so-called QGSP_BIC physics list, but only for the secondaries from incoming beam protons with momentum less than 12 GeV/c. For the secondaries from beam protons at 12 and 15 GeV/c momentum, and from beam pions at all momenta, we found the standard physics lists of Geant4 unsuitable [8].

To overcome this problem, we built our own HARP_CDP physics list for the production of secondaries from incoming beam pions. It starts from Geant4's standard QBBC physics list, but the Quark–Gluon String Model is replaced by the FRITIOF string fragmentation model for kinetic energy $E > 6$ GeV; for $E < 6$ GeV, the Bertini Cascade is used for pions, and the Binary Cascade for protons; elastic and quasi-elastic scattering is disabled. Examples of the good performance of the HARP_CDP physics list are given in Ref. [8].

[2)] A right-handed Cartesian and/or spherical polar coordinate system is employed; the z axis coincides with the beam line, with $+z$ pointing downstream; the coordinate origin is at the upstream end of the tantalum target, 500 mm downstream of the TPC's pad plane; looking downstream, the $+x$ coordinate points to the left and the $+y$ coordinate points up; the polar angle θ is the angle with respect to the $+z$ axis.

[3)] The only relevant issue is that the trajectory of each individual beam particle is known, whether shifted or not, and therefore the amount of matter to be traversed by the secondary hadrons.

5 SYSTEMATIC ERRORS

The systematic precision of our inclusive cross-sections is at the few-per-cent level, from errors in the normalization, in the momentum measurement, in particle identification, and in the corrections applied to the data.

The systematic error of the absolute flux normalization is taken as 2%. This error arises from uncertainties in the target thickness, in the contribution of large-angle scattering of beam particles, in the attenuation of beam particles in the target, and in the subtraction of the muon and electron contaminations of the beam. Another contribution comes from the removal of events with an abnormally large number of TPC hits[4)].

The systematic error of the track finding efficiency is taken as 1% which reflects differences between results from different persons who conducted eyeball scans. We also take the statistical errors of the parameters of a fit to scan results as systematic error into account [1]. The systematic error of the correction for losses from the requirement of at least 10 TPC clusters per track is taken as 20% of the correction which itself is in the range of 5 to 30%. This estimate arose from differences between the four TPC sectors that were used in our analysis, and from the observed variations with time.

The systematic error of the p_{T} scale is taken as 2% as discussed in Ref. [3]. For the data from the -3 GeV/*c* and $+15$ GeV/*c* beams, this error was doubled to account for a larger than usual uncertainty of the correction for dynamic TPC track distortions.

The systematic errors of the proton, pion, and electron abundances are taken as 10%. We stress that errors on abundances only lead to cross-section errors in case of a strong overlap of the resolution functions of both identification variables, $\mathrm{d}E/\mathrm{d}x$ and β. The systematic error of the correction for migration, absorption of secondary protons and pions in materials, and for pion decay into muons, is taken as 20% of the correction, or 1% of the cross-section, whichever is larger. These estimates reflect our experience with remanent differences between data and Monte Carlo simulations after weighting Monte Carlo events with smooth functions with a view to reproducing the data simultaneously in several variables in the best possible way.

All systematic errors are propagated into the momentum spectra of secondaries and then added in quadrature.

6 CROSS-SECTION RESULTS

In Tables A.1–A.45, collated in the Appendix of this paper, we give the double-differential inclusive cross-sections $\mathrm{d}^2\sigma/\mathrm{d}p\mathrm{d}\Omega$ for various combinations of incoming beam particle and secondary particle, including statistical and systematic errors. In each bin, the average momentum at the vertex and the average polar angle are also given.

The data of Tables A.1–A.45 are available in ASCII format in Ref. [9].

Some bins in the tables are empty. Cross-sections are only given if the total error is not larger than the cross-section itself. Since our track reconstruction algorithm is optimized for tracks with p_{T} above $\sim$70 MeV/*c* in the TPC volume, we do not give cross-sections from tracks with p_{T} below this value. Because of the absorption of slow protons in the material between the vertex and the TPC gas, and with a view to keeping the correction for absorption losses below 30%, cross-sections from protons are limited to $p > 450$ MeV/*c* at the interaction vertex. Proton cross-sections are also not given if a 10% error on the proton energy loss in materials between the interaction vertex and the TPC volume leads to a momentum change larger than

[4)] In less than 0.5% of the number of good events, because of apparatus malfunction, the number of TPC hits was much larger than possible for a physics event. Such events were considered unphysical and eliminated.

2%. Since the proton energy loss is large in the tantalum target, particularly at polar angles close to 90 degrees, the latter condition imposes significant restrictions. Pion cross-sections are not given if pions are separated from protons by less than twice the time-of-flight resolution.

The absence of results from the $+12$ GeV/*c* and $+15$ GeV/*c* pion beams is caused by scarce statistics because the beam composition was dominated by protons.

We present in Figs. 1 to 7 what we consider salient features of our cross-sections.

Figure 1 shows the inclusive cross-sections of the production of protons, π^+'s, and π^-'s, from incoming protons between 3 GeV/*c* and 12 GeV/*c* momentum, as a function of their charge-signed p_{T}. The data refer to the polar-angle range $20^\circ < \theta < 30^\circ$. Figures 2 and 3 show the same for incoming π^+'s and π^-'s.

Figure 4 shows the inclusive cross-sections of the production of protons, π^+'s, and π^-'s, from incoming protons between 3 GeV/*c* and 15 GeV/*c* momentum, this time as a function of their charge-signed polar angle θ. The data refer to the p_{T} range $0.24 < p_{\mathrm{T}} < 0.30$ GeV/*c*. In this p_{T} range pions populate nearly all polar angles, whereas protons are absorbed at large polar angle and thus escape measurement. Figures 5 and 6 show the same for incoming π^+'s and π^-'s.

In Fig. 7, we present the inclusive cross-sections of the production of secondary π^+'s and π^-'s, integrated over the momentum range $0.2 < p < 1.0$ GeV/*c* and the polar-angle range $30^\circ < \theta < 90^\circ$ in the forward hemisphere, as a function of the beam momentum.

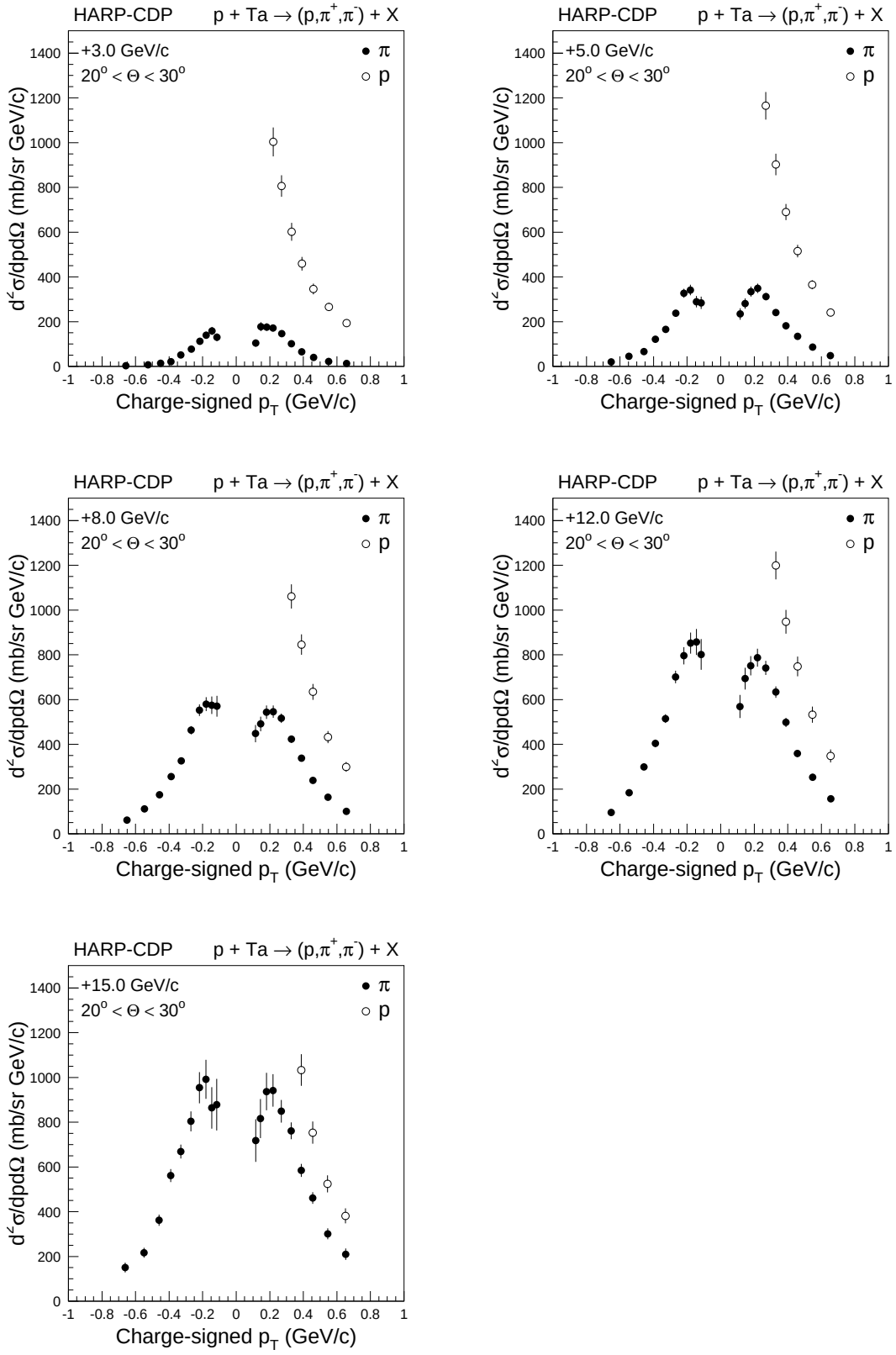

Fig. 1: Inclusive cross-sections of the production of secondary protons, π^+'s, and π^-'s, by protons on tantalum nuclei, in the polar-angle range $20^\circ < \theta < 30^\circ$, for different proton beam momenta, as a function of the charge-signed p_{T} of the secondaries; the shown errors are total errors.

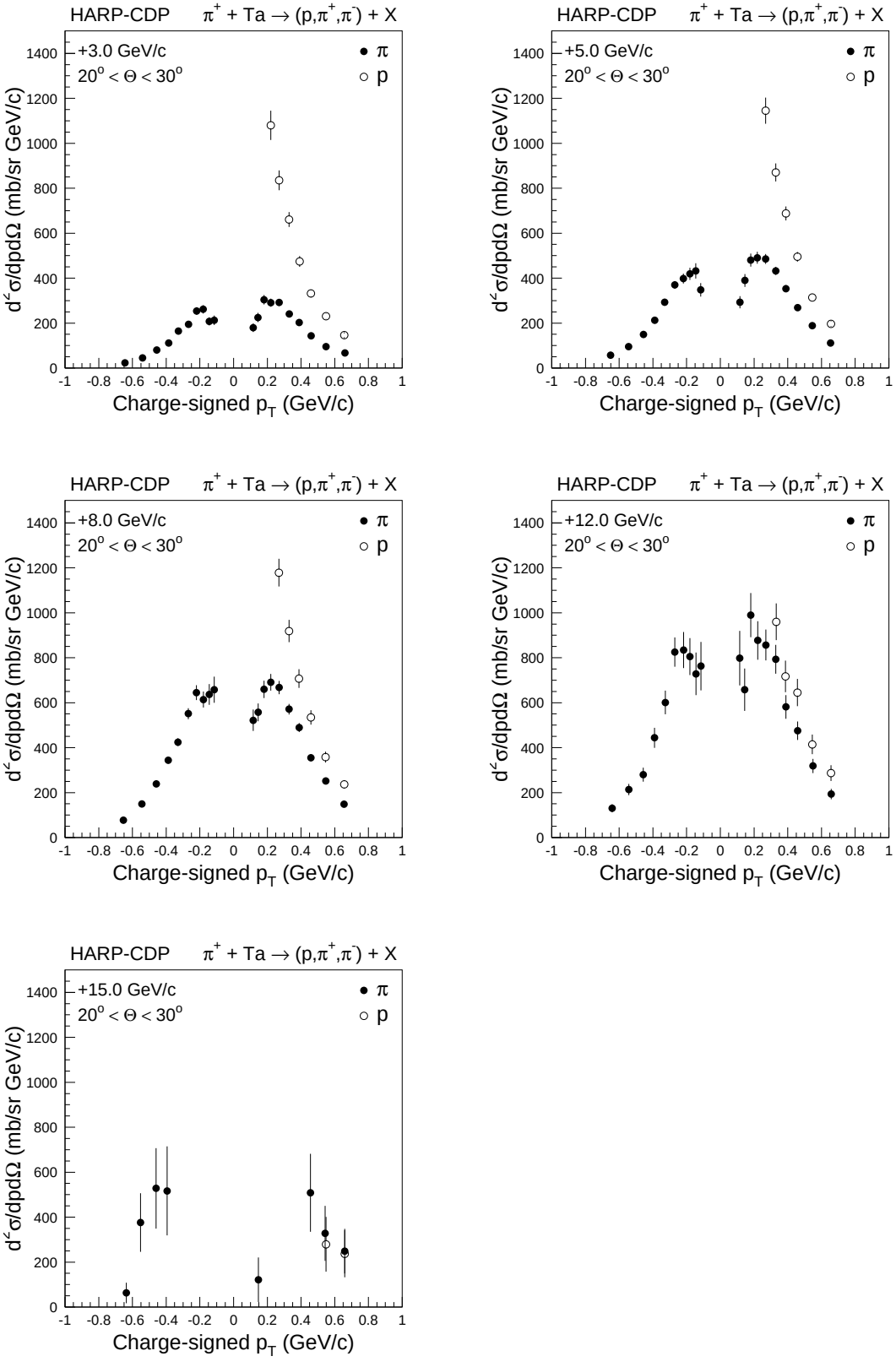

Fig. 2: Inclusive cross-sections of the production of secondary protons, π^+'s, and π^-'s, by π^+'s on tantalum nuclei, in the polar-angle range $20^\circ < \theta < 30^\circ$, for different π^+ beam momenta, as a function of the charge-signed $p_{\rm T}$ of the secondaries; the shown errors are total errors.

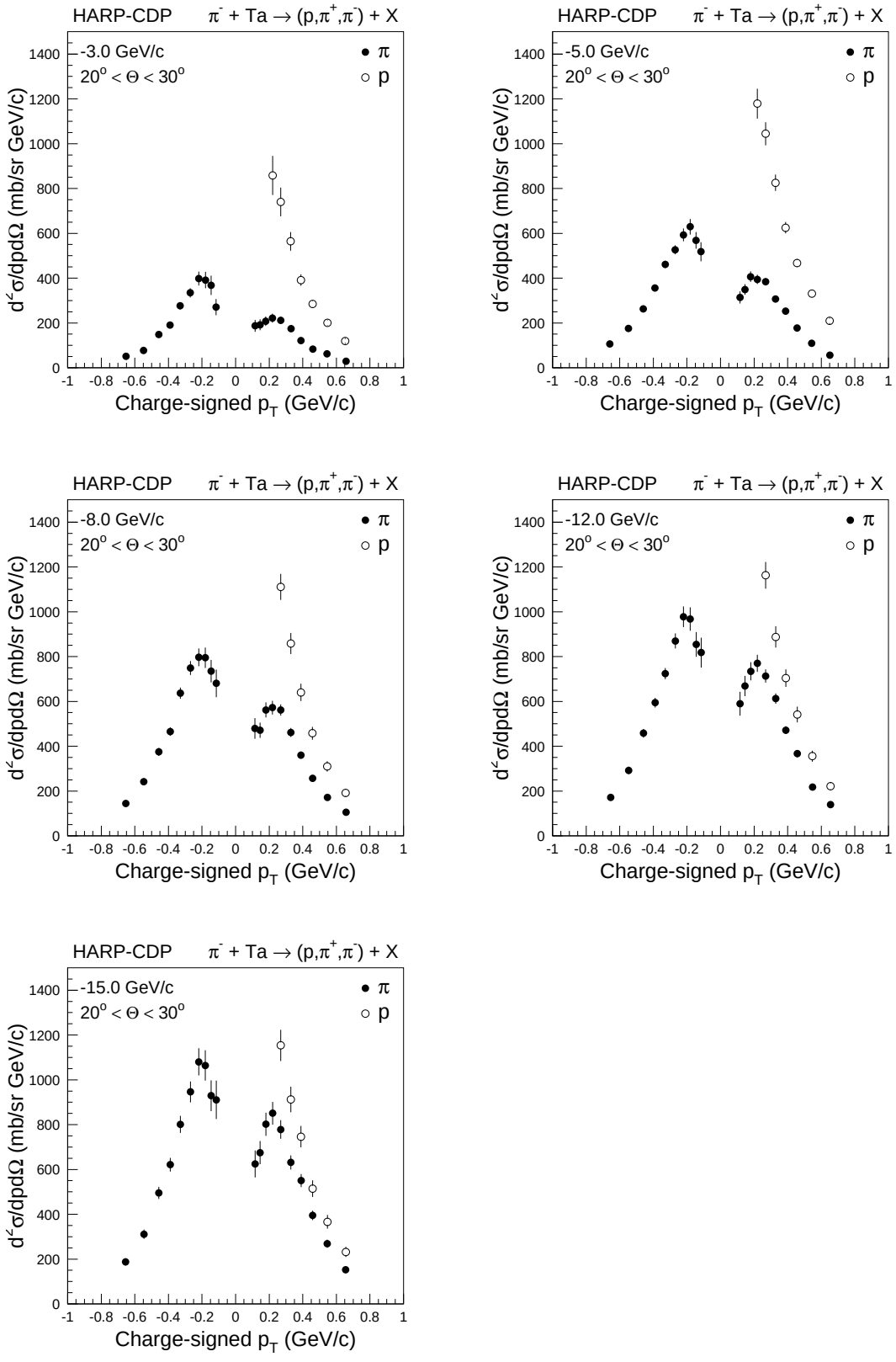

Fig. 3: Inclusive cross-sections of the production of secondary protons, π^+'s, and π^-'s, by π^-'s on tantalum nuclei, in the polar-angle range $20^\circ < \theta < 30^\circ$, for different π^- beam momenta, as a function of the charge-signed p_{T} of the secondaries; the shown errors are total errors.

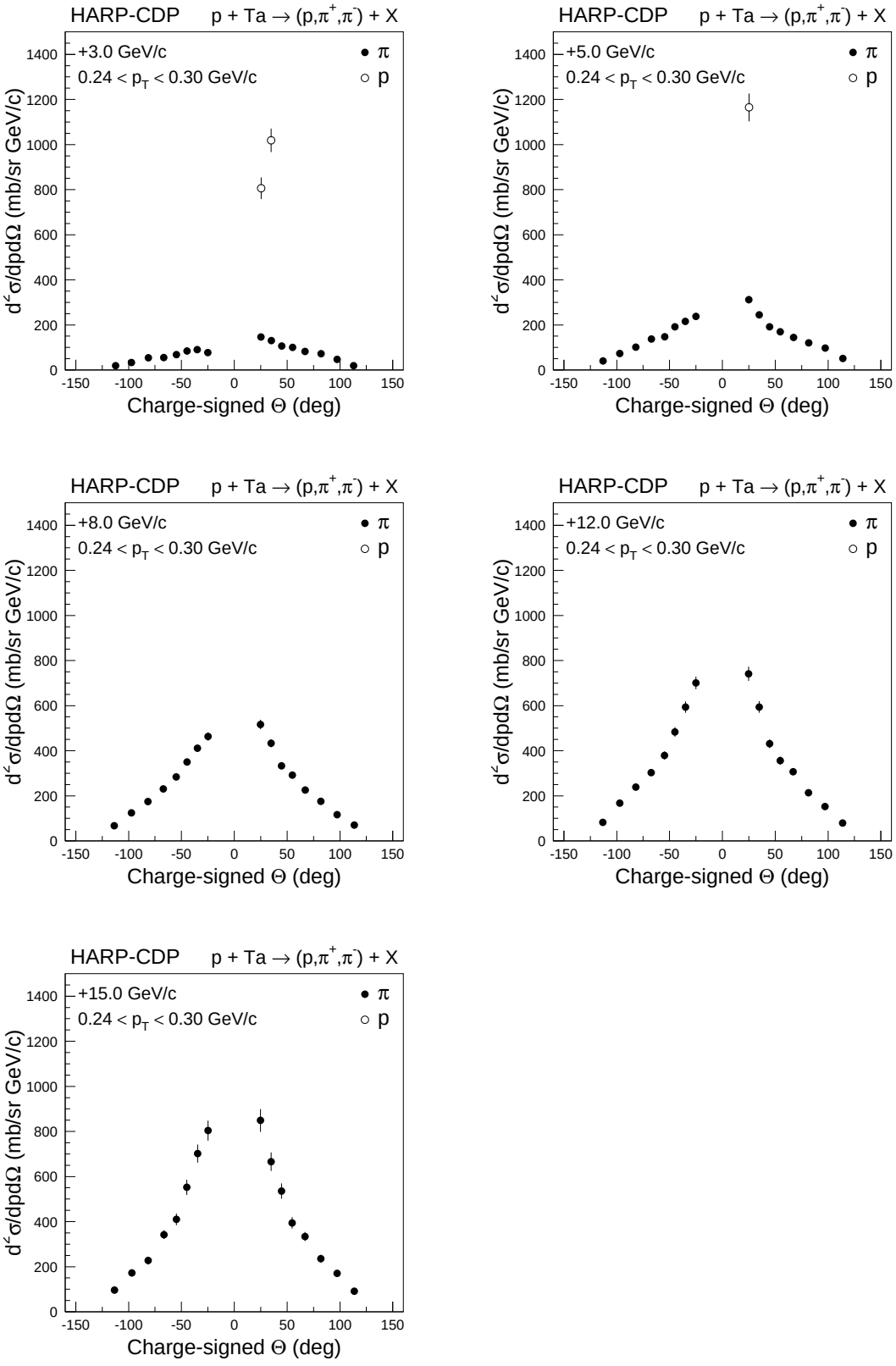

Fig. 4: Inclusive cross-sections of the production of secondary protons, π^+'s, and π^-'s, with p_{T} in the range 0.24–0.30 GeV/c, by protons on tantalum nuclei, for different proton beam momenta, as a function of the charge-signed polar angle θ of the secondaries; the shown errors are total errors.

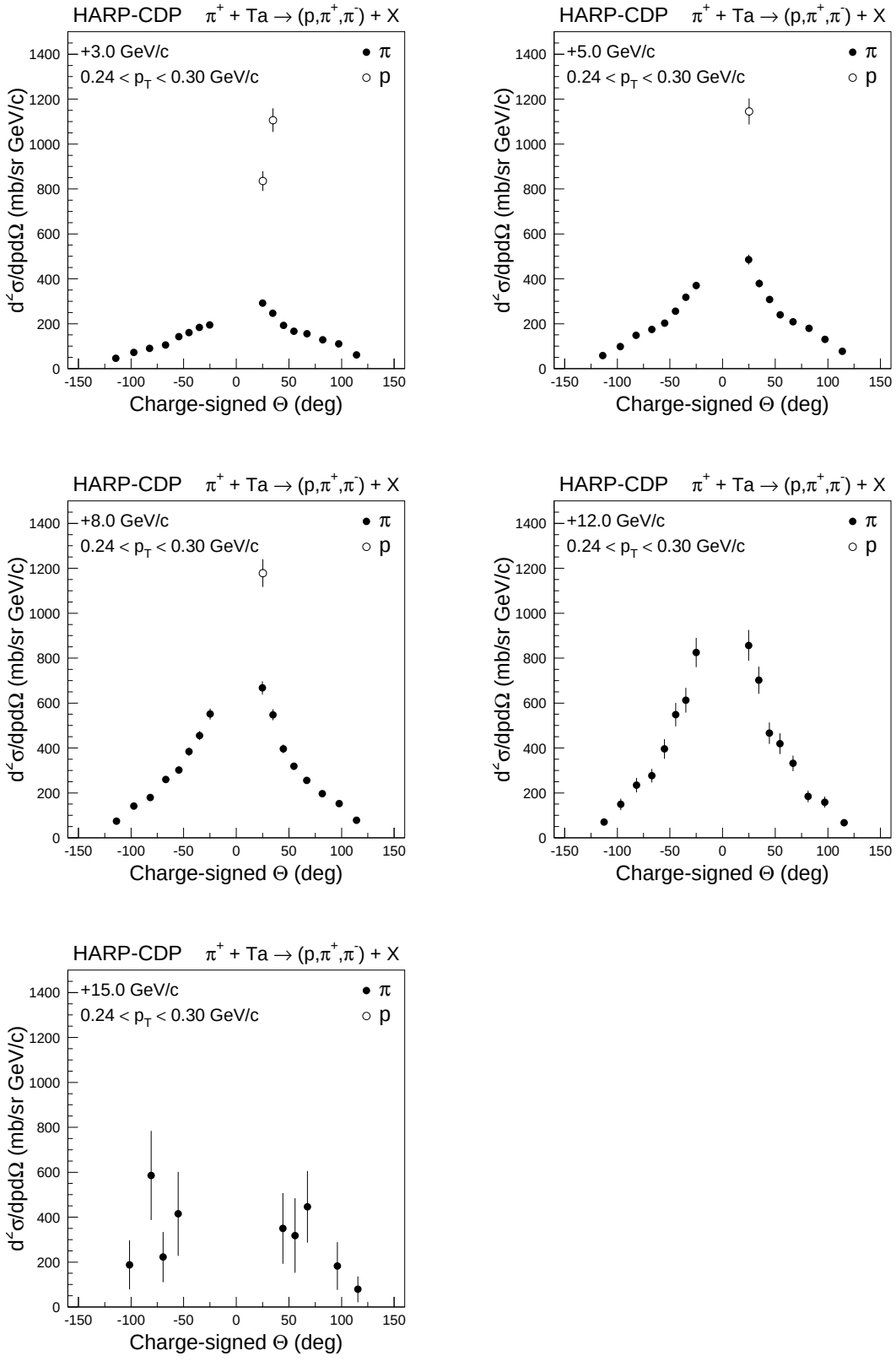

Fig. 5: Inclusive cross-sections of the production of secondary protons, π^+'s, and π^-'s, with $p_{\rm T}$ in the range 0.24–0.30 GeV/c, by π^+'s on tantalum nuclei, for different π^+ beam momenta, as a function of the charge-signed polar angle θ of the secondaries; the shown errors are total errors.

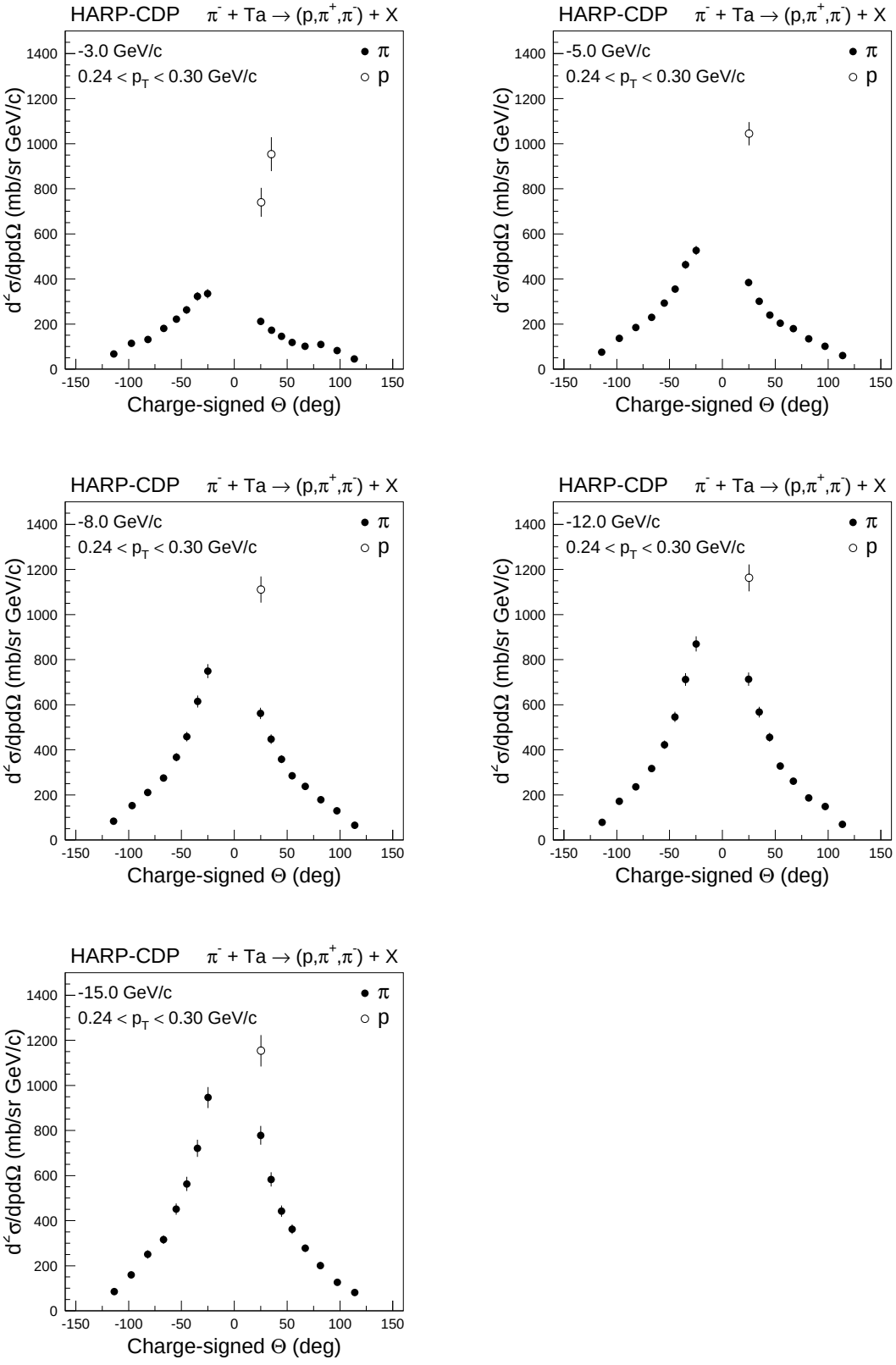

Fig. 6: Inclusive cross-sections of the production of secondary protons, π^+'s, and π^-'s, with p_{T} in the range 0.24–0.30 GeV/c, by π^-'s on tantalum nuclei, for different π^- beam momenta, as a function of the charge-signed polar angle θ of the secondaries; the shown errors are total errors.

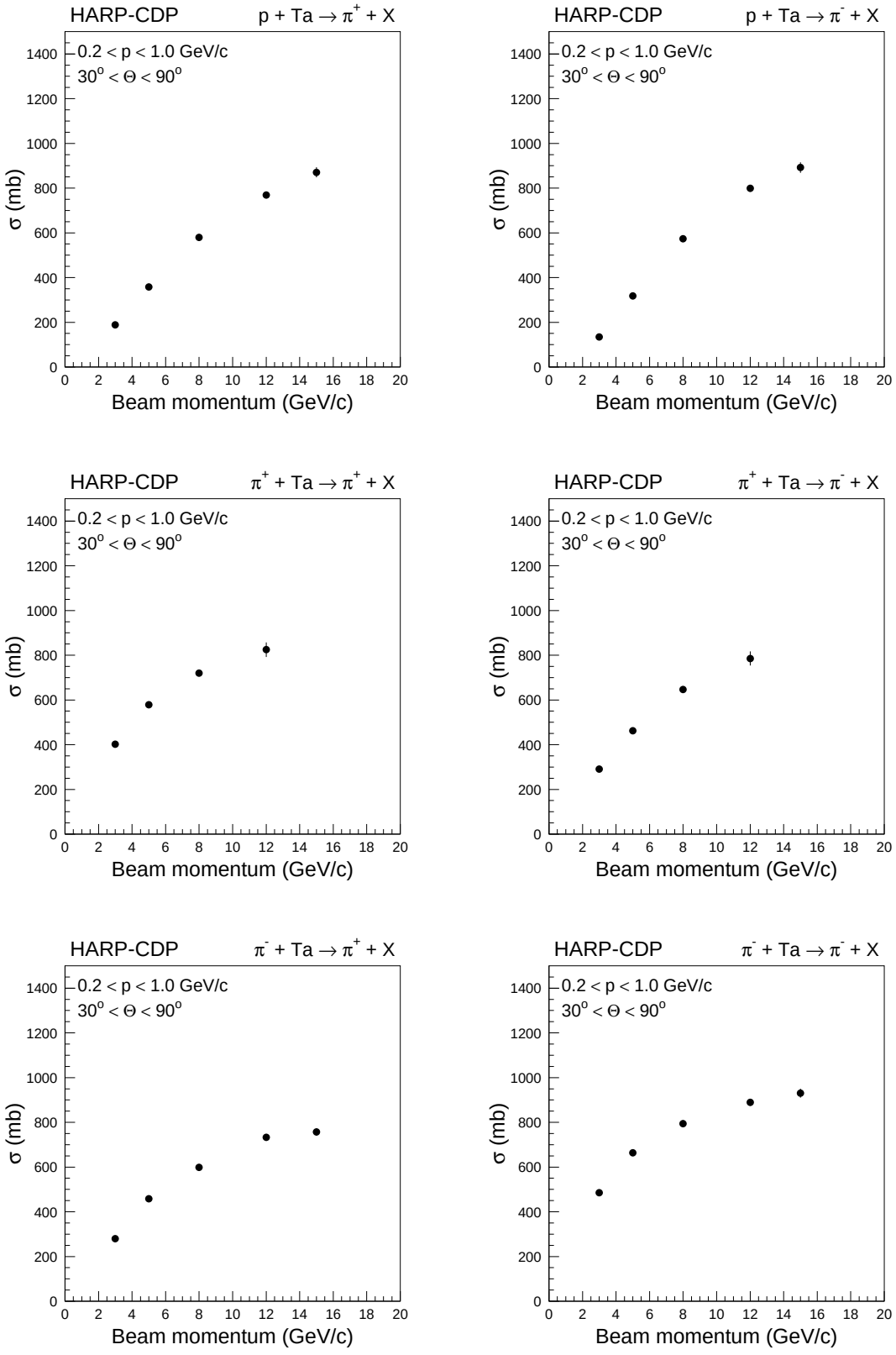

Fig. 7: Inclusive cross-sections of the production of secondary π^+'s and π^-'s, integrated over the momentum range $0.2 < p < 1.0$ GeV/c and the polar-angle range $30^\circ < \theta < 90^\circ$, from the interactions on tantalum nuclei of protons (top row), π^+'s (middle row), and π^-'s (bottom row), as a function of the beam momentum; the shown errors are total errors and mostly smaller than the symbol size.

7 DEUTERON PRODUCTION

Besides pions and protons, also deuterons are produced in sizeable quantities on tantalum nuclei. Up to momenta of about 1 GeV/c, deuterons are easily separated from protons both by $\mathrm{d}E/\mathrm{d}x$ and by time of flight.

Table 3 gives the ratio of deuteron to proton production as a function of the momentum at the vertex, for the momenta of beam protons of 3 GeV/c, 8 GeV/c, and 15 GeV/c. Table 4 gives the same for incoming π^- and Table 5 for incoming π^+. Cross-section ratios are not given if the data are scarce and the statistical error becomes comparable with the ratio itself—which is the case for deuterons at the high-momentum end of the spectrum.

The measured deuteron to proton production ratios are illustrated in Fig. 8, and compared with the predictions of Geant4's BIC and FRITIOF models. FRITIOF's predictions are shown for the same beam particles for which measured values are plotted, albeit only for beam momenta of 8 and 15 GeV/c, for its use at lower energies is discouraged. There is virtually no difference between its predictions for incoming protons, π^+'s and π^-'s. BIC's predictions are shown for incoming protons only. Both models, especially the BIC model, largely underestimate deuteron production.

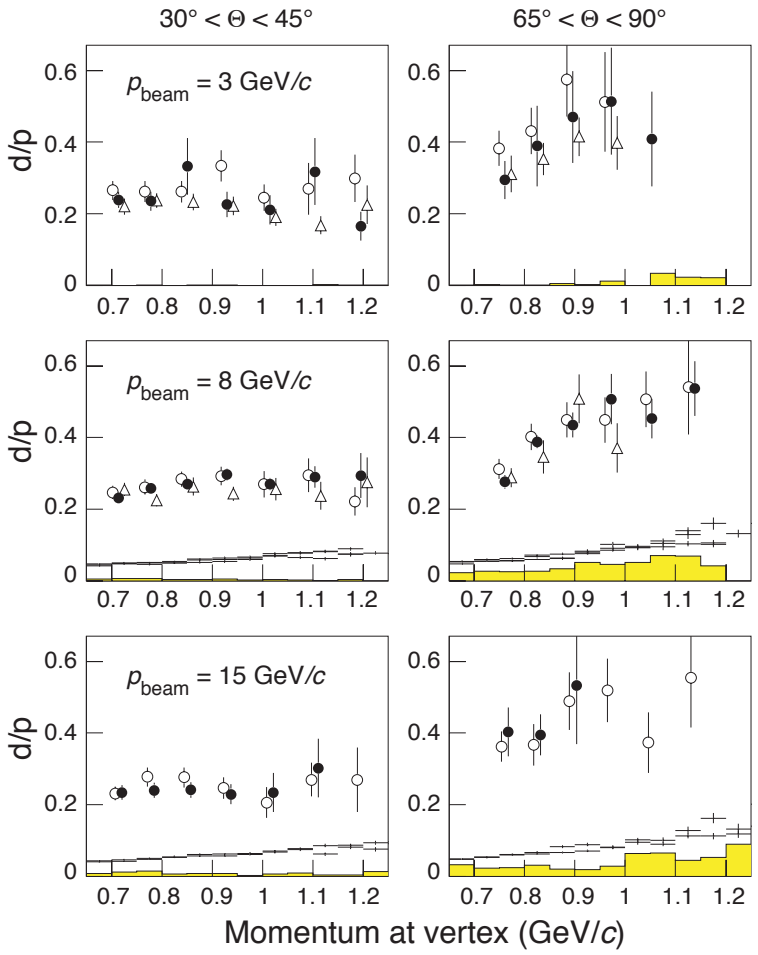

Fig. 8: Deuteron to proton ratio for beam particles of 3 GeV/c, 8 GeV/c, and 15 GeV/c on tantalum nuclei, as a function of the momentum at the vertex, for the polar-angle regions $30^\circ < \theta < 45^\circ$ (left panels) and $65^\circ < \theta < 90^\circ$ (right panels); black circles denote beam protons, triangles beam π^+, and open circles beam π^-; crosses denote predictions of Geant4's FRITIOF model, the shaded (yellow) histograms of its BIC model.

Table 3: Deuteron to proton ratio for beam protons of 3 GeV/c, 8 GeV/c, and 15 GeV/c on tantalum nuclei, as a function of the particle momentum p [GeV/c] at the vertex, for five polar-angle regions.

Polar angle		3 GeV/c protons	8 GeV/c protons	15 GeV/c protons
θ	p	d/p	d/p	d/p
$20^\circ - 30^\circ$	0.731	0.204 ± 0.030	0.200 ± 0.012	0.190 ± 0.027
	0.793	0.211 ± 0.031	0.202 ± 0.012	0.205 ± 0.025
	0.863	0.221 ± 0.035	0.241 ± 0.012	0.223 ± 0.028
	0.940	0.224 ± 0.040	0.242 ± 0.021	0.212 ± 0.029
	1.023	0.187 ± 0.031	0.222 ± 0.021	0.224 ± 0.056
	1.110	0.134 ± 0.032	0.213 ± 0.019	0.217 ± 0.036
	1.201	0.246 ± 0.085	0.284 ± 0.056	
$30^\circ - 45^\circ$	0.714	0.239 ± 0.023	0.232 ± 0.014	0.234 ± 0.021
	0.778	0.235 ± 0.027	0.259 ± 0.012	0.240 ± 0.021
	0.851	0.332 ± 0.079	0.270 ± 0.013	0.241 ± 0.022
	0.930	0.226 ± 0.035	0.297 ± 0.016	0.229 ± 0.028
	1.015	0.211 ± 0.041	0.270 ± 0.017	0.234 ± 0.055
	1.104	0.318 ± 0.093	0.290 ± 0.030	0.302 ± 0.082
	1.196	0.165 ± 0.040	0.294 ± 0.063	
$45^\circ - 65^\circ$	0.717	0.282 ± 0.036	0.277 ± 0.014	0.269 ± 0.027
	0.783	0.280 ± 0.036	0.326 ± 0.016	0.263 ± 0.023
	0.856	0.373 ± 0.064	0.323 ± 0.015	0.329 ± 0.053
	0.935	0.307 ± 0.047	0.402 ± 0.031	0.260 ± 0.046
	1.020	0.347 ± 0.081	0.388 ± 0.047	0.382 ± 0.118
	1.108	0.447 ± 0.201	0.424 ± 0.075	0.392 ± 0.124
	1.200		0.354 ± 0.041	
$65^\circ - 90^\circ$	0.761	0.294 ± 0.053	0.276 ± 0.019	0.403 ± 0.068
	0.825	0.389 ± 0.112	0.388 ± 0.018	0.395 ± 0.057
	0.896	0.470 ± 0.128	0.435 ± 0.035	0.533 ± 0.164
	0.972	0.514 ± 0.149	0.507 ± 0.070	
	1.053	0.409 ± 0.132	0.453 ± 0.055	
	1.138		0.537 ± 0.076	
$90^\circ - 125^\circ$	0.759		0.408 ± 0.027	0.497 ± 0.070
	0.824		0.590 ± 0.054	0.636 ± 0.086
	0.896		0.687 ± 0.080	
	0.974		0.754 ± 0.118	
	1.057		1.075 ± 0.241	

Table 4: Deuteron to proton ratio for beam π^-'s of 3 GeV/c, 8 GeV/c, and 15 GeV/c on tantalum nuclei, as a function of the particle momentum p [GeV/c] at the vertex, for five polar-angle regions.

Polar angle		3 GeV/c π^-	8 GeV/c π^-	15 GeV/c π^-
θ	p	d/p	d/p	d/p
$20^\circ - 30^\circ$	0.731	0.203 ± 0.032	0.185 ± 0.023	0.189 ± 0.022
	0.793	0.268 ± 0.038	0.235 ± 0.023	0.216 ± 0.026
	0.863	0.290 ± 0.053	0.223 ± 0.028	0.231 ± 0.026
	0.940	0.289 ± 0.041	0.248 ± 0.030	0.181 ± 0.025
	1.023	0.261 ± 0.058	0.213 ± 0.031	0.203 ± 0.031
	1.110	0.238 ± 0.048	0.232 ± 0.036	0.192 ± 0.032
	1.201	0.211 ± 0.043	0.215 ± 0.034	0.210 ± 0.034
$30^\circ - 45^\circ$	0.714	0.265 ± 0.026	0.247 ± 0.018	0.231 ± 0.019
	0.778	0.262 ± 0.029	0.262 ± 0.021	0.277 ± 0.027
	0.851	0.261 ± 0.030	0.284 ± 0.021	0.276 ± 0.028
	0.930	0.334 ± 0.044	0.293 ± 0.026	0.246 ± 0.030
	1.015	0.245 ± 0.037	0.270 ± 0.037	0.206 ± 0.043
	1.104	0.270 ± 0.072	0.295 ± 0.047	0.270 ± 0.047
	1.196	0.299 ± 0.066	0.222 ± 0.040	0.270 ± 0.090
$45^\circ - 65^\circ$	0.717	0.334 ± 0.033	0.308 ± 0.019	0.268 ± 0.024
	0.783	0.369 ± 0.037	0.336 ± 0.025	0.306 ± 0.026
	0.856	0.437 ± 0.052	0.368 ± 0.034	0.340 ± 0.038
	0.935	0.411 ± 0.067	0.377 ± 0.033	0.291 ± 0.038
	1.020	0.325 ± 0.066	0.448 ± 0.060	0.324 ± 0.039
	1.108	0.305 ± 0.062	0.407 ± 0.075	0.415 ± 0.099
$65^\circ - 90^\circ$	0.761	0.383 ± 0.049	0.312 ± 0.028	0.362 ± 0.042
	0.825	0.431 ± 0.065	0.402 ± 0.037	0.367 ± 0.058
	0.896	0.575 ± 0.103	0.450 ± 0.049	0.489 ± 0.080
	0.972	0.512 ± 0.139	0.449 ± 0.063	0.519 ± 0.089
	1.053		0.507 ± 0.078	0.373 ± 0.085
	1.138		0.541 ± 0.133	0.555 ± 0.140
$90^\circ - 125^\circ$	0.759		0.515 ± 0.053	0.445 ± 0.058
	0.824		0.631 ± 0.062	0.540 ± 0.088
	0.896		0.954 ± 0.189	1.001 ± 0.323
	0.974		0.802 ± 0.149	0.725 ± 0.169
	1.057		0.901 ± 0.335	

Table 5: Deuteron to proton ratio for beam π^+'s of 3 GeV/c and 8 GeV/c on tantalum nuclei, as a function of the particle momentum p [GeV/c] at the vertex, for five polar-angle regions.

Polar angle		3 GeV/c π^+	8 GeV/c π^+
θ	p	d/p	d/p
$20^\circ - 30^\circ$	0.731	0.224 $\pm$ 0.025	0.195 $\pm$ 0.021
	0.793	0.183 $\pm$ 0.021	0.171 $\pm$ 0.017
	0.863	0.225 $\pm$ 0.027	0.220 $\pm$ 0.028
	0.940	0.249 $\pm$ 0.034	0.203 $\pm$ 0.024
	1.023	0.207 $\pm$ 0.034	0.213 $\pm$ 0.031
	1.110	0.199 $\pm$ 0.040	0.243 $\pm$ 0.047
	1.201	0.173 $\pm$ 0.044	0.185 $\pm$ 0.032
$30^\circ - 45^\circ$	0.714	0.220 $\pm$ 0.022	0.255 $\pm$ 0.018
	0.778	0.237 $\pm$ 0.021	0.225 $\pm$ 0.017
	0.851	0.233 $\pm$ 0.023	0.263 $\pm$ 0.025
	0.930	0.222 $\pm$ 0.026	0.243 $\pm$ 0.020
	1.015	0.190 $\pm$ 0.024	0.256 $\pm$ 0.031
	1.104	0.168 $\pm$ 0.025	0.237 $\pm$ 0.039
	1.196	0.225 $\pm$ 0.054	0.275 $\pm$ 0.069
$45^\circ - 65^\circ$	0.717	0.243 $\pm$ 0.022	0.265 $\pm$ 0.018
	0.783	0.306 $\pm$ 0.037	0.289 $\pm$ 0.021
	0.856	0.304 $\pm$ 0.034	0.311 $\pm$ 0.031
	0.935	0.278 $\pm$ 0.044	0.312 $\pm$ 0.038
	1.020	0.319 $\pm$ 0.050	0.392 $\pm$ 0.066
	1.108	0.326 $\pm$ 0.087	0.274 $\pm$ 0.038
	1.200	0.245 $\pm$ 0.046	0.312 $\pm$ 0.084
$65^\circ - 90^\circ$	0.761	0.311 $\pm$ 0.051	0.288 $\pm$ 0.026
	0.825	0.353 $\pm$ 0.045	0.346 $\pm$ 0.047
	0.896	0.415 $\pm$ 0.054	0.508 $\pm$ 0.068
	0.972	0.398 $\pm$ 0.075	0.371 $\pm$ 0.069
$90^\circ - 125^\circ$	0.759		0.348 $\pm$ 0.039
	0.824		0.562 $\pm$ 0.078
	0.896		0.636 $\pm$ 0.106
	0.974		0.615 $\pm$ 0.107

8 COMPARISON OF PARTICLE PRODUCTION ON BERYLLIUM AND TANTALUM NUCLEI

Figure 9 demonstrates the rather striking differences in the production of pions, protons, and deuterons, in the interactions of protons with beryllium (A = 9.01) and tantalum (A = 181.0) nuclei. Reinteractions of secondaries in the nuclear matter of the heavy tantalum nucleus lead to a stark increase of the production of protons, deuterons, and even tritons, on tantalum nuclei with respect to beryllium nuclei.

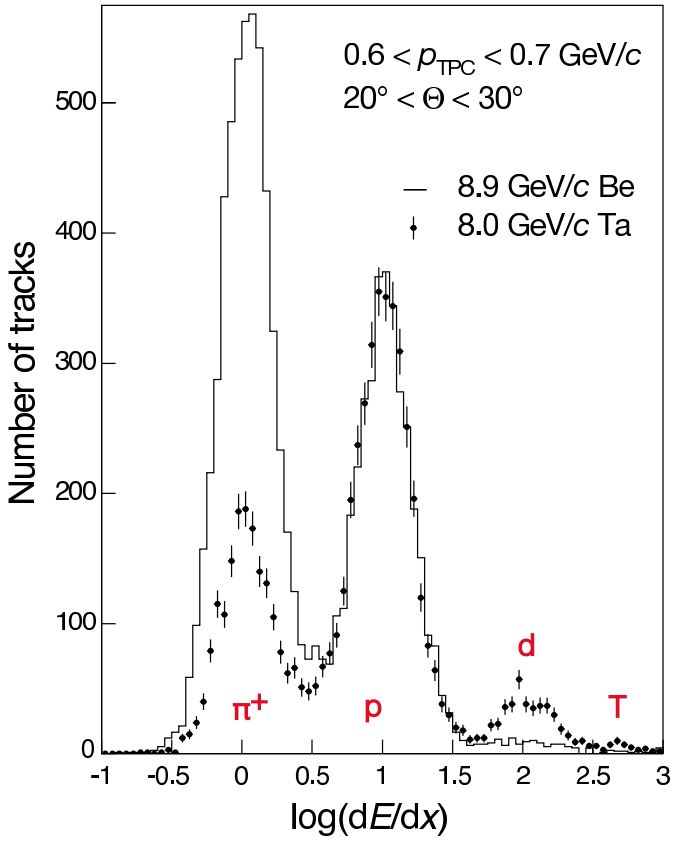

Fig. 9: Comparison of pion, proton, deuteron and triton production by protons between beryllium (histogram) and tantalum (black dots) target nuclei; the beryllium data are normalized such that the number of protons produced on beryllium and on tantalum agree; the momentum range refers to particle momentum in the TPC.

9 COMPARISON OF OUR RESULTS WITH RESULTS FROM OTHER EXPERIMENTS

9.1 Comparison with E802 results

Experiment E802 [10] at Brookhaven National Laboratory (BNL) measured secondary π^+'s in the polar-angle range $5^\circ < \theta < 58^\circ$ from the interactions of $+14.6$ GeV/c protons with gold (A = 197.0) nuclei.

Figure 10 shows their published Lorentz-invariant cross-section of π^+ and π^- production by $+14.6$ GeV/c protons, in the rapidity range $1.2 < y < 1.4$, as a function of $m_{\rm T} - m_\pi$, where $m_{\rm T}$ denotes the pion transverse mass. Their data are compared with our cross-sections from the interactions of $+15.0$ GeV/c protons with tantalum nuclei, expressed in the same unit as used by E802, but scaled up by 7% to compensate for the increase of the inclusive cross-section from tantalum to gold. Since E802 quoted only statistical errors, our data in Fig. 10 are also shown with their statistical errors.

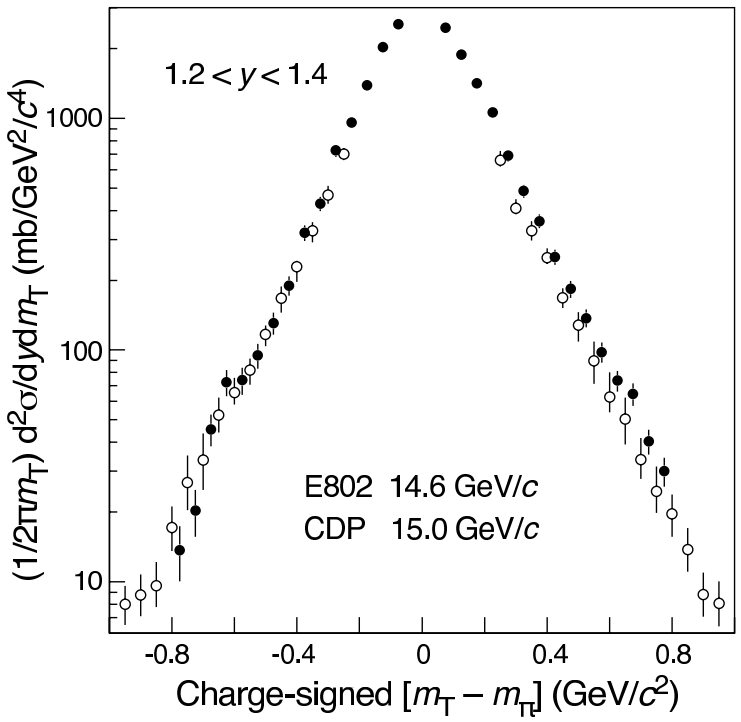

Fig. 10: Comparison of our cross-sections (black circles) of $\pi^\pm$ production by $+15.0$ GeV/c protons off tantalum nuclei, scaled up by 7% (see text), with the cross-sections on gold nuclei published by the E802 Collaboration for the proton beam momentum of $+14.6$ GeV/c (open circles); all errors are statistical only.

The E802 $\pi^\pm$ cross-sections are in good agreement with our cross-sections measured nearly at the same proton beam momentum, taking into account the normalization uncertainty of (10–15)% quoted by E802. We draw attention to the good agreement of the slopes of the cross-sections over two orders of magnitude.

9.2 Comparison with E910 results

BNL experiment E910 [11] measured secondary charged pions in the momentum range 0.1–6 GeV/c from the interactions of $+12.3$ GeV/c protons with gold (A = 197.0) nuclei. This experiment used a TPC for the measurement of secondaries, with a comfortably large track length of $\sim$1.5 m. This feature, together with a magnetic field strength of 0.5 T, is of particular significance, since it permits considerably better charge identification and proton–pion separation by $\mathrm{d}E/\mathrm{d}x$ than is possible in the HARP detector. Figure 11 shows their published cross-section $\mathrm{d}^2\sigma/\mathrm{d}p\mathrm{d}\Omega$ of $\pi^{\pm}$ production by $+12.3$ GeV/c protons, in the polar-angle range $0.8 < \cos\theta < 0.9$. Since E910 quoted only statistical errors, our data in Fig. 11 from the interactions of $+12.0$ GeV/c protons with tantalum, scaled up by 7% to compensate for the increase of the inclusive cross-section from tantalum to gold, are also shown with their statistical errors. The normalization uncertainty quoted by E910 is $\leq$5%.

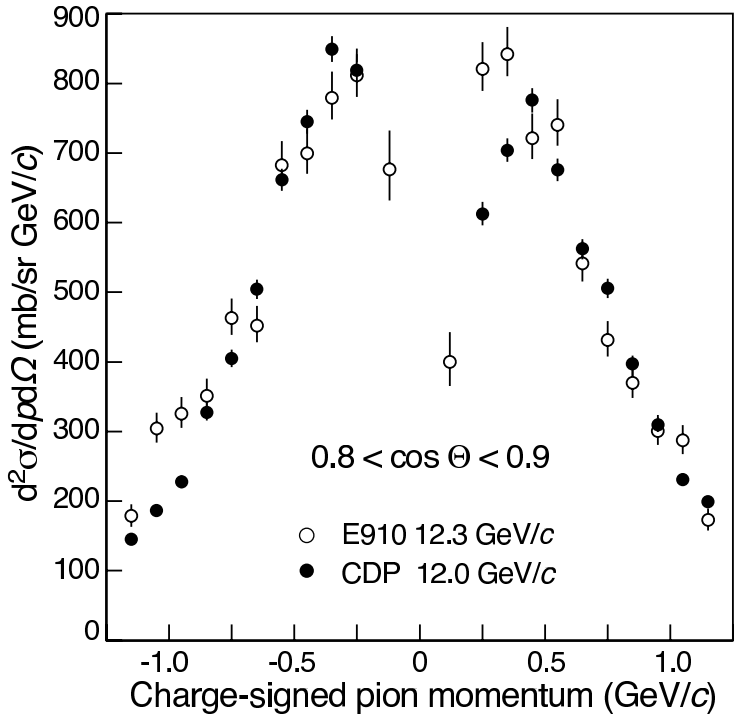

Fig. 11: Comparison of our cross-sections of $\pi^{\pm}$ production by $+12.0$ GeV/c protons off tantalum nuclei, scaled up by 7% (see text), with the cross-sections on gold nuclei published by the E910 Collaboration for the proton beam momentum of $+12.3$ GeV/c (open circles); all errors are statistical only.

Also here, the E910 data are shown as published, and our data are expressed in the same unit as used by E910. We draw attention to the good agreement in the π^+/π^- ratio between the cross-sections from E910 and our cross-sections.

9.3 Comparison with results from the HARP Collaboration

Figure 12 (a) shows the comparison of our cross-sections of pion production by $+12.0$ GeV/c protons off tantalum nuclei with the ones published by the HARP Collaboration [12], in the

polar-angle range $0.35 < \theta < 0.55$ rad. The latter cross-sections are plotted as published, while we expressed our cross-sections in the unit used by the HARP Collaboration. Figure 12 (b) shows our ratio π^+/π^- as a function of the polar angle θ in comparison with the ratios published by the E910 Collaboration (at the slightly different proton beam momentum of $+12.3$ GeV/c, and for gold nuclei) and by the HARP Collaboration.

The discrepancy between our results and those published by the HARP Collaboration is evident. We note the difference especially of the π^+ cross-section, and the difference in the reported momentum range. The discrepancy is even more serious as the same data set has been analysed by both groups.

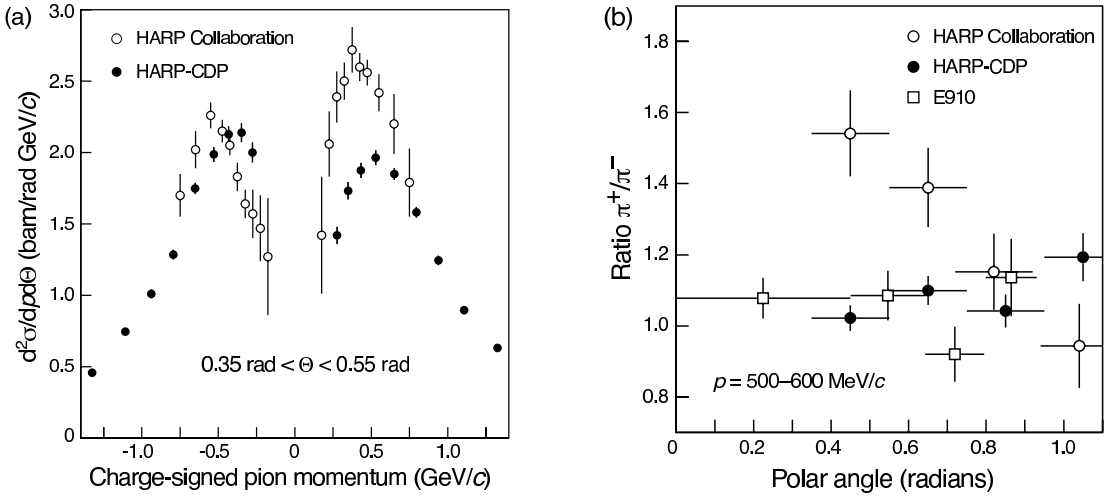

Fig. 12: (a) Comparison of our cross-sections (black circles) of $\pi^\pm$ production by $+12.0$ GeV/c protons off tantalum nuclei with the cross-sections published by the HARP Collaboration (open circles); (b) Comparison of our ratio π^+/π^- at $+12.0$ GeV/c beam momentum as a function of the polar angle θ with the ratios published by the HARP Collaboration; also shown are the ratios π^+/π^- published by the E910 Collaboration for a $+12.3$ GeV/c beam momentum and for gold nuclei; for the HARP Collaboration, total errors are shown; for E910 and our group, the shown errors are statistical only.

We hold that the discrepancy is caused by problems in the HARP Collaboration's data analysis. They result primarily, but not exclusively, from a lack of understanding TPC track distortions and RPC timing signals. These problems, together with others that affect the HARP Collaboration's data analysis, are discussed in detail in Refs [13–15] and summarized in the Appendix of Ref. [1].

We hold that the tantalum results published by the HARP Collaboration [12, 16] are not suitable for the optimization of the proton driver of a neutrino factory.

10 SUMMARY

From the analysis of data from the HARP large-angle spectrometer (polar angle θ in the range $20^\circ < \theta < 125^\circ$), double-differential cross-sections $\mathrm{d}^2\sigma/\mathrm{d}p\mathrm{d}\Omega$ of the production of secondary protons, π^+'s, and π^-'s, and of deuterons, have been obtained. The incoming beam particles were protons and pions with momenta from ± 3 to ± 15 GeV/c, impinging on a 5% λ_{abs} thick stationary tantalum target. Our cross-sections for π^+ and π^- production agree with results from

BNL experiments E802 and E910 but disagree with the results of the HARP Collaboration that were obtained from the same raw data. The inclusive cross-sections reported in this paper are of particular relevance for the optimization of the design parameters of the proton driver of a neutrino factory.

ACKNOWLEDGEMENTS

We are greatly indebted to many technical collaborators whose diligent and hard work made the HARP detector a well-functioning instrument. We thank all HARP colleagues who devoted time and effort to the design and construction of the detector, to data taking, and to setting up the computing and software infrastructure. We express our sincere gratitude to HARP's funding agencies for their support.

REFERENCES

[1] A. Bolshakova *et al.*, Cross-sections of large-angle hadron production in proton– and pion–nucleus interactions I: beryllium nuclei and beam momenta of $+8.9$ GeV/*c* and -8.0 GeV/*c*, Preprint CERN–PH–EP–2008–022 [arXiv:0901.3648], accepted for publication in Eur. Phys. J. C

[2] A. Bolshakova *et al.*, Cross-sections of large-angle hadron production in proton– and pion–nucleus interactions II: beryllium nuclei and beam momenta from ± 3 GeV/*c* to ± 15 GeV/*c*, Preprint CERN–PH–EP–2008–025 [arXiv:0903.2145], to be published in Eur. Phys. J. C

[3] V. Ammosov *et al.*, Nucl. Instrum. Methods Phys. Res. **A588** (2008) 294

[4] V. Ammosov *et al.*, Nucl. Instrum. Methods Phys. Res. **A578** (2007) 119

[5] V. Ammosov *et al.*, CERN–HARP–CDP–2008–001 (HARP Memo 08–101)

[6] V. Ammosov *et al.*, CERN–HARP–CDP–2008–002 (HARP Memo 08–102)

[7] S. Agostinelli *et al.*, Nucl. Instrum. Methods Phys. Res. **A506** (2003) 250; J. Allison *et al.*, IEEE Trans. Nucl. Sci. **53** (2006) 270

[8] A. Bolshakova *et al.*, Eur. Phys. J. **C56** (2008) 323

[9] A. Bolshakova *et al.*, Tables of cross-sections of large-angle hadron production in proton– and pion–nucleus interactions III: tantalum nuclei and beam momenta from ± 3 GeV/*c* to ± 15 GeV/*c*, CERN–HARP–CDP–2009–003

[10] T. Abbott *et al.*, Phys. Rev. **D45** (1992) 3906

[11] I. Chemakin *et al.*, Phys. Rev. **C65** (2002) 024904

[12] M.G. Catanesi *et al.*, Phys. Rev. **C77** (2008) 055207

[13] V. Ammosov *et al.*, J. Instrum. **3** (2008) P01002

[14] V. Ammosov *et al.*, Eur. Phys. J. **C54** (2008) 169

[15] V. Ammosov *et al.*, CERN–HARP–CDP–2006–003 (HARP Memo 06–101); CERN–HARP–CDP–2006–007 (HARP Memo 06–105); CERN–HARP–CDP–2007–001 (HARP Memo 07–101)

[16] M.G. Catanesi *et al.*, Eur. Phys. J. **C51** (2007) 787

APPENDIX A: CROSS-SECTION TABLES

Table A.1: Double-differential inclusive cross-section $\mathrm{d}^2\sigma/\mathrm{d}p\mathrm{d}\Omega$ [mb/(GeV/c sr)] of the production of protons in p + Ta $\rightarrow$ p + X interactions with $+3.0$ GeV/c beam momentum; the first error is statistical, the second systematic; p_T in GeV/c, polar angle θ in degrees.

	$20 < \theta < 30$					$30 < \theta < 40$				
p_T	$\langle p_\mathrm{T}\rangle$	$\langle\theta\rangle$	$\mathrm{d}^2\sigma/\mathrm{d}p\mathrm{d}\Omega$			$\langle p_\mathrm{T}\rangle$	$\langle\theta\rangle$	$\mathrm{d}^2\sigma/\mathrm{d}p\mathrm{d}\Omega$		
0.20–0.24	0.221	25.2	1003.26 ± 33.03	±	55.11					
0.24–0.30	0.270	25.4	806.42 ± 24.05	±	41.46	0.272	35.0	1018.58 ± 26.98	±	44.58
0.30–0.36	0.331	25.4	601.76 ± 21.42	±	33.60	0.331	35.0	893.51 ± 23.89	±	34.39
0.36–0.42	0.391	25.3	458.79 ± 18.45	±	24.92	0.390	35.1	649.01 ± 21.31	±	27.11
0.42–0.50	0.461	25.2	345.97 ± 14.16	±	19.41	0.459	35.2	483.57 ± 16.57	±	24.30
0.50–0.60	0.552	25.2	265.32 ± 10.84	±	13.20	0.551	35.1	346.54 ± 12.57	±	18.65
0.60–0.72	0.658	25.2	193.54 ± 8.50	±	10.46	0.658	35.3	202.39 ± 8.93	±	13.48
0.72–0.90						0.806	35.4	101.59 ± 5.20	±	8.14

	$40 < \theta < 50$					$50 < \theta < 60$				
p_T	$\langle p_\mathrm{T}\rangle$	$\langle\theta\rangle$	$\mathrm{d}^2\sigma/\mathrm{d}p\mathrm{d}\Omega$			$\langle p_\mathrm{T}\rangle$	$\langle\theta\rangle$	$\mathrm{d}^2\sigma/\mathrm{d}p\mathrm{d}\Omega$		
0.30–0.36	0.331	45.1	1033.78 ± 24.63	±	32.79					
0.36–0.42	0.392	45.1	823.20 ± 22.64	±	24.04	0.392	55.1	862.94 ± 21.83	±	26.36
0.42–0.50	0.462	45.1	563.79 ± 17.15	±	22.34	0.462	55.0	704.63 ± 18.18	±	20.46
0.50–0.60	0.552	45.2	408.29 ± 13.96	±	25.06	0.554	55.0	421.73 ± 13.41	±	19.05
0.60–0.72	0.663	45.0	225.69 ± 9.62	±	17.26	0.663	55.1	237.13 ± 9.97	±	18.69
0.72–0.90	0.811	45.0	108.66 ± 5.68	±	11.16	0.810	55.1	110.47 ± 5.75	±	12.28

	$60 < \theta < 75$					$75 < \theta < 90$				
p_T	$\langle p_\mathrm{T}\rangle$	$\langle\theta\rangle$	$\mathrm{d}^2\sigma/\mathrm{d}p\mathrm{d}\Omega$			$\langle p_\mathrm{T}\rangle$	$\langle\theta\rangle$	$\mathrm{d}^2\sigma/\mathrm{d}p\mathrm{d}\Omega$		
0.50–0.60	0.555	67.2	424.37 ± 10.14	±	15.95					
0.60–0.72	0.668	67.0	245.16 ± 7.66	±	15.51	0.664	81.7	170.86 ± 5.72	±	12.23
0.72–0.90	0.814	67.2	99.16 ± 4.42	±	11.30	0.809	81.8	65.97 ± 3.34	±	7.29

	$90 < \theta < 105$					$105 < \theta < 125$				
p_T	$\langle p_\mathrm{T}\rangle$	$\langle\theta\rangle$	$\mathrm{d}^2\sigma/\mathrm{d}p\mathrm{d}\Omega$			$\langle p_\mathrm{T}\rangle$	$\langle\theta\rangle$	$\mathrm{d}^2\sigma/\mathrm{d}p\mathrm{d}\Omega$		
0.42–0.50						0.464	113.5	212.84 ± 6.74	±	11.98
0.50–0.60						0.554	112.7	79.60 ± 3.90	±	7.89
0.60–0.72	0.663	97.1	84.47 ± 4.02	±	7.72					
0.72–0.90	0.811	96.6	19.49 ± 1.93	±	2.96					

Table A.2: Double-differential inclusive cross-section $\mathrm{d}^2\sigma/\mathrm{d}p\mathrm{d}\Omega$ [mb/(GeV/c sr)] of the production of π^+'s in p + Ta $\rightarrow \pi^+$ + X interactions with $+3.0$ GeV/c beam momentum; the first error is statistical, the second systematic; p_T in GeV/c, polar angle θ in degrees.

	$20 < \theta < 30$					$30 < \theta < 40$				
p_T	$\langle p_\mathrm{T}\rangle$	$\langle\theta\rangle$	$\mathrm{d}^2\sigma/\mathrm{d}p\mathrm{d}\Omega$			$\langle p_\mathrm{T}\rangle$	$\langle\theta\rangle$	$\mathrm{d}^2\sigma/\mathrm{d}p\mathrm{d}\Omega$		
0.10–0.13	0.117	24.7	104.14 ±	13.28 ±	8.40	0.116	34.9	132.51 ±	14.94 ±	10.56
0.13–0.16	0.146	24.6	177.45 ±	16.58 ±	12.08	0.144	35.1	105.39 ±	11.54 ±	6.75
0.16–0.20	0.182	25.0	175.91 ±	13.46 ±	9.31	0.181	35.0	163.67 ±	12.42 ±	8.79
0.20–0.24	0.220	24.9	171.46 ±	12.80 ±	7.85	0.220	34.8	164.56 ±	12.56 ±	7.56
0.24–0.30	0.272	25.3	146.16 ±	9.81 ±	5.67	0.268	35.1	130.84 ±	9.24 ±	5.13
0.30–0.36	0.329	25.3	101.17 ±	7.96 ±	3.67	0.330	34.6	101.57 ±	7.88 ±	3.62
0.36–0.42	0.390	24.9	65.53 ±	6.25 ±	2.57	0.390	35.3	75.72 ±	6.92 ±	2.82
0.42–0.50	0.462	25.5	39.68 ±	4.10 ±	1.79	0.460	35.0	49.06 ±	4.79 ±	2.09
0.50–0.60	0.551	25.7	22.01 ±	2.51 ±	1.33	0.552	35.2	25.52 ±	2.80 ±	1.39
0.60–0.72	0.658	25.4	13.43 ±	1.58 ±	1.20	0.664	34.8	16.34 ±	1.98 ±	1.29
0.72–0.90						0.807	35.1	8.90 ±	1.13 ±	1.11

	$40 < \theta < 50$					$50 < \theta < 60$				
p_T	$\langle p_\mathrm{T}\rangle$	$\langle\theta\rangle$	$\mathrm{d}^2\sigma/\mathrm{d}p\mathrm{d}\Omega$			$\langle p_\mathrm{T}\rangle$	$\langle\theta\rangle$	$\mathrm{d}^2\sigma/\mathrm{d}p\mathrm{d}\Omega$		
0.10–0.13	0.116	45.7	136.69 ±	16.41 ±	11.71					
0.13–0.16	0.144	44.9	138.77 ±	13.21 ±	8.66	0.146	55.1	113.92 ±	12.28 ±	7.37
0.16–0.20	0.180	44.8	148.31 ±	11.98 ±	7.88	0.181	54.3	125.41 ±	10.96 ±	6.49
0.20–0.24	0.220	44.9	134.80 ±	11.15 ±	6.42	0.218	55.0	119.67 ±	10.75 ±	5.62
0.24–0.30	0.271	44.9	106.22 ±	8.17 ±	4.16	0.269	55.2	100.46 ±	7.95 ±	3.92
0.30–0.36	0.333	45.0	76.19 ±	6.93 ±	2.74	0.331	54.6	69.31 ±	6.66 ±	2.54
0.36–0.42	0.391	44.9	73.20 ±	6.76 ±	2.77	0.392	54.7	58.79 ±	6.21 ±	2.46
0.42–0.50	0.461	45.0	39.47 ±	4.37 ±	1.75	0.465	55.2	47.74 ±	4.89 ±	2.26
0.50–0.60	0.554	45.2	21.65 ±	2.72 ±	1.15	0.557	54.9	24.47 ±	3.03 ±	1.45
0.60–0.72	0.664	44.6	15.24 ±	1.98 ±	1.17	0.666	54.1	15.18 ±	2.12 ±	1.22
0.72–0.90	0.813	44.9	9.29 ±	1.17 ±	1.02	0.803	54.2	6.78 ±	1.10 ±	0.76
0.90–1.25						1.009	54.1	1.67 ±	0.31 ±	0.29

	$60 < \theta < 75$					$75 < \theta < 90$				
p_T	$\langle p_\mathrm{T}\rangle$	$\langle\theta\rangle$	$\mathrm{d}^2\sigma/\mathrm{d}p\mathrm{d}\Omega$			$\langle p_\mathrm{T}\rangle$	$\langle\theta\rangle$	$\mathrm{d}^2\sigma/\mathrm{d}p\mathrm{d}\Omega$		
0.13–0.16	0.145	67.0	158.00 ±	15.05 ±	14.89					
0.16–0.20	0.180	66.8	145.47 ±	9.67 ±	7.32	0.184	82.1	118.00 ±	10.74 ±	10.65
0.20–0.24	0.220	66.9	118.76 ±	8.73 ±	5.17	0.220	82.5	105.59 ±	8.85 ±	5.34
0.24–0.30	0.271	66.9	82.08 ±	5.94 ±	3.11	0.267	82.1	72.56 ±	5.96 ±	3.73
0.30–0.36	0.329	66.9	53.33 ±	4.81 ±	1.94	0.329	81.3	42.32 ±	4.61 ±	2.47
0.36–0.42	0.393	66.8	45.09 ±	4.50 ±	1.95	0.392	81.6	28.70 ±	3.74 ±	1.67
0.42–0.50	0.465	67.3	24.89 ±	2.86 ±	1.28	0.467	81.6	14.20 ±	2.27 ±	1.03
0.50–0.60	0.547	66.6	16.32 ±	2.07 ±	1.11	0.547	82.2	12.99 ±	1.97 ±	1.22
0.60–0.72	0.671	66.2	5.83 ±	1.09 ±	0.54	0.663	82.4	4.53 ±	1.02 ±	0.53
0.72–0.90	0.800	66.5	4.00 ±	0.69 ±	0.51	0.839	80.9	0.97 ±	0.33 ±	0.15
0.90–1.25	1.057	66.6	0.57 ±	0.15 ±	0.11	0.987	82.7	0.18 ±	0.08 ±	0.05

	$90 < \theta < 105$					$105 < \theta < 125$				
p_T	$\langle p_\mathrm{T}\rangle$	$\langle\theta\rangle$	$\mathrm{d}^2\sigma/\mathrm{d}p\mathrm{d}\Omega$			$\langle p_\mathrm{T}\rangle$	$\langle\theta\rangle$	$\mathrm{d}^2\sigma/\mathrm{d}p\mathrm{d}\Omega$		
0.13–0.16						0.145	114.8	133.66 ±	11.55 ±	8.58
0.16–0.20	0.180	97.2	109.79 ±	10.97 ±	10.74	0.178	114.5	89.93 ±	6.80 ±	3.54
0.20–0.24	0.219	97.7	81.63 ±	8.03 ±	4.70	0.221	114.1	56.70 ±	5.38 ±	2.34
0.24–0.30	0.269	97.2	46.91 ±	4.79 ±	2.25	0.263	113.0	19.30 ±	2.51 ±	1.01
0.30–0.36	0.334	97.0	31.40 ±	3.89 ±	1.79	0.330	113.6	12.43 ±	2.07 ±	0.90
0.36–0.42	0.394	96.0	9.61 ±	2.17 ±	0.73	0.386	112.0	6.55 ±	1.58 ±	0.66
0.42–0.50	0.465	95.7	7.50 ±	1.73 ±	0.77	0.456	109.4	4.07 ±	1.04 ±	0.51
0.50–0.60	0.573	96.4	2.26 ±	0.80 ±	0.28	0.552	112.1	1.75 ±	0.57 ±	0.30
0.60–0.72	0.692	93.3	2.01 ±	0.68 ±	0.34					
0.72–0.90	0.774	98.9	0.21 ±	0.12 ±	0.05					

Table A.3: Double-differential inclusive cross-section $\mathrm{d}^2\sigma/\mathrm{d}p\mathrm{d}\Omega$ [mb/(GeV/c sr)] of the production of π^-'s in p + Ta $\rightarrow \pi^-$ + X interactions with $+3.0$ GeV/c beam momentum; the first error is statistical, the second systematic; p_T in GeV/c, polar angle θ in degrees.

	$20 < \theta < 30$					$30 < \theta < 40$				
p_T	$\langle p_\mathrm{T}\rangle$	$\langle\theta\rangle$	$\mathrm{d}^2\sigma/\mathrm{d}p\mathrm{d}\Omega$			$\langle p_\mathrm{T}\rangle$	$\langle\theta\rangle$	$\mathrm{d}^2\sigma/\mathrm{d}p\mathrm{d}\Omega$		
0.10–0.13	0.115	24.9	129.88 ± 14.68	±	9.98	0.114	35.1	138.65 ± 14.80	±	10.97
0.13–0.16	0.145	24.6	158.29 ± 15.00	±	10.43	0.145	34.4	139.10 ± 13.51	±	9.17
0.16–0.20	0.179	25.0	139.70 ± 12.02	±	7.89	0.179	34.9	107.53 ± 9.93	±	5.97
0.20–0.24	0.217	25.8	112.64 ± 10.81	±	5.80	0.219	34.7	110.66 ± 10.30	±	5.43
0.24–0.30	0.268	25.0	77.11 ± 7.07	±	3.31	0.266	35.1	90.17 ± 7.55	±	3.61
0.30–0.36	0.330	25.7	51.53 ± 5.94	±	2.44	0.329	35.0	64.73 ± 6.33	±	2.53
0.36–0.42	0.390	25.0	20.83 ± 3.63	±	1.10	0.386	35.2	46.73 ± 5.34	±	2.11
0.42–0.50	0.451	26.0	14.13 ± 2.63	±	0.91	0.453	35.3	24.62 ± 3.46	±	1.37
0.50–0.60	0.525	26.1	6.85 ± 1.66	±	0.59	0.554	34.9	7.04 ± 1.66	±	0.52
0.60–0.72	0.658	25.6	2.78 ± 0.98	±	0.32	0.647	36.2	5.03 ± 1.26	±	0.54
0.72–0.90						0.772	35.7	1.02 ± 0.51	±	0.17

	$40 < \theta < 50$					$50 < \theta < 60$				
p_T	$\langle p_\mathrm{T}\rangle$	$\langle\theta\rangle$	$\mathrm{d}^2\sigma/\mathrm{d}p\mathrm{d}\Omega$			$\langle p_\mathrm{T}\rangle$	$\langle\theta\rangle$	$\mathrm{d}^2\sigma/\mathrm{d}p\mathrm{d}\Omega$		
0.10–0.13	0.114	45.2	169.94 ± 17.86	±	14.14					
0.13–0.16	0.144	45.4	163.99 ± 14.85	±	10.62	0.146	54.6	134.35 ± 13.70	±	8.83
0.16–0.20	0.180	45.4	106.42 ± 9.79	±	5.88	0.178	54.5	120.78 ± 10.45	±	6.47
0.20–0.24	0.218	45.0	91.08 ± 9.29	±	4.70	0.219	54.8	88.78 ± 8.95	±	4.24
0.24–0.30	0.267	44.6	84.14 ± 7.09	±	3.32	0.267	54.7	68.63 ± 6.57	±	2.78
0.30–0.36	0.330	45.0	55.60 ± 5.80	±	2.09	0.326	54.4	53.86 ± 5.78	±	2.06
0.36–0.42	0.385	44.4	40.39 ± 4.99	±	1.75	0.384	55.5	37.30 ± 4.83	±	1.66
0.42–0.50	0.452	44.8	23.10 ± 3.31	±	1.19	0.452	54.0	25.25 ± 3.58	±	1.46
0.50–0.60	0.540	45.4	13.38 ± 2.27	±	0.95	0.546	55.9	10.92 ± 2.03	±	0.77
0.60–0.72	0.639	44.5	4.06 ± 1.17	±	0.42	0.649	55.7	7.16 ± 1.60	±	0.73
0.72–0.90	0.764	44.7	1.19 ± 0.49	±	0.17	0.765	54.6	2.58 ± 0.75	±	0.35
0.90–1.25						0.952	53.2	0.10 ± 0.08	±	0.02

	$60 < \theta < 75$					$75 < \theta < 90$				
p_T	$\langle p_\mathrm{T}\rangle$	$\langle\theta\rangle$	$\mathrm{d}^2\sigma/\mathrm{d}p\mathrm{d}\Omega$			$\langle p_\mathrm{T}\rangle$	$\langle\theta\rangle$	$\mathrm{d}^2\sigma/\mathrm{d}p\mathrm{d}\Omega$		
0.13–0.16	0.143	67.0	149.70 ± 14.29	±	11.27	0.150	81.2	233.16 ± 37.59	±	153.40
0.16–0.20	0.179	67.0	110.86 ± 8.36	±	5.40	0.178	80.9	111.55 ± 10.58	±	10.06
0.20–0.24	0.217	66.8	102.08 ± 8.03	±	4.46	0.218	81.7	68.46 ± 7.03	±	3.76
0.24–0.30	0.264	66.7	55.53 ± 4.72	±	2.03	0.269	81.2	54.24 ± 5.16	±	3.12
0.30–0.36	0.325	67.1	47.02 ± 4.45	±	1.78	0.324	82.2	32.37 ± 4.01	±	2.04
0.36–0.42	0.385	66.7	32.57 ± 3.84	±	1.64	0.382	83.1	18.17 ± 2.96	±	1.19
0.42–0.50	0.449	67.2	20.05 ± 2.61	±	1.21	0.456	81.2	16.52 ± 2.41	±	1.28
0.50–0.60	0.531	66.4	10.12 ± 1.65	±	0.78	0.531	80.9	7.18 ± 1.41	±	0.72
0.60–0.72	0.634	65.6	4.47 ± 1.00	±	0.47	0.643	79.6	0.91 ± 0.46	±	0.13
0.72–0.90	0.786	65.4	1.40 ± 0.44	±	0.21	0.774	82.8	0.31 ± 0.22	±	0.07
0.90–1.25	0.998	65.3	0.35 ± 0.13	±	0.08					

	$90 < \theta < 105$					$105 < \theta < 125$				
p_T	$\langle p_\mathrm{T}\rangle$	$\langle\theta\rangle$	$\mathrm{d}^2\sigma/\mathrm{d}p\mathrm{d}\Omega$			$\langle p_\mathrm{T}\rangle$	$\langle\theta\rangle$	$\mathrm{d}^2\sigma/\mathrm{d}p\mathrm{d}\Omega$		
0.13–0.16	0.146	96.9	264.67 ± 81.53	±	117.96	0.144	114.0	114.60 ± 9.70	±	5.99
0.16–0.20	0.179	97.8	100.65 ± 10.00	±	7.52	0.177	114.1	67.91 ± 5.98	±	2.80
0.20–0.24	0.216	97.4	74.89 ± 7.96	±	5.52	0.219	114.5	45.71 ± 4.95	±	2.37
0.24–0.30	0.265	97.4	32.73 ± 4.00	±	1.76	0.264	112.3	18.78 ± 2.49	±	1.06
0.30–0.36	0.326	96.3	22.52 ± 3.29	±	1.46	0.323	111.7	11.53 ± 1.95	±	0.91
0.36–0.42	0.385	96.9	10.64 ± 2.22	±	0.84	0.377	114.8	7.76 ± 1.58	±	0.81
0.42–0.50	0.449	97.2	8.49 ± 1.77	±	0.90	0.466	112.4	2.86 ± 0.83	±	0.39
0.50–0.60	0.530	96.8	2.14 ± 0.76	±	0.31	0.553	110.9	0.86 ± 0.38	±	0.18
0.60–0.72	0.635	97.2	0.45 ± 0.32	±	0.11	0.616	106.7	0.40 ± 0.20	±	0.15

Table A.4: Double-differential inclusive cross-section $\mathrm{d}^2\sigma/\mathrm{d}p\mathrm{d}\Omega$ [mb/(GeV/c sr)] of the production of protons in π^+ + Ta $\rightarrow$ p + X interactions with $+3.0$ GeV/c beam momentum; the first error is statistical, the second systematic; p_T in GeV/c, polar angle θ in degrees.

	$20 < \theta < 30$						$30 < \theta < 40$					
p_T	$\langle p_\mathrm{T}\rangle$	$\langle\theta\rangle$	$\mathrm{d}^2\sigma/\mathrm{d}p\mathrm{d}\Omega$				$\langle p_\mathrm{T}\rangle$	$\langle\theta\rangle$	$\mathrm{d}^2\sigma/\mathrm{d}p\mathrm{d}\Omega$			
0.20–0.24	0.221	25.4	1080.23	$\pm$	25.48	$\pm$ 59.93						
0.24–0.30	0.269	25.3	835.17	$\pm$	17.66	$\pm$ 40.36	0.271	34.9	1106.28	$\pm$	20.05	$\pm$ 48.75
0.30–0.36	0.329	25.5	660.90	$\pm$	15.88	$\pm$ 29.12	0.330	35.2	916.42	$\pm$	17.78	$\pm$ 34.52
0.36–0.42	0.391	25.5	474.29	$\pm$	13.40	$\pm$ 20.25	0.390	35.2	690.93	$\pm$	15.92	$\pm$ 24.74
0.42–0.50	0.459	25.6	332.14	$\pm$	9.83	$\pm$ 13.88	0.460	35.3	520.88	$\pm$	12.20	$\pm$ 18.48
0.50–0.60	0.548	25.5	230.57	$\pm$	7.18	$\pm$ 9.45	0.549	35.3	348.17	$\pm$	8.95	$\pm$ 13.83
0.60–0.72	0.657	25.4	146.01	$\pm$	5.20	$\pm$ 7.10	0.659	35.3	203.02	$\pm$	6.23	$\pm$ 10.13
0.72–0.90							0.803	35.2	106.33	$\pm$	3.64	$\pm$ 6.87

	$40 < \theta < 50$						$50 < \theta < 60$					
p_T	$\langle p_\mathrm{T}\rangle$	$\langle\theta\rangle$	$\mathrm{d}^2\sigma/\mathrm{d}p\mathrm{d}\Omega$				$\langle p_\mathrm{T}\rangle$	$\langle\theta\rangle$	$\mathrm{d}^2\sigma/\mathrm{d}p\mathrm{d}\Omega$			
0.30–0.36	0.331	45.1	1061.21	$\pm$	18.75	$\pm$ 34.55						
0.36–0.42	0.392	45.1	890.86	$\pm$	17.38	$\pm$ 25.51	0.391	55.2	931.12	$\pm$	16.89	$\pm$ 28.51
0.42–0.50	0.462	45.2	656.16	$\pm$	13.28	$\pm$ 19.63	0.462	55.0	752.30	$\pm$	13.80	$\pm$ 20.96
0.50–0.60	0.553	45.1	436.35	$\pm$	10.11	$\pm$ 17.48	0.553	55.0	508.84	$\pm$	10.54	$\pm$ 18.27
0.60–0.72	0.663	45.0	258.72	$\pm$	7.19	$\pm$ 13.97	0.663	55.0	291.74	$\pm$	7.64	$\pm$ 15.78
0.72–0.90	0.809	45.2	131.53	$\pm$	4.28	$\pm$ 9.66	0.810	55.0	129.63	$\pm$	4.20	$\pm$ 9.77
0.90–1.25	1.052	45.2	27.45	$\pm$	1.28	$\pm$ 3.36	1.051	55.2	27.64	$\pm$	1.31	$\pm$ 3.60

	$60 < \theta < 75$						$75 < \theta < 90$					
p_T	$\langle p_\mathrm{T}\rangle$	$\langle\theta\rangle$	$\mathrm{d}^2\sigma/\mathrm{d}p\mathrm{d}\Omega$				$\langle p_\mathrm{T}\rangle$	$\langle\theta\rangle$	$\mathrm{d}^2\sigma/\mathrm{d}p\mathrm{d}\Omega$			
0.50–0.60	0.555	67.4	508.18	$\pm$	8.16	$\pm$ 18.59						
0.60–0.72	0.667	67.4	286.56	$\pm$	5.92	$\pm$ 16.08	0.665	81.8	219.70	$\pm$	4.76	$\pm$ 15.58
0.72–0.90	0.816	67.2	125.46	$\pm$	3.38	$\pm$ 11.17	0.812	81.5	90.32	$\pm$	2.73	$\pm$ 9.09
0.90–1.25	1.062	67.2	23.07	$\pm$	1.03	$\pm$ 3.91						

	$90 < \theta < 105$						$105 < \theta < 125$					
p_T	$\langle p_\mathrm{T}\rangle$	$\langle\theta\rangle$	$\mathrm{d}^2\sigma/\mathrm{d}p\mathrm{d}\Omega$				$\langle p_\mathrm{T}\rangle$	$\langle\theta\rangle$	$\mathrm{d}^2\sigma/\mathrm{d}p\mathrm{d}\Omega$			
0.42–0.50							0.464	113.7	321.81	$\pm$	6.13	$\pm$ 17.24
0.50–0.60							0.550	112.8	148.88	$\pm$	3.74	$\pm$ 13.67
0.60–0.72	0.663	97.1	132.46	$\pm$	3.64	$\pm$ 11.93	0.662	112.9	46.40	$\pm$	2.10	$\pm$ 6.76
0.72–0.90	0.808	96.8	42.31	$\pm$	1.84	$\pm$ 4.98						

Table A.5: Double-differential inclusive cross-section $\mathrm{d}^2\sigma/\mathrm{d}p\mathrm{d}\Omega$ [mb/(GeV/c sr)] of the production of π^+'s in π^+ + Ta $\rightarrow \pi^+$ + X interactions with $+3.0$ GeV/c beam momentum; the first error is statistical, the second systematic; p_T in GeV/c, polar angle θ in degrees.

	$20 < \theta < 30$			$30 < \theta < 40$		
p_T	$\langle p_\mathrm{T}\rangle$	$\langle\theta\rangle$	$\mathrm{d}^2\sigma/\mathrm{d}p\mathrm{d}\Omega$	$\langle p_\mathrm{T}\rangle$	$\langle\theta\rangle$	$\mathrm{d}^2\sigma/\mathrm{d}p\mathrm{d}\Omega$
0.10–0.13	0.116	24.9	179.27 ± 12.88 ± 13.97	0.115	35.2	205.87 ± 13.25 ± 15.63
0.13–0.16	0.145	24.7	224.82 ± 13.81 ± 15.15	0.146	34.9	176.48 ± 11.15 ± 10.93
0.16–0.20	0.181	25.0	303.43 ± 13.25 ± 16.27	0.181	34.8	211.70 ± 10.38 ± 11.10
0.20–0.24	0.220	25.2	290.88 ± 12.44 ± 12.87	0.220	34.8	233.79 ± 11.05 ± 10.42
0.24–0.30	0.270	24.9	292.17 ± 10.22 ± 10.92	0.270	34.7	246.78 ± 9.33 ± 9.35
0.30–0.36	0.330	24.9	240.76 ± 9.13 ± 7.82	0.331	35.0	217.57 ± 8.56 ± 6.98
0.36–0.42	0.390	25.1	203.00 ± 8.40 ± 6.80	0.390	34.9	182.18 ± 7.91 ± 5.76
0.42–0.50	0.460	25.3	143.64 ± 6.01 ± 5.54	0.461	34.9	139.90 ± 5.99 ± 5.06
0.50–0.60	0.548	25.1	95.45 ± 4.19 ± 5.10	0.549	34.7	96.57 ± 4.22 ± 4.66
0.60–0.72	0.660	25.0	67.35 ± 3.27 ± 5.57	0.661	35.0	65.95 ± 3.15 ± 4.77
0.72–0.90				0.803	34.9	35.15 ± 1.86 ± 4.17

	$40 < \theta < 50$			$50 < \theta < 60$		
p_T	$\langle p_\mathrm{T}\rangle$	$\langle\theta\rangle$	$\mathrm{d}^2\sigma/\mathrm{d}p\mathrm{d}\Omega$	$\langle p_\mathrm{T}\rangle$	$\langle\theta\rangle$	$\mathrm{d}^2\sigma/\mathrm{d}p\mathrm{d}\Omega$
0.10–0.13	0.115	45.1	210.79 ± 14.59 ± 16.77			
0.13–0.16	0.145	44.8	227.31 ± 12.69 ± 13.80	0.145	55.2	209.81 ± 12.41 ± 13.16
0.16–0.20	0.180	45.0	226.16 ± 10.97 ± 11.67	0.180	54.9	240.62 ± 11.29 ± 12.09
0.20–0.24	0.221	45.2	195.21 ± 9.88 ± 8.87	0.220	54.8	184.29 ± 9.74 ± 8.16
0.24–0.30	0.270	44.8	192.67 ± 8.17 ± 7.15	0.272	54.7	165.95 ± 7.46 ± 5.99
0.30–0.36	0.331	44.9	178.82 ± 7.81 ± 5.80	0.331	54.8	156.16 ± 7.38 ± 5.12
0.36–0.42	0.391	44.7	150.14 ± 7.15 ± 4.86	0.390	55.0	125.57 ± 6.78 ± 4.75
0.42–0.50	0.463	44.8	124.08 ± 5.80 ± 4.93	0.463	54.8	103.41 ± 5.34 ± 4.46
0.50–0.60	0.553	44.8	89.94 ± 4.26 ± 4.24	0.553	54.9	77.05 ± 4.08 ± 4.12
0.60–0.72	0.665	44.6	60.53 ± 3.19 ± 4.26	0.665	54.7	54.31 ± 3.08 ± 3.99
0.72–0.90	0.809	44.6	26.52 ± 1.63 ± 2.78	0.804	54.7	25.19 ± 1.67 ± 2.66
0.90–1.25				1.050	54.7	6.56 ± 0.51 ± 1.06

	$60 < \theta < 75$			$75 < \theta < 90$		
p_T	$\langle p_\mathrm{T}\rangle$	$\langle\theta\rangle$	$\mathrm{d}^2\sigma/\mathrm{d}p\mathrm{d}\Omega$	$\langle p_\mathrm{T}\rangle$	$\langle\theta\rangle$	$\mathrm{d}^2\sigma/\mathrm{d}p\mathrm{d}\Omega$
0.13–0.16	0.146	67.2	245.29 ± 13.37 ± 20.12			
0.16–0.20	0.182	67.3	200.76 ± 8.45 ± 9.91	0.182	81.9	203.35 ± 10.24 ± 15.27
0.20–0.24	0.222	67.6	182.36 ± 8.00 ± 7.60	0.221	81.8	176.41 ± 8.57 ± 9.48
0.24–0.30	0.271	67.2	155.05 ± 6.04 ± 5.52	0.271	82.1	128.06 ± 5.94 ± 6.91
0.30–0.36	0.332	66.9	115.21 ± 5.24 ± 3.83	0.332	82.0	93.11 ± 5.12 ± 5.45
0.36–0.42	0.394	66.9	99.86 ± 4.97 ± 4.02	0.394	81.9	64.40 ± 4.14 ± 3.46
0.42–0.50	0.465	67.0	77.00 ± 3.76 ± 3.68	0.465	82.0	52.04 ± 3.24 ± 3.44
0.50–0.60	0.555	67.0	57.95 ± 2.92 ± 3.68	0.556	81.5	40.97 ± 2.60 ± 3.58
0.60–0.72	0.667	66.3	35.66 ± 2.07 ± 3.10	0.665	81.4	20.83 ± 1.63 ± 2.22
0.72–0.90	0.814	66.7	16.58 ± 1.11 ± 1.99	0.812	81.5	7.48 ± 0.72 ± 1.05
0.90–1.25	1.057	66.8	3.39 ± 0.29 ± 0.63	1.081	81.8	1.59 ± 0.19 ± 0.36

	$90 < \theta < 105$			$105 < \theta < 125$		
p_T	$\langle p_\mathrm{T}\rangle$	$\langle\theta\rangle$	$\mathrm{d}^2\sigma/\mathrm{d}p\mathrm{d}\Omega$	$\langle p_\mathrm{T}\rangle$	$\langle\theta\rangle$	$\mathrm{d}^2\sigma/\mathrm{d}p\mathrm{d}\Omega$
0.13–0.16				0.146	115.1	207.22 ± 10.40 ± 11.75
0.16–0.20	0.181	98.1	177.78 ± 9.55 ± 12.57	0.180	114.7	154.18 ± 6.58 ± 5.74
0.20–0.24	0.221	98.0	168.72 ± 8.73 ± 10.50	0.220	113.9	112.63 ± 5.57 ± 4.05
0.24–0.30	0.269	97.4	109.90 ± 5.45 ± 5.39	0.270	114.2	61.23 ± 3.23 ± 2.65
0.30–0.36	0.332	97.0	60.96 ± 4.02 ± 3.22	0.331	114.3	39.40 ± 2.68 ± 2.38
0.36–0.42	0.393	97.0	48.69 ± 3.62 ± 3.27	0.394	113.4	35.26 ± 2.65 ± 2.99
0.42–0.50	0.465	96.5	38.59 ± 2.86 ± 3.50	0.464	112.5	16.61 ± 1.51 ± 1.75
0.50–0.60	0.550	96.9	21.01 ± 1.80 ± 2.26	0.554	112.7	7.27 ± 0.87 ± 1.02
0.60–0.72	0.673	96.8	6.92 ± 0.89 ± 0.98	0.665	112.0	1.91 ± 0.36 ± 0.38
0.72–0.90	0.805	96.5	2.82 ± 0.41 ± 0.55	0.818	112.2	0.19 ± 0.06 ± 0.06
0.90–1.25	1.042	94.4	0.17 ± 0.04 ± 0.06			

Table A.6: Double-differential inclusive cross-section $\mathrm{d}^2\sigma/\mathrm{d}p\mathrm{d}\Omega$ [mb/(GeV/c sr)] of the production of π^-'s in π^+ + Ta $\rightarrow$ π^- + X interactions with $+3.0$ GeV/c beam momentum; the first error is statistical, the second systematic; p_T in GeV/c, polar angle θ in degrees.

	$20 < \theta < 30$			$30 < \theta < 40$		
p_T	$\langle p_\mathrm{T}\rangle$	$\langle\theta\rangle$	$\mathrm{d}^2\sigma/\mathrm{d}p\mathrm{d}\Omega$	$\langle p_\mathrm{T}\rangle$	$\langle\theta\rangle$	$\mathrm{d}^2\sigma/\mathrm{d}p\mathrm{d}\Omega$
0.10–0.13	0.115	24.9	212.60 ± 13.59 ± 16.32	0.114	35.3	218.69 ± 13.15 ± 17.04
0.13–0.16	0.144	25.3	207.46 ± 12.50 ± 13.17	0.144	35.0	212.85 ± 12.17 ± 13.52
0.16–0.20	0.180	25.1	261.45 ± 12.08 ± 13.98	0.180	35.0	204.29 ± 10.19 ± 10.76
0.20–0.24	0.220	24.9	253.62 ± 11.72 ± 11.83	0.220	34.9	223.18 ± 10.81 ± 10.26
0.24–0.30	0.268	25.2	194.95 ± 8.38 ± 7.29	0.268	35.0	183.24 ± 7.94 ± 6.73
0.30–0.36	0.327	25.1	164.85 ± 7.83 ± 6.21	0.328	35.0	147.08 ± 7.08 ± 4.77
0.36–0.42	0.385	25.4	111.56 ± 6.22 ± 3.90	0.387	35.1	109.17 ± 6.03 ± 3.76
0.42–0.50	0.456	25.3	79.76 ± 4.63 ± 3.40	0.454	34.9	81.87 ± 4.65 ± 3.47
0.50–0.60	0.541	25.3	44.68 ± 3.08 ± 2.55	0.543	34.9	53.64 ± 3.39 ± 2.99
0.60–0.72	0.644	25.3	22.77 ± 2.04 ± 1.80	0.647	34.6	22.87 ± 1.97 ± 1.72
0.72–0.90				0.789	35.2	8.80 ± 1.06 ± 0.95

	$40 < \theta < 50$			$50 < \theta < 60$		
p_T	$\langle p_\mathrm{T}\rangle$	$\langle\theta\rangle$	$\mathrm{d}^2\sigma/\mathrm{d}p\mathrm{d}\Omega$	$\langle p_\mathrm{T}\rangle$	$\langle\theta\rangle$	$\mathrm{d}^2\sigma/\mathrm{d}p\mathrm{d}\Omega$
0.10–0.13	0.115	45.3	262.44 ± 15.55 ± 20.73			
0.13–0.16	0.144	45.0	224.32 ± 12.65 ± 14.06	0.145	55.1	248.91 ± 13.81 ± 15.83
0.16–0.20	0.179	45.0	194.47 ± 9.68 ± 10.31	0.179	54.6	173.88 ± 9.29 ± 8.99
0.20–0.24	0.218	45.0	196.73 ± 10.14 ± 9.74	0.218	55.1	150.80 ± 8.64 ± 6.78
0.24–0.30	0.266	44.8	160.11 ± 7.28 ± 5.84	0.268	54.6	142.20 ± 6.93 ± 5.49
0.30–0.36	0.326	45.0	143.74 ± 6.94 ± 4.68	0.326	54.7	111.67 ± 6.12 ± 3.72
0.36–0.42	0.385	44.9	102.88 ± 5.93 ± 3.63	0.385	54.8	89.01 ± 5.49 ± 3.27
0.42–0.50	0.453	44.8	81.96 ± 4.63 ± 3.45	0.453	54.6	77.58 ± 4.65 ± 3.87
0.50–0.60	0.536	45.0	44.21 ± 3.05 ± 2.52	0.540	54.6	39.86 ± 2.84 ± 2.35
0.60–0.72	0.646	44.8	29.45 ± 2.34 ± 2.42	0.646	54.8	19.32 ± 1.91 ± 1.64
0.72–0.90	0.781	44.6	9.05 ± 1.02 ± 1.00	0.788	54.8	7.74 ± 0.95 ± 0.88
0.90–1.25				0.995	54.6	1.55 ± 0.25 ± 0.29

	$60 < \theta < 75$			$75 < \theta < 90$		
p_T	$\langle p_\mathrm{T}\rangle$	$\langle\theta\rangle$	$\mathrm{d}^2\sigma/\mathrm{d}p\mathrm{d}\Omega$	$\langle p_\mathrm{T}\rangle$	$\langle\theta\rangle$	$\mathrm{d}^2\sigma/\mathrm{d}p\mathrm{d}\Omega$
0.13–0.16	0.145	67.2	250.72 ± 13.07 ± 16.69	0.147	81.3	232.77 ± 30.80 ± 78.08
0.16–0.20	0.178	67.3	177.06 ± 7.93 ± 8.39	0.180	81.9	215.18 ± 11.16 ± 21.35
0.20–0.24	0.218	67.5	156.50 ± 7.47 ± 6.67	0.218	82.3	143.43 ± 7.69 ± 7.36
0.24–0.30	0.265	67.1	105.76 ± 4.84 ± 3.60	0.265	82.2	90.71 ± 5.01 ± 5.23
0.30–0.36	0.326	67.2	86.15 ± 4.47 ± 2.97	0.323	81.7	71.50 ± 4.47 ± 4.53
0.36–0.42	0.383	67.2	73.51 ± 4.27 ± 3.29	0.384	82.1	48.88 ± 3.66 ± 3.12
0.42–0.50	0.451	67.1	58.30 ± 3.30 ± 3.13	0.453	81.8	39.42 ± 2.81 ± 2.85
0.50–0.60	0.535	67.6	34.36 ± 2.25 ± 2.35	0.537	81.4	23.84 ± 1.92 ± 2.11
0.60–0.72	0.640	67.2	15.36 ± 1.37 ± 1.40	0.639	82.2	9.84 ± 1.09 ± 1.12
0.72–0.90	0.771	67.4	5.54 ± 0.65 ± 0.69	0.761	81.5	3.59 ± 0.51 ± 0.56
0.90–1.25	0.983	65.9	1.10 ± 0.18 ± 0.22	0.973	81.2	0.28 ± 0.07 ± 0.08

	$90 < \theta < 105$			$105 < \theta < 125$		
p_T	$\langle p_\mathrm{T}\rangle$	$\langle\theta\rangle$	$\mathrm{d}^2\sigma/\mathrm{d}p\mathrm{d}\Omega$	$\langle p_\mathrm{T}\rangle$	$\langle\theta\rangle$	$\mathrm{d}^2\sigma/\mathrm{d}p\mathrm{d}\Omega$
0.13–0.16				0.143	113.9	224.68 ± 26.89 ± 13.61
0.16–0.20	0.178	98.2	184.45 ± 11.40 ± 19.79	0.177	114.6	119.46 ± 5.88 ± 4.58
0.20–0.24	0.217	97.3	122.72 ± 7.37 ± 7.53	0.217	113.8	73.48 ± 4.71 ± 3.54
0.24–0.30	0.264	97.3	72.61 ± 4.41 ± 3.57	0.266	114.4	46.32 ± 2.88 ± 2.33
0.30–0.36	0.321	97.4	42.95 ± 3.40 ± 2.65	0.324	114.8	29.57 ± 2.31 ± 2.09
0.36–0.42	0.381	97.5	32.78 ± 2.93 ± 2.39	0.384	113.6	19.64 ± 1.89 ± 1.85
0.42–0.50	0.452	96.9	27.34 ± 2.39 ± 2.70	0.447	114.1	12.84 ± 1.30 ± 1.57
0.50–0.60	0.533	96.4	16.03 ± 1.57 ± 1.93	0.532	111.5	4.03 ± 0.61 ± 0.67
0.60–0.72	0.635	97.3	5.11 ± 0.78 ± 0.82	0.642	111.6	1.54 ± 0.30 ± 0.37
0.72–0.90	0.765	97.4	0.92 ± 0.22 ± 0.22	0.806	112.8	0.17 ± 0.08 ± 0.06
0.90–1.25	1.052	97.4	0.05 ± 0.03 ± 0.02			

Table A.7: Double-differential inclusive cross-section $\mathrm{d}^2\sigma/\mathrm{d}p\mathrm{d}\Omega$ [mb/(GeV/c sr)] of the production of protons in π^- + Ta $\rightarrow$ p + X interactions with -3.0 GeV/c beam momentum; the first error is statistical, the second systematic; p_T in GeV/c, polar angle θ in degrees.

	$20 < \theta < 30$					$30 < \theta < 40$				
p_T	$\langle p_\mathrm{T}\rangle$	$\langle\theta\rangle$	$\mathrm{d}^2\sigma/\mathrm{d}p\mathrm{d}\Omega$			$\langle p_\mathrm{T}\rangle$	$\langle\theta\rangle$	$\mathrm{d}^2\sigma/\mathrm{d}p\mathrm{d}\Omega$		
0.20–0.24	0.220	25.3	858.52 ± 27.63	±	82.96					
0.24–0.30	0.269	25.5	739.97 ± 20.06	±	61.03	0.271	35.1	953.68 ± 22.82	±	71.38
0.30–0.36	0.328	25.3	564.01 ± 17.63	±	37.86	0.329	35.2	803.47 ± 20.45	±	47.24
0.36–0.42	0.389	25.4	391.13 ± 14.80	±	20.94	0.389	35.3	629.02 ± 18.41	±	28.29
0.42–0.50	0.458	25.4	284.31 ± 10.68	±	11.62	0.458	35.3	457.96 ± 13.75	±	15.45
0.50–0.60	0.546	25.6	200.78 ± 8.21	±	7.64	0.546	35.3	301.99 ± 10.00	±	11.01
0.60–0.72	0.652	25.7	119.51 ± 5.71	±	6.52	0.657	35.1	178.74 ± 6.97	±	10.40
0.72–0.90						0.799	35.0	84.25 ± 3.92	±	8.29

	$40 < \theta < 50$					$50 < \theta < 60$				
p_T	$\langle p_\mathrm{T}\rangle$	$\langle\theta\rangle$	$\mathrm{d}^2\sigma/\mathrm{d}p\mathrm{d}\Omega$			$\langle p_\mathrm{T}\rangle$	$\langle\theta\rangle$	$\mathrm{d}^2\sigma/\mathrm{d}p\mathrm{d}\Omega$		
0.30–0.36	0.329	45.1	954.12 ± 21.69	±	41.81					
0.36–0.42	0.388	45.2	818.51 ± 20.17	±	26.76	0.389	55.3	821.62 ± 19.31	±	26.24
0.42–0.50	0.458	45.1	577.81 ± 14.97	±	16.06	0.458	55.2	633.88 ± 15.28	±	19.47
0.50–0.60	0.546	45.2	399.89 ± 11.53	±	16.12	0.545	55.0	426.34 ± 11.56	±	20.55
0.60–0.72	0.656	45.2	244.70 ± 8.39	±	16.17	0.654	55.1	264.32 ± 8.70	±	20.46
0.72–0.90	0.795	45.1	105.00 ± 4.42	±	11.05	0.799	55.0	114.35 ± 4.65	±	13.33
0.90–1.25	1.039	45.1	26.50 ± 1.57	±	4.85	1.026	55.1	24.20 ± 1.45	±	4.76

	$60 < \theta < 75$					$75 < \theta < 90$				
p_T	$\langle p_\mathrm{T}\rangle$	$\langle\theta\rangle$	$\mathrm{d}^2\sigma/\mathrm{d}p\mathrm{d}\Omega$			$\langle p_\mathrm{T}\rangle$	$\langle\theta\rangle$	$\mathrm{d}^2\sigma/\mathrm{d}p\mathrm{d}\Omega$		
0.50–0.60	0.541	67.7	440.45 ± 9.25	±	24.97					
0.60–0.72	0.649	67.4	250.36 ± 6.70	±	24.44	0.647	81.9	200.69 ± 5.61	±	26.63
0.72–0.90	0.790	67.0	107.39 ± 3.71	±	16.85	0.789	82.0	73.84 ± 2.95	±	14.17
0.90–1.25	1.018	66.6	20.10 ± 1.10	±	5.37	1.014	81.4	10.45 ± 0.81	±	3.20

	$90 < \theta < 105$					$105 < \theta < 125$				
p_T	$\langle p_\mathrm{T}\rangle$	$\langle\theta\rangle$	$\mathrm{d}^2\sigma/\mathrm{d}p\mathrm{d}\Omega$			$\langle p_\mathrm{T}\rangle$	$\langle\theta\rangle$	$\mathrm{d}^2\sigma/\mathrm{d}p\mathrm{d}\Omega$		
0.42–0.50						0.457	114.4	277.17 ± 7.03	±	25.58
0.50–0.60						0.539	113.0	133.33 ± 4.30	±	23.11
0.60–0.72	0.648	97.5	117.27 ± 4.19	±	19.95	0.648	112.9	54.35 ± 2.67	±	14.85
0.72–0.90	0.789	97.4	40.90 ± 2.22	±	9.14	0.781	112.6	11.92 ± 1.13	±	5.00

Table A.8: Double-differential inclusive cross-section $\mathrm{d}^2\sigma/\mathrm{d}p\mathrm{d}\Omega$ [mb/(GeV/c sr)] of the production of π^+'s in π^- + Ta $\rightarrow$ π^+ + X interactions with -3.0 GeV/c beam momentum; the first error is statistical, the second systematic; p_T in GeV/c, polar angle θ in degrees.

	$20 < \theta < 30$					$30 < \theta < 40$				
p_T	$\langle p_\mathrm{T}\rangle$	$\langle\theta\rangle$	$\mathrm{d}^2\sigma/\mathrm{d}p\mathrm{d}\Omega$			$\langle p_\mathrm{T}\rangle$	$\langle\theta\rangle$	$\mathrm{d}^2\sigma/\mathrm{d}p\mathrm{d}\Omega$		
0.10–0.13	0.116	24.8	187.11 ± 15.88	±	21.39	0.116	35.2	202.30 ± 15.75	±	22.25
0.13–0.16	0.145	25.0	191.81 ± 15.20	±	19.04	0.144	35.2	169.53 ± 13.10	±	15.98
0.16–0.20	0.180	25.3	207.74 ± 12.55	±	16.73	0.180	34.9	178.16 ± 11.29	±	14.14
0.20–0.24	0.219	25.1	221.54 ± 13.27	±	15.57	0.221	34.7	199.42 ± 12.65	±	14.22
0.24–0.30	0.269	25.1	211.10 ± 10.49	±	11.19	0.269	35.2	172.68 ± 9.31	±	8.53
0.30–0.36	0.331	25.1	174.07 ± 9.45	±	6.78	0.330	34.4	145.10 ± 8.43	±	5.29
0.36–0.42	0.389	25.1	121.61 ± 7.80	±	4.22	0.389	34.9	114.74 ± 7.48	±	3.88
0.42–0.50	0.460	25.1	83.54 ± 5.51	±	3.83	0.458	34.7	94.51 ± 5.89	±	4.24
0.50–0.60	0.544	25.0	61.91 ± 4.21	±	4.67	0.549	35.1	55.24 ± 4.02	±	4.10
0.60–0.72	0.657	25.4	29.53 ± 2.45	±	3.41	0.656	34.4	27.97 ± 2.36	±	3.16
0.72–0.90						0.798	34.6	14.17 ± 1.38	±	2.52

	$40 < \theta < 50$					$50 < \theta < 60$				
p_T	$\langle p_\mathrm{T}\rangle$	$\langle\theta\rangle$	$\mathrm{d}^2\sigma/\mathrm{d}p\mathrm{d}\Omega$			$\langle p_\mathrm{T}\rangle$	$\langle\theta\rangle$	$\mathrm{d}^2\sigma/\mathrm{d}p\mathrm{d}\Omega$		
0.10–0.13	0.115	44.9	207.70 ± 17.97	±	24.27					
0.13–0.16	0.145	44.7	166.64 ± 12.86	±	15.62	0.146	55.0	158.29 ± 12.96	±	14.62
0.16–0.20	0.180	45.5	165.52 ± 10.94	±	13.13	0.179	55.0	180.95 ± 11.66	±	13.73
0.20–0.24	0.220	44.9	160.05 ± 10.53	±	10.53	0.222	54.9	117.54 ± 9.04	±	7.33
0.24–0.30	0.270	44.7	144.89 ± 8.53	±	7.29	0.267	54.8	118.33 ± 7.58	±	5.45
0.30–0.36	0.330	45.0	131.13 ± 8.16	±	4.91	0.330	54.6	96.20 ± 6.94	±	3.48
0.36–0.42	0.391	44.9	103.82 ± 7.16	±	3.64	0.389	54.9	93.92 ± 7.01	±	3.95
0.42–0.50	0.456	45.1	88.21 ± 5.93	±	4.61	0.458	55.0	74.54 ± 5.41	±	4.33
0.50–0.60	0.547	44.7	49.00 ± 3.79	±	3.73	0.545	54.8	48.94 ± 3.91	±	4.31
0.60–0.72	0.650	44.3	26.20 ± 2.41	±	3.01	0.653	55.0	29.29 ± 2.59	±	3.72
0.72–0.90	0.799	44.9	13.26 ± 1.33	±	2.30	0.792	54.7	11.62 ± 1.31	±	2.16
0.90–1.25						1.028	54.8	2.63 ± 0.36	±	0.78

	$60 < \theta < 75$					$75 < \theta < 90$				
p_T	$\langle p_\mathrm{T}\rangle$	$\langle\theta\rangle$	$\mathrm{d}^2\sigma/\mathrm{d}p\mathrm{d}\Omega$			$\langle p_\mathrm{T}\rangle$	$\langle\theta\rangle$	$\mathrm{d}^2\sigma/\mathrm{d}p\mathrm{d}\Omega$		
0.13–0.16	0.146	67.3	166.02 ± 13.12	±	17.25	0.148	82.0	154.52 ± 28.69	±	54.88
0.16–0.20	0.180	66.8	170.09 ± 9.49	±	12.86	0.181	81.6	165.04 ± 11.77	±	18.59
0.20–0.24	0.219	67.5	144.14 ± 8.73	±	8.75	0.218	81.8	112.47 ± 8.06	±	6.48
0.24–0.30	0.269	67.0	100.88 ± 5.86	±	4.37	0.269	82.0	109.60 ± 6.72	±	6.30
0.30–0.36	0.328	67.0	89.91 ± 5.65	±	3.58	0.325	81.9	67.37 ± 5.33	±	4.62
0.36–0.42	0.389	67.2	72.44 ± 4.99	±	3.36	0.390	81.6	46.84 ± 4.33	±	3.65
0.42–0.50	0.457	67.2	51.94 ± 3.77	±	3.85	0.456	81.8	32.55 ± 2.99	±	3.18
0.50–0.60	0.543	66.3	34.12 ± 2.61	±	3.68	0.539	82.0	27.01 ± 2.45	±	3.78
0.60–0.72	0.648	67.0	16.08 ± 1.59	±	2.51	0.648	81.6	12.89 ± 1.55	±	2.53
0.72–0.90	0.796	67.1	8.34 ± 0.90	±	1.87	0.792	81.4	3.77 ± 0.60	±	1.02
0.90–1.25	1.023	66.6	1.34 ± 0.20	±	0.47	0.980	80.9	0.44 ± 0.10	±	0.19

	$90 < \theta < 105$					$105 < \theta < 125$				
p_T	$\langle p_\mathrm{T}\rangle$	$\langle\theta\rangle$	$\mathrm{d}^2\sigma/\mathrm{d}p\mathrm{d}\Omega$			$\langle p_\mathrm{T}\rangle$	$\langle\theta\rangle$	$\mathrm{d}^2\sigma/\mathrm{d}p\mathrm{d}\Omega$		
0.13–0.16	0.149	98.0	109.74 ± 17.20	±	29.49	0.144	115.1	163.50 ± 11.25	±	11.50
0.16–0.20	0.179	98.0	133.60 ± 10.43	±	12.53	0.179	114.6	112.59 ± 7.04	±	4.65
0.20–0.24	0.218	97.1	121.50 ± 8.71	±	6.55	0.219	114.4	71.80 ± 5.38	±	2.98
0.24–0.30	0.268	97.3	82.34 ± 5.75	±	4.28	0.265	113.5	45.14 ± 3.47	±	2.91
0.30–0.36	0.325	97.4	49.53 ± 4.35	±	3.47	0.326	114.3	26.73 ± 2.62	±	2.80
0.36–0.42	0.389	97.0	42.08 ± 3.85	±	4.24	0.386	113.4	17.47 ± 2.23	±	2.61
0.42–0.50	0.455	96.8	23.82 ± 2.59	±	3.46	0.453	112.6	12.62 ± 1.58	±	2.53
0.50–0.60	0.545	97.6	13.99 ± 1.79	±	2.85	0.545	114.1	4.99 ± 0.82	±	1.34
0.60–0.72	0.646	96.3	5.98 ± 0.97	±	1.63	0.638	111.7	1.19 ± 0.28	±	0.45
0.72–0.90	0.788	96.9	0.79 ± 0.23	±	0.30	0.772	114.0	0.45 ± 0.16	±	0.23
0.90–1.25	0.999	99.2	0.14 ± 0.05	±	0.09					

Table A.9: Double-differential inclusive cross-section $\mathrm{d}^2\sigma/\mathrm{d}p\mathrm{d}\Omega$ [mb/(GeV/c sr)] of the production of π^-'s in π^- + Ta $\rightarrow \pi^-$ + X interactions with -3.0 GeV/c beam momentum; the first error is statistical, the second systematic; p_T in GeV/c, polar angle θ in degrees.

	$20 < \theta < 30$					$30 < \theta < 40$				
p_T	$\langle p_\mathrm{T}\rangle$	$\langle\theta\rangle$	$\mathrm{d}^2\sigma/\mathrm{d}p\mathrm{d}\Omega$			$\langle p_\mathrm{T}\rangle$	$\langle\theta\rangle$	$\mathrm{d}^2\sigma/\mathrm{d}p\mathrm{d}\Omega$		
0.10–0.13	0.116	24.4	270.77 ± 18.51	±	30.56	0.114	34.9	330.03 ± 20.73	±	37.62
0.13–0.16	0.146	25.1	368.02 ± 21.48	±	36.87	0.146	34.7	316.66 ± 18.26	±	30.47
0.16–0.20	0.179	24.7	391.34 ± 18.20	±	31.77	0.181	34.9	322.45 ± 15.93	±	25.79
0.20–0.24	0.220	24.9	398.28 ± 17.90	±	25.28	0.220	34.9	368.95 ± 17.07	±	23.59
0.24–0.30	0.270	25.2	334.52 ± 13.52	±	15.47	0.270	34.9	322.74 ± 12.90	±	14.73
0.30–0.36	0.330	25.3	276.31 ± 12.33	±	9.27	0.329	35.1	254.73 ± 11.49	±	7.99
0.36–0.42	0.390	25.4	190.82 ± 10.15	±	6.73	0.388	34.9	198.33 ± 10.14	±	6.70
0.42–0.50	0.458	25.1	148.68 ± 7.69	±	8.31	0.457	35.0	149.19 ± 7.66	±	7.89
0.50–0.60	0.548	25.1	76.93 ± 4.93	±	6.95	0.546	34.9	82.30 ± 5.02	±	7.08
0.60–0.72	0.653	25.1	51.06 ± 3.84	±	7.03	0.653	35.0	61.12 ± 4.08	±	7.95
0.72–0.90						0.799	35.3	29.16 ± 2.41	±	5.62

	$40 < \theta < 50$					$50 < \theta < 60$				
p_T	$\langle p_\mathrm{T}\rangle$	$\langle\theta\rangle$	$\mathrm{d}^2\sigma/\mathrm{d}p\mathrm{d}\Omega$			$\langle p_\mathrm{T}\rangle$	$\langle\theta\rangle$	$\mathrm{d}^2\sigma/\mathrm{d}p\mathrm{d}\Omega$		
0.10–0.13	0.115	45.4	424.11 ± 26.18	±	50.06					
0.13–0.16	0.145	45.2	345.99 ± 19.87	±	33.40	0.145	55.3	279.17 ± 18.18	±	26.28
0.16–0.20	0.180	45.3	292.53 ± 15.25	±	23.47	0.179	54.9	271.30 ± 14.37	±	20.74
0.20–0.24	0.220	44.9	296.61 ± 15.15	±	19.04	0.219	55.0	239.20 ± 13.79	±	14.55
0.24–0.30	0.270	45.1	262.35 ± 11.74	±	11.78	0.269	54.8	221.53 ± 10.78	±	9.52
0.30–0.36	0.328	44.8	233.62 ± 10.97	±	7.24	0.330	55.0	177.80 ± 9.77	±	5.89
0.36–0.42	0.387	44.6	169.73 ± 9.31	±	6.09	0.389	55.1	149.56 ± 9.02	±	6.27
0.42–0.50	0.456	44.8	144.27 ± 7.66	±	8.48	0.458	54.5	126.28 ± 7.21	±	8.12
0.50–0.60	0.547	45.2	102.83 ± 5.73	±	9.53	0.547	54.7	78.12 ± 4.96	±	7.59
0.60–0.72	0.660	45.3	60.93 ± 4.11	±	8.48	0.655	55.1	42.25 ± 3.44	±	6.10
0.72–0.90	0.797	44.8	29.23 ± 2.32	±	5.91	0.795	54.5	18.41 ± 1.85	±	3.81
0.90–1.25						1.030	55.1	3.92 ± 0.54	±	1.26

	$60 < \theta < 75$					$75 < \theta < 90$				
p_T	$\langle p_\mathrm{T}\rangle$	$\langle\theta\rangle$	$\mathrm{d}^2\sigma/\mathrm{d}p\mathrm{d}\Omega$			$\langle p_\mathrm{T}\rangle$	$\langle\theta\rangle$	$\mathrm{d}^2\sigma/\mathrm{d}p\mathrm{d}\Omega$		
0.13–0.16	0.146	67.2	360.65 ± 20.43	±	38.31	0.145	81.1	396.47 ± 79.47	±	149.22
0.16–0.20	0.180	67.3	316.17 ± 13.63	±	22.01	0.180	81.8	319.21 ± 17.52	±	35.25
0.20–0.24	0.219	66.9	227.52 ± 10.98	±	11.86	0.220	82.1	193.01 ± 11.00	±	10.65
0.24–0.30	0.270	66.8	180.06 ± 8.02	±	6.71	0.268	81.7	131.11 ± 7.28	±	6.16
0.30–0.36	0.330	67.3	135.26 ± 7.09	±	5.19	0.330	82.2	119.64 ± 7.12	±	7.93
0.36–0.42	0.391	66.6	116.99 ± 6.49	±	5.82	0.390	81.5	88.07 ± 6.01	±	7.20
0.42–0.50	0.458	67.0	92.06 ± 5.13	±	7.35	0.463	81.8	64.14 ± 4.46	±	7.28
0.50–0.60	0.551	66.5	61.50 ± 3.69	±	7.13	0.545	82.0	44.25 ± 3.24	±	6.82
0.60–0.72	0.652	66.9	37.16 ± 2.68	±	6.16	0.656	82.0	19.57 ± 1.97	±	4.12
0.72–0.90	0.806	67.3	16.81 ± 1.44	±	3.89	0.798	80.9	6.53 ± 0.84	±	1.88
0.90–1.25	1.022	66.3	2.16 ± 0.31	±	0.76	1.031	81.5	1.14 ± 0.20	±	0.50

	$90 < \theta < 105$					$105 < \theta < 125$				
p_T	$\langle p_\mathrm{T}\rangle$	$\langle\theta\rangle$	$\mathrm{d}^2\sigma/\mathrm{d}p\mathrm{d}\Omega$			$\langle p_\mathrm{T}\rangle$	$\langle\theta\rangle$	$\mathrm{d}^2\sigma/\mathrm{d}p\mathrm{d}\Omega$		
0.13–0.16						0.142	113.1	383.64 ± 50.84	±	33.04
0.16–0.20	0.181	97.9	265.44 ± 15.04	±	24.15	0.178	114.3	181.68 ± 9.27	±	7.41
0.20–0.24	0.218	97.8	142.91 ± 9.44	±	6.67	0.219	113.9	106.45 ± 6.86	±	5.06
0.24–0.30	0.267	97.3	114.71 ± 7.04	±	7.21	0.268	114.1	67.13 ± 4.31	±	5.11
0.30–0.36	0.328	97.1	74.54 ± 5.53	±	6.07	0.327	113.3	42.60 ± 3.43	±	5.21
0.36–0.42	0.390	97.1	60.55 ± 4.93	±	7.03	0.391	114.0	28.15 ± 2.80	±	4.81
0.42–0.50	0.460	97.2	41.54 ± 3.60	±	6.82	0.458	112.7	18.85 ± 1.95	±	4.29
0.50–0.60	0.545	97.2	19.23 ± 2.12	±	4.27	0.537	112.0	7.01 ± 1.03	±	2.12
0.60–0.72	0.655	96.3	8.00 ± 1.18	±	2.38	0.640	112.4	1.38 ± 0.38	±	0.55
0.72–0.90	0.786	96.1	2.29 ± 0.42	±	0.94	0.784	108.5	0.24 ± 0.11	±	0.13
0.90–1.25	0.991	95.5	0.13 ± 0.05	±	0.08					

Table A.10: Double-differential inclusive cross-section $\mathrm{d}^2\sigma/\mathrm{d}p\mathrm{d}\Omega$ [mb/(GeV/c sr)] of the production of protons in p + Ta $\rightarrow$ p + X interactions with $+5.0$ GeV/c beam momentum; the first error is statistical, the second systematic; p_T in GeV/c, polar angle θ in degrees.

	$20 < \theta < 30$					$30 < \theta < 40$				
p_T	$\langle p_\mathrm{T}\rangle$	$\langle\theta\rangle$	$\mathrm{d}^2\sigma/\mathrm{d}p\mathrm{d}\Omega$			$\langle p_\mathrm{T}\rangle$	$\langle\theta\rangle$	$\mathrm{d}^2\sigma/\mathrm{d}p\mathrm{d}\Omega$		
0.20–0.24	0.221	25.1	1423.27	± 32.37	± 80.07					
0.24–0.30	0.269	25.3	1164.94	± 22.95	± 57.39	0.271	34.9	1334.11	± 24.05	± 58.24
0.30–0.36	0.329	25.4	902.05	± 20.41	± 43.52	0.329	35.1	1237.17	± 22.78	± 46.64
0.36–0.42	0.389	25.4	690.09	± 17.95	± 31.57	0.389	35.1	951.98	± 20.58	± 36.12
0.42–0.50	0.458	25.3	515.66	± 13.51	± 24.54	0.458	35.2	683.50	± 15.55	± 29.78
0.50–0.60	0.546	25.3	364.88	± 10.03	± 17.17	0.546	35.2	512.08	± 12.19	± 24.18
0.60–0.72	0.655	25.3	240.75	± 7.33	± 12.27	0.656	35.3	305.07	± 8.54	± 17.88
0.72–0.90						0.800	35.2	170.04	± 5.16	± 11.89

	$40 < \theta < 50$					$50 < \theta < 60$				
p_T	$\langle p_\mathrm{T}\rangle$	$\langle\theta\rangle$	$\mathrm{d}^2\sigma/\mathrm{d}p\mathrm{d}\Omega$			$\langle p_\mathrm{T}\rangle$	$\langle\theta\rangle$	$\mathrm{d}^2\sigma/\mathrm{d}p\mathrm{d}\Omega$		
0.30–0.36	0.331	45.1	1332.60	± 22.94	± 41.93					
0.36–0.42	0.392	45.2	1123.91	± 21.47	± 32.02	0.391	55.1	1194.50	± 22.21	± 34.52
0.42–0.50	0.462	45.1	836.53	± 16.71	± 29.07	0.462	55.0	934.03	± 16.88	± 26.15
0.50–0.60	0.553	45.1	551.17	± 12.76	± 28.77	0.553	55.1	628.81	± 12.98	± 25.29
0.60–0.72	0.664	45.1	349.73	± 9.45	± 22.83	0.664	55.0	368.16	± 9.66	± 24.36
0.72–0.90	0.812	45.1	189.80	± 5.79	± 15.90	0.812	55.1	187.05	± 5.81	± 16.84
0.90–1.25	1.057	44.9	55.63	± 2.18	± 6.27	1.045	55.0	44.52	± 2.00	± 6.19

	$60 < \theta < 75$					$75 < \theta < 90$				
p_T	$\langle p_\mathrm{T}\rangle$	$\langle\theta\rangle$	$\mathrm{d}^2\sigma/\mathrm{d}p\mathrm{d}\Omega$			$\langle p_\mathrm{T}\rangle$	$\langle\theta\rangle$	$\mathrm{d}^2\sigma/\mathrm{d}p\mathrm{d}\Omega$		
0.50–0.60	0.551	67.5	621.69	± 9.87	± 22.81					
0.60–0.72	0.662	67.1	375.29	± 7.52	± 21.96	0.659	81.6	261.32	± 5.69	± 18.62
0.72–0.90	0.809	66.9	143.80	± 4.06	± 14.27	0.808	81.5	93.54	± 3.11	± 9.83

	$90 < \theta < 105$					$105 < \theta < 125$				
p_T	$\langle p_\mathrm{T}\rangle$	$\langle\theta\rangle$	$\mathrm{d}^2\sigma/\mathrm{d}p\mathrm{d}\Omega$			$\langle p_\mathrm{T}\rangle$	$\langle\theta\rangle$	$\mathrm{d}^2\sigma/\mathrm{d}p\mathrm{d}\Omega$		
0.42–0.50						0.462	113.7	304.84	± 6.60	± 16.30
0.50–0.60						0.549	112.7	137.44	± 4.05	± 12.98
0.60–0.72	0.660	97.4	152.77	± 4.33	± 13.80	0.661	113.1	50.76	± 2.57	± 8.07
0.72–0.90	0.802	97.1	42.75	± 2.19	± 5.68					

Table A.11: Double-differential inclusive cross-section $\mathrm{d}^2\sigma/\mathrm{d}p\mathrm{d}\Omega$ [mb/(GeV/c sr)] of the production of π^+'s in p + Ta $\rightarrow \pi^+$ + X interactions with $+5.0$ GeV/c beam momentum; the first error is statistical, the second systematic; p_T in GeV/c, polar angle θ in degrees.

	$20 < \theta < 30$					$30 < \theta < 40$				
p_T	$\langle p_\mathrm{T}\rangle$	$\langle\theta\rangle$	$\mathrm{d}^2\sigma/\mathrm{d}p\mathrm{d}\Omega$			$\langle p_\mathrm{T}\rangle$	$\langle\theta\rangle$	$\mathrm{d}^2\sigma/\mathrm{d}p\mathrm{d}\Omega$		
0.10–0.13	0.116	24.8	234.34 ± 16.47	±	19.28	0.115	35.0	265.93 ± 16.76	±	20.16
0.13–0.16	0.146	24.8	280.35 ± 15.94	±	16.73	0.146	35.0	264.70 ± 14.96	±	15.88
0.16–0.20	0.180	24.8	334.26 ± 14.64	±	16.82	0.180	34.7	256.75 ± 12.38	±	12.94
0.20–0.24	0.221	24.8	349.03 ± 14.65	±	15.11	0.220	34.6	257.50 ± 12.62	±	11.19
0.24–0.30	0.270	25.0	311.82 ± 11.34	±	11.42	0.269	34.8	244.86 ± 9.85	±	8.73
0.30–0.36	0.328	24.8	240.48 ± 9.85	±	7.84	0.330	34.8	212.65 ± 9.31	±	6.69
0.36–0.42	0.388	24.9	181.28 ± 8.42	±	5.99	0.388	34.9	170.29 ± 8.32	±	5.32
0.42–0.50	0.459	25.0	134.61 ± 6.23	±	5.51	0.457	34.6	118.03 ± 5.87	±	4.20
0.50–0.60	0.548	24.9	86.36 ± 4.12	±	4.61	0.548	34.6	84.81 ± 4.30	±	4.20
0.60–0.72	0.654	24.9	48.24 ± 2.57	±	3.82	0.653	34.8	47.07 ± 2.74	±	3.41
0.72–0.90						0.803	34.7	22.77 ± 1.38	±	2.56

	$40 < \theta < 50$					$50 < \theta < 60$				
p_T	$\langle p_\mathrm{T}\rangle$	$\langle\theta\rangle$	$\mathrm{d}^2\sigma/\mathrm{d}p\mathrm{d}\Omega$			$\langle p_\mathrm{T}\rangle$	$\langle\theta\rangle$	$\mathrm{d}^2\sigma/\mathrm{d}p\mathrm{d}\Omega$		
0.10–0.13	0.116	45.1	245.87 ± 16.66	±	18.86					
0.13–0.16	0.145	45.1	266.90 ± 15.47	±	15.96	0.145	54.8	235.34 ± 14.27	±	14.67
0.16–0.20	0.181	45.1	237.75 ± 11.92	±	12.04	0.181	55.0	211.86 ± 11.05	±	10.61
0.20–0.24	0.221	44.8	226.65 ± 11.77	±	10.01	0.220	54.5	198.49 ± 10.86	±	8.65
0.24–0.30	0.271	44.6	191.81 ± 8.82	±	6.91	0.270	54.7	169.82 ± 8.25	±	6.11
0.30–0.36	0.332	44.8	168.55 ± 8.23	±	5.33	0.332	54.6	136.25 ± 7.53	±	4.66
0.36–0.42	0.392	44.7	150.90 ± 7.93	±	5.02	0.390	55.0	103.56 ± 6.69	±	3.92
0.42–0.50	0.462	44.8	98.84 ± 5.55	±	3.76	0.461	54.6	76.09 ± 4.90	±	3.23
0.50–0.60	0.551	44.7	63.98 ± 3.82	±	3.06	0.549	54.8	50.56 ± 3.54	±	2.75
0.60–0.72	0.661	44.7	41.04 ± 2.71	±	2.83	0.664	54.6	33.30 ± 2.54	±	2.49
0.72–0.90	0.805	44.5	19.21 ± 1.37	±	1.96	0.811	54.8	16.61 ± 1.35	±	1.71
0.90–1.25						1.046	54.2	4.87 ± 0.46	±	0.80

	$60 < \theta < 75$					$75 < \theta < 90$				
p_T	$\langle p_\mathrm{T}\rangle$	$\langle\theta\rangle$	$\mathrm{d}^2\sigma/\mathrm{d}p\mathrm{d}\Omega$			$\langle p_\mathrm{T}\rangle$	$\langle\theta\rangle$	$\mathrm{d}^2\sigma/\mathrm{d}p\mathrm{d}\Omega$		
0.13–0.16	0.146	67.2	239.90 ± 13.76	±	15.35					
0.16–0.20	0.181	67.4	197.82 ± 9.15	±	9.74	0.181	81.9	192.21 ± 11.02	±	14.62
0.20–0.24	0.220	67.0	177.38 ± 8.57	±	7.38	0.221	81.6	155.22 ± 8.76	±	8.38
0.24–0.30	0.270	67.3	144.03 ± 6.38	±	5.21	0.269	81.7	120.54 ± 6.23	±	6.16
0.30–0.36	0.331	67.3	102.16 ± 5.54	±	4.18	0.331	82.0	68.20 ± 4.63	±	3.45
0.36–0.42	0.392	66.7	86.44 ± 5.04	±	3.63	0.390	81.7	50.36 ± 3.93	±	2.51
0.42–0.50	0.461	67.2	56.45 ± 3.47	±	2.65	0.464	82.2	33.48 ± 2.87	±	2.43
0.50–0.60	0.550	67.0	41.12 ± 2.67	±	2.65	0.553	81.6	22.99 ± 2.06	±	1.91
0.60–0.72	0.659	66.4	20.04 ± 1.67	±	1.80	0.656	81.6	12.80 ± 1.37	±	1.39
0.72–0.90	0.813	65.9	8.92 ± 0.83	±	1.08	0.808	81.0	2.85 ± 0.48	±	0.41
0.90–1.25	1.051	66.4	2.40 ± 0.26	±	0.45	1.047	81.1	0.83 ± 0.14	±	0.19

	$90 < \theta < 105$					$105 < \theta < 125$				
p_T	$\langle p_\mathrm{T}\rangle$	$\langle\theta\rangle$	$\mathrm{d}^2\sigma/\mathrm{d}p\mathrm{d}\Omega$			$\langle p_\mathrm{T}\rangle$	$\langle\theta\rangle$	$\mathrm{d}^2\sigma/\mathrm{d}p\mathrm{d}\Omega$		
0.13–0.16						0.146	114.8	213.68 ± 11.93	±	14.31
0.16–0.20	0.180	97.8	189.46 ± 11.28	±	17.21	0.179	114.5	126.49 ± 6.51	±	4.81
0.20–0.24	0.220	98.2	135.03 ± 8.03	±	5.81	0.218	114.1	83.79 ± 5.15	±	3.18
0.24–0.30	0.269	97.4	97.53 ± 5.56	±	4.56	0.271	113.9	50.79 ± 3.40	±	2.39
0.30–0.36	0.330	97.5	46.45 ± 3.81	±	2.40	0.333	113.5	25.85 ± 2.42	±	1.66
0.36–0.42	0.391	97.3	32.82 ± 3.29	±	2.34	0.391	114.1	15.97 ± 1.89	±	1.36
0.42–0.50	0.463	97.3	19.81 ± 2.16	±	1.68	0.458	113.4	8.37 ± 1.18	±	0.92
0.50–0.60	0.552	97.4	13.28 ± 1.56	±	1.46	0.557	110.7	3.92 ± 0.68	±	0.57
0.60–0.72	0.655	97.8	5.10 ± 0.79	±	0.74	0.678	109.4	0.46 ± 0.20	±	0.09
0.72–0.90	0.810	94.4	1.67 ± 0.35	±	0.34	0.800	114.0	0.35 ± 0.12	±	0.11
0.90–1.25	1.044	97.5	0.21 ± 0.06	±	0.07					

Table A.12: Double-differential inclusive cross-section $\mathrm{d}^2\sigma/\mathrm{d}p\mathrm{d}\Omega$ [mb/(GeV/c sr)] of the production of π^-'s in p + Ta $\rightarrow$ π^- + X interactions with $+5.0$ GeV/c beam momentum; the first error is statistical, the second systematic; p_T in GeV/c, polar angle θ in degrees.

	$20 < \theta < 30$			$30 < \theta < 40$		
p_T	$\langle p_\mathrm{T}\rangle$	$\langle\theta\rangle$	$\mathrm{d}^2\sigma/\mathrm{d}p\mathrm{d}\Omega$	$\langle p_\mathrm{T}\rangle$	$\langle\theta\rangle$	$\mathrm{d}^2\sigma/\mathrm{d}p\mathrm{d}\Omega$
0.10–0.13	0.116	25.1	284.21 ± 17.26 ± 21.71	0.115	35.2	328.76 ± 18.71 ± 25.78
0.13–0.16	0.145	25.0	289.02 ± 16.62 ± 19.22	0.145	34.8	290.86 ± 15.71 ± 17.98
0.16–0.20	0.180	25.1	341.41 ± 15.03 ± 18.14	0.179	34.9	273.45 ± 12.90 ± 14.04
0.20–0.24	0.220	25.2	327.09 ± 14.11 ± 14.00	0.220	34.6	257.39 ± 12.33 ± 11.17
0.24–0.30	0.268	25.1	237.95 ± 9.88 ± 8.36	0.269	35.0	215.71 ± 9.35 ± 7.58
0.30–0.36	0.328	25.1	165.71 ± 8.35 ± 5.60	0.328	35.0	168.52 ± 8.24 ± 5.29
0.36–0.42	0.389	25.2	121.03 ± 7.04 ± 4.14	0.387	34.9	125.41 ± 7.17 ± 4.22
0.42–0.50	0.457	25.2	66.68 ± 4.56 ± 2.75	0.456	34.9	84.79 ± 5.21 ± 3.62
0.50–0.60	0.547	25.1	45.52 ± 3.34 ± 2.57	0.542	34.7	50.24 ± 3.52 ± 2.75
0.60–0.72	0.653	25.3	19.98 ± 2.01 ± 1.58	0.650	35.4	24.74 ± 2.22 ± 1.88
0.72–0.90				0.793	35.1	12.77 ± 1.36 ± 1.37

	$40 < \theta < 50$			$50 < \theta < 60$		
p_T	$\langle p_\mathrm{T}\rangle$	$\langle\theta\rangle$	$\mathrm{d}^2\sigma/\mathrm{d}p\mathrm{d}\Omega$	$\langle p_\mathrm{T}\rangle$	$\langle\theta\rangle$	$\mathrm{d}^2\sigma/\mathrm{d}p\mathrm{d}\Omega$
0.10–0.13	0.113	45.0	329.91 ± 19.10 ± 25.73			
0.13–0.16	0.144	45.0	260.53 ± 14.72 ± 16.04	0.144	55.3	299.43 ± 16.63 ± 18.80
0.16–0.20	0.178	45.1	227.54 ± 11.65 ± 11.82	0.179	54.9	243.38 ± 12.22 ± 12.41
0.20–0.24	0.218	44.8	230.00 ± 11.94 ± 10.79	0.219	54.7	179.19 ± 10.26 ± 7.94
0.24–0.30	0.268	45.0	191.77 ± 8.89 ± 7.08	0.267	54.6	147.89 ± 7.75 ± 5.53
0.30–0.36	0.328	44.8	143.55 ± 7.64 ± 4.66	0.326	55.0	118.41 ± 6.98 ± 3.83
0.36–0.42	0.386	44.9	106.92 ± 6.68 ± 3.81	0.384	55.1	92.89 ± 6.22 ± 3.38
0.42–0.50	0.452	44.9	81.81 ± 5.05 ± 3.44	0.451	54.6	72.36 ± 4.79 ± 3.29
0.50–0.60	0.539	44.7	42.77 ± 3.22 ± 2.44	0.537	55.0	45.23 ± 3.44 ± 2.82
0.60–0.72	0.646	45.2	25.31 ± 2.28 ± 2.02	0.636	55.1	20.10 ± 2.06 ± 1.67
0.72–0.90	0.775	44.4	11.69 ± 1.28 ± 1.31	0.791	54.8	6.20 ± 0.93 ± 0.71
0.90–1.25				1.017	55.2	1.75 ± 0.35 ± 0.31

	$60 < \theta < 75$			$75 < \theta < 90$		
p_T	$\langle p_\mathrm{T}\rangle$	$\langle\theta\rangle$	$\mathrm{d}^2\sigma/\mathrm{d}p\mathrm{d}\Omega$	$\langle p_\mathrm{T}\rangle$	$\langle\theta\rangle$	$\mathrm{d}^2\sigma/\mathrm{d}p\mathrm{d}\Omega$
0.13–0.16	0.145	67.2	308.63 ± 15.31 ± 18.71			
0.16–0.20	0.179	67.3	224.57 ± 9.84 ± 10.54	0.179	81.7	204.89 ± 11.11 ± 13.69
0.20–0.24	0.218	67.3	157.42 ± 7.87 ± 6.30	0.218	81.8	151.21 ± 8.50 ± 7.31
0.24–0.30	0.267	67.2	137.30 ± 6.16 ± 4.89	0.266	82.0	101.48 ± 5.70 ± 5.04
0.30–0.36	0.326	67.0	93.18 ± 5.19 ± 3.55	0.324	81.8	68.84 ± 4.52 ± 3.03
0.36–0.42	0.386	66.9	67.92 ± 4.40 ± 2.76	0.385	81.4	55.35 ± 4.16 ± 3.29
0.42–0.50	0.454	67.0	52.88 ± 3.34 ± 2.67	0.453	82.1	29.79 ± 2.63 ± 2.06
0.50–0.60	0.537	66.8	28.35 ± 2.22 ± 1.94	0.536	81.5	17.58 ± 1.81 ± 1.59
0.60–0.72	0.641	66.0	14.55 ± 1.45 ± 1.35	0.640	82.6	6.61 ± 1.01 ± 0.78
0.72–0.90	0.786	67.1	7.44 ± 0.85 ± 0.94	0.770	81.8	3.50 ± 0.58 ± 0.55
0.90–1.25	0.992	66.7	0.72 ± 0.17 ± 0.14	0.974	76.7	0.11 ± 0.05 ± 0.03

	$90 < \theta < 105$			$105 < \theta < 125$		
p_T	$\langle p_\mathrm{T}\rangle$	$\langle\theta\rangle$	$\mathrm{d}^2\sigma/\mathrm{d}p\mathrm{d}\Omega$	$\langle p_\mathrm{T}\rangle$	$\langle\theta\rangle$	$\mathrm{d}^2\sigma/\mathrm{d}p\mathrm{d}\Omega$
0.13–0.16				0.144	114.3	243.09 ± 12.49 ± 12.93
0.16–0.20	0.178	98.5	214.52 ± 11.63 ± 14.76	0.178	113.9	139.52 ± 6.86 ± 5.21
0.20–0.24	0.218	97.4	123.21 ± 7.58 ± 5.08	0.219	113.7	74.79 ± 4.82 ± 3.01
0.24–0.30	0.264	97.1	73.14 ± 4.72 ± 3.14	0.266	112.8	40.52 ± 2.97 ± 2.09
0.30–0.36	0.326	97.4	38.70 ± 3.44 ± 2.19	0.327	113.4	22.05 ± 2.24 ± 1.67
0.36–0.42	0.389	97.7	36.71 ± 3.47 ± 2.94	0.386	113.2	15.13 ± 1.82 ± 1.49
0.42–0.50	0.452	97.0	18.17 ± 2.03 ± 1.69	0.450	111.7	8.18 ± 1.18 ± 1.05
0.50–0.60	0.540	96.2	9.22 ± 1.34 ± 1.18	0.534	112.4	2.74 ± 0.60 ± 0.48
0.60–0.72	0.649	97.1	2.75 ± 0.62 ± 0.46	0.652	109.0	0.52 ± 0.20 ± 0.13
0.72–0.90	0.767	96.7	1.02 ± 0.27 ± 0.25	0.792	113.3	0.12 ± 0.06 ± 0.06
0.90–1.25	0.987	93.4	0.09 ± 0.05 ± 0.04			

Table A.13: Double-differential inclusive cross-section $\mathrm{d}^2\sigma/\mathrm{d}p\mathrm{d}\Omega$ [mb/(GeV/c sr)] of the production of protons in π^+ + Ta $\rightarrow$ p + X interactions with $+5.0$ GeV/c beam momentum; the first error is statistical, the second systematic; p_T in GeV/c, polar angle θ in degrees.

	$20 < \theta < 30$						$30 < \theta < 40$					
p_T	$\langle p_\mathrm{T}\rangle$	$\langle\theta\rangle$	$\mathrm{d}^2\sigma/\mathrm{d}p\mathrm{d}\Omega$				$\langle p_\mathrm{T}\rangle$	$\langle\theta\rangle$	$\mathrm{d}^2\sigma/\mathrm{d}p\mathrm{d}\Omega$			
0.20–0.24	0.221	25.1	1347.48	$\pm$	28.36	$\pm$ 72.57						
0.24–0.30	0.268	25.2	1145.26	$\pm$	19.97	$\pm$ 54.57	0.271	35.0	1350.32	$\pm$	22.28	$\pm$ 59.35
0.30–0.36	0.329	25.3	870.18	$\pm$	17.37	$\pm$ 36.54	0.329	35.1	1160.86	$\pm$	19.70	$\pm$ 43.34
0.36–0.42	0.389	25.4	688.03	$\pm$	15.60	$\pm$ 26.59	0.389	35.2	918.76	$\pm$	17.80	$\pm$ 31.15
0.42–0.50	0.458	25.5	494.88	$\pm$	11.39	$\pm$ 18.12	0.458	35.3	693.57	$\pm$	13.50	$\pm$ 22.20
0.50–0.60	0.546	25.5	313.48	$\pm$	7.97	$\pm$ 11.73	0.547	35.2	475.19	$\pm$	10.10	$\pm$ 16.55
0.60–0.72	0.656	25.6	196.97	$\pm$	5.65	$\pm$ 8.52	0.654	35.3	300.44	$\pm$	7.18	$\pm$ 13.22
0.72–0.90							0.798	35.2	162.21	$\pm$	4.22	$\pm$ 9.57

	$40 < \theta < 50$						$50 < \theta < 60$					
p_T	$\langle p_\mathrm{T}\rangle$	$\langle\theta\rangle$	$\mathrm{d}^2\sigma/\mathrm{d}p\mathrm{d}\Omega$				$\langle p_\mathrm{T}\rangle$	$\langle\theta\rangle$	$\mathrm{d}^2\sigma/\mathrm{d}p\mathrm{d}\Omega$			
0.30–0.36	0.331	45.1	1317.17	$\pm$	20.63	$\pm$ 41.62						
0.36–0.42	0.393	45.1	1108.47	$\pm$	18.99	$\pm$ 31.31	0.391	55.1	1206.60	$\pm$	19.05	$\pm$ 34.69
0.42–0.50	0.462	45.1	854.58	$\pm$	14.72	$\pm$ 24.14	0.462	55.1	925.37	$\pm$	14.95	$\pm$ 25.42
0.50–0.60	0.553	45.1	584.67	$\pm$	11.20	$\pm$ 20.91	0.553	55.1	637.44	$\pm$	11.41	$\pm$ 22.04
0.60–0.72	0.663	45.1	345.20	$\pm$	7.98	$\pm$ 16.70	0.663	55.0	377.95	$\pm$	8.31	$\pm$ 18.80
0.72–0.90	0.810	45.1	182.38	$\pm$	4.75	$\pm$ 11.87	0.813	55.0	185.25	$\pm$	4.84	$\pm$ 12.89
0.90–1.25	1.049	45.2	56.25	$\pm$	1.84	$\pm$ 5.46	1.048	55.0	49.97	$\pm$	1.73	$\pm$ 5.40

	$60 < \theta < 75$						$75 < \theta < 90$					
p_T	$\langle p_\mathrm{T}\rangle$	$\langle\theta\rangle$	$\mathrm{d}^2\sigma/\mathrm{d}p\mathrm{d}\Omega$				$\langle p_\mathrm{T}\rangle$	$\langle\theta\rangle$	$\mathrm{d}^2\sigma/\mathrm{d}p\mathrm{d}\Omega$			
0.50–0.60	0.552	67.5	623.52	$\pm$	8.83	$\pm$ 22.62						
0.60–0.72	0.662	67.3	370.73	$\pm$	6.55	$\pm$ 20.34	0.661	81.8	284.51	$\pm$	5.32	$\pm$ 20.13
0.72–0.90	0.810	67.0	158.33	$\pm$	3.59	$\pm$ 13.46	0.806	81.6	112.28	$\pm$	2.92	$\pm$ 11.18
0.90–1.25	1.046	66.7	35.63	$\pm$	1.24	$\pm$ 5.30	1.042	81.5	18.55	$\pm$	0.90	$\pm$ 3.22

	$90 < \theta < 105$						$105 < \theta < 125$					
p_T	$\langle p_\mathrm{T}\rangle$	$\langle\theta\rangle$	$\mathrm{d}^2\sigma/\mathrm{d}p\mathrm{d}\Omega$				$\langle p_\mathrm{T}\rangle$	$\langle\theta\rangle$	$\mathrm{d}^2\sigma/\mathrm{d}p\mathrm{d}\Omega$			
0.42–0.50							0.463	113.8	375.13	$\pm$	6.55	$\pm$ 19.91
0.50–0.60							0.549	113.1	185.49	$\pm$	4.09	$\pm$ 16.91
0.60–0.72	0.659	97.2	169.77	$\pm$	4.06	$\pm$ 15.18	0.659	113.2	70.59	$\pm$	2.49	$\pm$ 10.01
0.72–0.90	0.805	97.3	63.44	$\pm$	2.18	$\pm$ 7.33	0.801	112.6	16.63	$\pm$	1.12	$\pm$ 3.92

Table A.14: Double-differential inclusive cross-section $\mathrm{d}^2\sigma/\mathrm{d}p\mathrm{d}\Omega$ [mb/(GeV/c sr)] of the production of π^+'s in π^+ + Ta $\rightarrow$ π^+ + X interactions with $+5.0$ GeV/c beam momentum; the first error is statistical, the second systematic; p_T in GeV/c, polar angle θ in degrees.

	$20 < \theta < 30$			$30 < \theta < 40$		
p_T	$\langle p_\mathrm{T}\rangle$	$\langle\theta\rangle$	$\mathrm{d}^2\sigma/\mathrm{d}p\mathrm{d}\Omega$	$\langle p_\mathrm{T}\rangle$	$\langle\theta\rangle$	$\mathrm{d}^2\sigma/\mathrm{d}p\mathrm{d}\Omega$
0.10–0.13	0.116	25.0	292.87 ± 16.03 ± 21.51	0.116	35.0	317.51 ± 16.01 ± 23.47
0.13–0.16	0.146	24.7	389.74 ± 16.95 ± 23.05	0.145	35.0	318.15 ± 14.84 ± 18.84
0.16–0.20	0.180	24.9	480.32 ± 15.99 ± 24.47	0.179	34.9	350.82 ± 13.20 ± 17.52
0.20–0.24	0.220	24.8	490.81 ± 15.70 ± 21.02	0.220	34.7	381.77 ± 13.89 ± 16.47
0.24–0.30	0.269	24.8	485.19 ± 12.79 ± 17.58	0.270	34.8	379.26 ± 11.13 ± 13.30
0.30–0.36	0.329	24.8	432.30 ± 11.94 ± 13.62	0.330	34.8	359.25 ± 10.93 ± 10.90
0.36–0.42	0.389	24.8	353.20 ± 10.71 ± 11.07	0.389	34.8	287.96 ± 9.74 ± 8.49
0.42–0.50	0.459	24.8	269.08 ± 8.05 ± 10.61	0.458	34.9	245.56 ± 7.75 ± 8.28
0.50–0.60	0.545	24.7	188.97 ± 5.77 ± 9.80	0.547	34.8	163.71 ± 5.52 ± 7.79
0.60–0.72	0.654	24.9	111.51 ± 3.94 ± 8.67	0.654	34.9	103.12 ± 3.85 ± 7.27
0.72–0.90				0.799	34.8	49.18 ± 2.00 ± 5.46

	$40 < \theta < 50$			$50 < \theta < 60$		
p_T	$\langle p_\mathrm{T}\rangle$	$\langle\theta\rangle$	$\mathrm{d}^2\sigma/\mathrm{d}p\mathrm{d}\Omega$	$\langle p_\mathrm{T}\rangle$	$\langle\theta\rangle$	$\mathrm{d}^2\sigma/\mathrm{d}p\mathrm{d}\Omega$
0.10–0.13	0.116	45.1	327.82 ± 17.15 ± 24.80			
0.13–0.16	0.146	44.8	334.35 ± 15.64 ± 19.83	0.146	54.9	309.60 ± 14.59 ± 18.96
0.16–0.20	0.181	44.9	334.01 ± 12.72 ± 16.71	0.180	55.0	300.22 ± 11.96 ± 14.83
0.20–0.24	0.221	45.1	300.07 ± 12.28 ± 13.12	0.220	54.8	258.87 ± 11.28 ± 11.06
0.24–0.30	0.271	44.8	307.38 ± 10.11 ± 10.90	0.270	54.8	240.05 ± 8.91 ± 8.40
0.30–0.36	0.331	44.8	276.68 ± 9.53 ± 8.39	0.330	54.8	214.45 ± 8.56 ± 7.12
0.36–0.42	0.392	44.6	249.99 ± 9.16 ± 7.78	0.393	54.7	202.08 ± 8.40 ± 7.28
0.42–0.50	0.461	44.7	200.83 ± 7.14 ± 7.19	0.462	54.9	155.62 ± 6.33 ± 6.11
0.50–0.60	0.555	44.7	131.50 ± 4.99 ± 6.01	0.552	54.7	108.08 ± 4.67 ± 5.49
0.60–0.72	0.664	44.6	78.55 ± 3.46 ± 5.21	0.661	54.7	59.44 ± 3.11 ± 4.23
0.72–0.90	0.805	44.5	36.44 ± 1.79 ± 3.65	0.812	54.7	29.34 ± 1.67 ± 2.95
0.90–1.25				1.046	54.4	8.74 ± 0.61 ± 1.41

	$60 < \theta < 75$			$75 < \theta < 90$		
p_T	$\langle p_\mathrm{T}\rangle$	$\langle\theta\rangle$	$\mathrm{d}^2\sigma/\mathrm{d}p\mathrm{d}\Omega$	$\langle p_\mathrm{T}\rangle$	$\langle\theta\rangle$	$\mathrm{d}^2\sigma/\mathrm{d}p\mathrm{d}\Omega$
0.13–0.16	0.146	67.0	331.63 ± 14.70 ± 23.27	0.150	82.0	215.92 ± 19.47 ± 63.53
0.16–0.20	0.181	67.4	269.72 ± 9.60 ± 13.14	0.181	82.0	256.45 ± 11.67 ± 22.71
0.20–0.24	0.220	67.3	259.48 ± 9.41 ± 10.82	0.221	81.8	235.34 ± 9.69 ± 12.28
0.24–0.30	0.269	67.1	208.82 ± 6.96 ± 7.74	0.269	82.0	179.65 ± 6.94 ± 9.91
0.30–0.36	0.332	66.8	165.54 ± 6.34 ± 6.79	0.330	81.8	110.23 ± 5.38 ± 5.87
0.36–0.42	0.392	66.9	127.19 ± 5.48 ± 5.14	0.392	81.4	84.48 ± 4.58 ± 4.16
0.42–0.50	0.462	67.1	99.32 ± 4.13 ± 4.40	0.462	82.2	60.90 ± 3.49 ± 4.33
0.50–0.60	0.550	66.9	73.06 ± 3.18 ± 4.47	0.553	81.6	44.56 ± 2.58 ± 3.56
0.60–0.72	0.664	67.1	43.14 ± 2.22 ± 3.71	0.660	81.0	25.04 ± 1.73 ± 2.61
0.72–0.90	0.814	66.0	16.63 ± 1.05 ± 1.97	0.807	81.1	8.08 ± 0.74 ± 1.13
0.90–1.25	1.035	65.9	4.14 ± 0.32 ± 0.76	1.041	81.4	1.59 ± 0.18 ± 0.35

	$90 < \theta < 105$			$105 < \theta < 125$		
p_T	$\langle p_\mathrm{T}\rangle$	$\langle\theta\rangle$	$\mathrm{d}^2\sigma/\mathrm{d}p\mathrm{d}\Omega$	$\langle p_\mathrm{T}\rangle$	$\langle\theta\rangle$	$\mathrm{d}^2\sigma/\mathrm{d}p\mathrm{d}\Omega$
0.13–0.16	0.150	98.9	214.54 ± 20.32 ± 69.19	0.145	114.7	355.83 ± 15.84 ± 48.40
0.16–0.20	0.181	98.1	271.15 ± 12.68 ± 30.45	0.180	114.6	175.92 ± 7.16 ± 6.75
0.20–0.24	0.220	97.8	197.85 ± 8.76 ± 8.27	0.220	113.9	119.21 ± 5.54 ± 4.30
0.24–0.30	0.269	97.3	130.15 ± 5.78 ± 5.94	0.269	113.9	76.96 ± 3.71 ± 3.32
0.30–0.36	0.331	97.3	81.08 ± 4.51 ± 4.05	0.328	114.7	41.80 ± 2.69 ± 2.49
0.36–0.42	0.391	97.0	57.27 ± 3.90 ± 3.96	0.389	113.6	35.78 ± 2.52 ± 2.86
0.42–0.50	0.461	96.7	41.28 ± 2.81 ± 3.41	0.460	113.8	19.80 ± 1.60 ± 2.07
0.50–0.60	0.555	96.5	25.54 ± 1.95 ± 2.74	0.549	112.7	10.16 ± 0.99 ± 1.43
0.60–0.72	0.663	96.2	10.24 ± 1.01 ± 1.45	0.654	111.1	2.28 ± 0.40 ± 0.45
0.72–0.90	0.810	95.3	2.82 ± 0.41 ± 0.55	0.789	113.0	0.46 ± 0.12 ± 0.15
0.90–1.25	1.058	97.7	0.30 ± 0.06 ± 0.10	1.050	108.8	0.03 ± 0.01 ± 0.02

Table A.15: Double-differential inclusive cross-section $\mathrm{d}^2\sigma/\mathrm{d}p\mathrm{d}\Omega$ [mb/(GeV/c sr)] of the production of π^-'s in π^+ + Ta $\rightarrow \pi^-$ + X interactions with $+5.0$ GeV/c beam momentum; the first error is statistical, the second systematic; p_T in GeV/c, polar angle θ in degrees.

	$20 < \theta < 30$					$30 < \theta < 40$				
p_T	$\langle p_\mathrm{T}\rangle$	$\langle\theta\rangle$	$\mathrm{d}^2\sigma/\mathrm{d}p\mathrm{d}\Omega$			$\langle p_\mathrm{T}\rangle$	$\langle\theta\rangle$	$\mathrm{d}^2\sigma/\mathrm{d}p\mathrm{d}\Omega$		
0.10–0.13	0.116	25.1	347.61 ± 16.34	±	25.26	0.115	34.9	403.30 ± 18.39	±	30.79
0.13–0.16	0.146	24.9	432.19 ± 18.29	±	29.17	0.144	34.7	341.59 ± 15.25	±	20.89
0.16–0.20	0.180	24.8	419.15 ± 14.88	±	22.63	0.180	34.9	356.21 ± 13.14	±	18.06
0.20–0.24	0.219	25.0	398.10 ± 13.94	±	16.75	0.220	34.9	339.92 ± 12.69	±	14.48
0.24–0.30	0.269	25.0	370.14 ± 11.02	±	12.70	0.269	34.9	318.02 ± 10.12	±	10.95
0.30–0.36	0.330	25.1	292.53 ± 9.93	±	9.58	0.329	35.0	238.02 ± 8.78	±	7.15
0.36–0.42	0.389	25.0	212.29 ± 8.35	±	6.79	0.390	34.9	192.97 ± 7.95	±	6.11
0.42–0.50	0.456	25.0	149.41 ± 6.10	±	5.79	0.456	34.8	150.64 ± 6.23	±	6.16
0.50–0.60	0.544	25.1	95.52 ± 4.34	±	5.06	0.546	34.9	87.61 ± 4.18	±	4.55
0.60–0.72	0.651	25.3	57.61 ± 3.10	±	4.26	0.656	34.8	43.86 ± 2.64	±	3.14
0.72–0.90						0.799	34.7	25.46 ± 1.73	±	2.61

	$40 < \theta < 50$					$50 < \theta < 60$				
p_T	$\langle p_\mathrm{T}\rangle$	$\langle\theta\rangle$	$\mathrm{d}^2\sigma/\mathrm{d}p\mathrm{d}\Omega$			$\langle p_\mathrm{T}\rangle$	$\langle\theta\rangle$	$\mathrm{d}^2\sigma/\mathrm{d}p\mathrm{d}\Omega$		
0.10–0.13	0.115	44.9	343.86 ± 17.17	±	26.69					
0.13–0.16	0.144	44.8	339.99 ± 14.99	±	20.73	0.144	55.0	369.57 ± 16.46	±	22.99
0.16–0.20	0.179	44.9	317.32 ± 12.18	±	16.24	0.178	55.1	297.92 ± 12.07	±	14.99
0.20–0.24	0.219	44.9	298.74 ± 12.09	±	13.74	0.218	55.1	231.89 ± 10.39	±	9.99
0.24–0.30	0.269	44.8	255.42 ± 9.15	±	9.27	0.268	54.9	202.63 ± 8.16	±	7.41
0.30–0.36	0.326	44.7	212.10 ± 8.34	±	6.63	0.327	54.9	183.99 ± 7.79	±	5.69
0.36–0.42	0.386	44.8	185.61 ± 7.91	±	6.28	0.386	54.9	136.55 ± 6.73	±	4.67
0.42–0.50	0.452	45.1	130.43 ± 5.74	±	5.22	0.454	54.8	104.88 ± 5.18	±	4.51
0.50–0.60	0.539	44.9	86.53 ± 4.12	±	4.69	0.539	54.5	63.95 ± 3.66	±	3.78
0.60–0.72	0.645	44.9	46.84 ± 2.77	±	3.55	0.645	54.5	39.53 ± 2.59	±	3.11
0.72–0.90	0.783	45.2	21.15 ± 1.57	±	2.28	0.781	54.9	15.76 ± 1.32	±	1.72
0.90–1.25						1.012	54.9	3.73 ± 0.45	±	0.62

	$60 < \theta < 75$					$75 < \theta < 90$				
p_T	$\langle p_\mathrm{T}\rangle$	$\langle\theta\rangle$	$\mathrm{d}^2\sigma/\mathrm{d}p\mathrm{d}\Omega$			$\langle p_\mathrm{T}\rangle$	$\langle\theta\rangle$	$\mathrm{d}^2\sigma/\mathrm{d}p\mathrm{d}\Omega$		
0.13–0.16	0.144	67.6	371.68 ± 15.75	±	24.42					
0.16–0.20	0.178	67.2	279.31 ± 9.78	±	13.01	0.179	81.9	271.72 ± 12.06	±	20.63
0.20–0.24	0.218	67.3	207.95 ± 8.12	±	8.17	0.217	81.7	189.68 ± 8.63	±	9.56
0.24–0.30	0.267	67.2	174.54 ± 6.25	±	6.17	0.266	82.1	147.92 ± 6.22	±	7.87
0.30–0.36	0.327	66.9	142.86 ± 5.77	±	5.35	0.324	81.9	89.47 ± 4.69	±	4.03
0.36–0.42	0.386	66.8	109.22 ± 5.01	±	4.25	0.387	81.5	73.90 ± 4.35	±	4.40
0.42–0.50	0.452	66.9	85.28 ± 3.83	±	4.11	0.452	82.0	57.83 ± 3.30	±	3.88
0.50–0.60	0.542	67.0	53.65 ± 2.73	±	3.51	0.537	82.3	33.47 ± 2.24	±	2.90
0.60–0.72	0.640	66.7	27.91 ± 1.80	±	2.47	0.637	81.6	17.57 ± 1.46	±	1.97
0.72–0.90	0.781	67.3	12.09 ± 0.96	±	1.47	0.767	82.2	5.84 ± 0.66	±	0.88
0.90–1.25	0.981	66.8	1.92 ± 0.25	±	0.36	0.997	82.1	0.83 ± 0.14	±	0.20

	$90 < \theta < 105$					$105 < \theta < 125$				
p_T	$\langle p_\mathrm{T}\rangle$	$\langle\theta\rangle$	$\mathrm{d}^2\sigma/\mathrm{d}p\mathrm{d}\Omega$			$\langle p_\mathrm{T}\rangle$	$\langle\theta\rangle$	$\mathrm{d}^2\sigma/\mathrm{d}p\mathrm{d}\Omega$		
0.13–0.16						0.144	114.5	322.38 ± 14.43	±	24.27
0.16–0.20	0.179	97.6	250.07 ± 11.96	±	23.80	0.177	113.7	175.36 ± 7.07	±	6.45
0.20–0.24	0.219	97.6	161.81 ± 8.04	±	7.49	0.217	113.8	89.08 ± 4.80	±	3.44
0.24–0.30	0.266	97.1	98.56 ± 4.99	±	4.45	0.267	113.7	57.69 ± 3.21	±	2.91
0.30–0.36	0.325	97.0	60.35 ± 3.90	±	3.37	0.326	113.8	37.81 ± 2.62	±	2.71
0.36–0.42	0.384	97.2	45.21 ± 3.45	±	3.48	0.387	112.5	26.31 ± 2.14	±	2.44
0.42–0.50	0.451	97.3	35.68 ± 2.55	±	3.16	0.447	112.7	14.94 ± 1.42	±	1.81
0.50–0.60	0.543	97.3	20.38 ± 1.78	±	2.49	0.540	111.7	4.83 ± 0.71	±	0.78
0.60–0.72	0.639	96.6	6.65 ± 0.85	±	1.05	0.647	111.8	1.18 ± 0.28	±	0.27
0.72–0.90	0.787	96.0	1.44 ± 0.29	±	0.33	0.797	108.7	0.18 ± 0.07	±	0.08
0.90–1.25	1.061	92.3	0.18 ± 0.07	±	0.07					

Table A.16: Double-differential inclusive cross-section $\mathrm{d}^2\sigma/\mathrm{d}p\mathrm{d}\Omega$ [mb/(GeV/c sr)] of the production of protons in π^- + Ta $\rightarrow$ p + X interactions with -5.0 GeV/c beam momentum; the first error is statistical, the second systematic; p_T in GeV/c, polar angle θ in degrees.

	$20 < \theta < 30$						$30 < \theta < 40$					
p_T	$\langle p_\mathrm{T}\rangle$	$\langle\theta\rangle$	$\mathrm{d}^2\sigma/\mathrm{d}p\mathrm{d}\Omega$				$\langle p_\mathrm{T}\rangle$	$\langle\theta\rangle$	$\mathrm{d}^2\sigma/\mathrm{d}p\mathrm{d}\Omega$			
0.20–0.24	0.220	25.2	1178.83	$\pm$	20.56	$\pm$ 63.58						
0.24–0.30	0.268	25.3	1044.47	$\pm$	14.69	$\pm$ 49.58	0.270	34.9	1238.38	$\pm$	16.23	$\pm$ 54.48
0.30–0.36	0.327	25.3	825.63	$\pm$	13.09	$\pm$ 34.18	0.328	35.1	1083.32	$\pm$	14.53	$\pm$ 40.42
0.36–0.42	0.387	25.4	624.77	$\pm$	11.42	$\pm$ 22.93	0.387	35.2	880.69	$\pm$	13.39	$\pm$ 28.60
0.42–0.50	0.456	25.4	467.31	$\pm$	8.41	$\pm$ 15.44	0.456	35.2	643.96	$\pm$	9.84	$\pm$ 18.92
0.50–0.60	0.544	25.5	330.89	$\pm$	6.31	$\pm$ 11.03	0.543	35.3	454.06	$\pm$	7.50	$\pm$ 14.16
0.60–0.72	0.650	25.5	209.49	$\pm$	4.52	$\pm$ 8.49	0.650	35.2	295.35	$\pm$	5.45	$\pm$ 11.69
0.72–0.90							0.792	35.2	154.68	$\pm$	3.22	$\pm$ 8.88

	$40 < \theta < 50$						$50 < \theta < 60$					
p_T	$\langle p_\mathrm{T}\rangle$	$\langle\theta\rangle$	$\mathrm{d}^2\sigma/\mathrm{d}p\mathrm{d}\Omega$				$\langle p_\mathrm{T}\rangle$	$\langle\theta\rangle$	$\mathrm{d}^2\sigma/\mathrm{d}p\mathrm{d}\Omega$			
0.30–0.36	0.329	45.1	1245.06	$\pm$	15.31	$\pm$ 39.98						
0.36–0.42	0.389	45.1	1044.40	$\pm$	14.28	$\pm$ 29.34	0.389	55.1	1105.28	$\pm$	14.03	$\pm$ 33.13
0.42–0.50	0.458	45.1	787.92	$\pm$	10.75	$\pm$ 21.18	0.457	55.1	869.97	$\pm$	11.07	$\pm$ 23.77
0.50–0.60	0.547	45.2	568.95	$\pm$	8.41	$\pm$ 17.93	0.547	55.0	604.58	$\pm$	8.46	$\pm$ 20.12
0.60–0.72	0.654	45.1	350.49	$\pm$	6.06	$\pm$ 14.61	0.654	55.0	367.91	$\pm$	6.21	$\pm$ 16.81
0.72–0.90	0.798	45.0	167.71	$\pm$	3.41	$\pm$ 10.06	0.797	55.1	173.38	$\pm$	3.50	$\pm$ 11.19
0.90–1.25	1.032	44.9	48.13	$\pm$	1.29	$\pm$ 4.60	1.024	55.1	39.02	$\pm$	1.15	$\pm$ 4.01

	$60 < \theta < 75$						$75 < \theta < 90$					
p_T	$\langle p_\mathrm{T}\rangle$	$\langle\theta\rangle$	$\mathrm{d}^2\sigma/\mathrm{d}p\mathrm{d}\Omega$				$\langle p_\mathrm{T}\rangle$	$\langle\theta\rangle$	$\mathrm{d}^2\sigma/\mathrm{d}p\mathrm{d}\Omega$			
0.50–0.60	0.545	67.6	579.90	$\pm$	6.54	$\pm$ 20.96						
0.60–0.72	0.653	67.2	333.91	$\pm$	4.71	$\pm$ 18.06	0.652	81.9	253.03	$\pm$	3.87	$\pm$ 17.88
0.72–0.90	0.796	67.1	145.55	$\pm$	2.62	$\pm$ 12.06	0.793	81.6	94.39	$\pm$	2.03	$\pm$ 9.35
0.90–1.25	1.026	66.6	32.92	$\pm$	0.88	$\pm$ 4.53	1.015	81.6	14.62	$\pm$	0.59	$\pm$ 2.36

	$90 < \theta < 105$						$105 < \theta < 125$					
p_T	$\langle p_\mathrm{T}\rangle$	$\langle\theta\rangle$	$\mathrm{d}^2\sigma/\mathrm{d}p\mathrm{d}\Omega$				$\langle p_\mathrm{T}\rangle$	$\langle\theta\rangle$	$\mathrm{d}^2\sigma/\mathrm{d}p\mathrm{d}\Omega$			
0.42–0.50							0.458	113.6	352.54	$\pm$	4.92	$\pm$ 18.54
0.50–0.60							0.543	113.0	163.19	$\pm$	2.94	$\pm$ 14.94
0.60–0.72	0.651	97.3	149.06	$\pm$	2.91	$\pm$ 13.42	0.651	113.0	61.54	$\pm$	1.75	$\pm$ 8.59
0.72–0.90	0.792	97.1	51.49	$\pm$	1.52	$\pm$ 5.95	0.792	112.7	15.09	$\pm$	0.77	$\pm$ 3.31
0.90–1.25	1.015	96.7	5.67	$\pm$	0.37	$\pm$ 1.11						

Table A.17: Double-differential inclusive cross-section $\mathrm{d}^2\sigma/\mathrm{d}p\mathrm{d}\Omega$ [mb/(GeV/c sr)] of the production of π^+'s in π^- + Ta $\rightarrow \pi^+$ + X interactions with -5.0 GeV/c beam momentum; the first error is statistical, the second systematic; p_T in GeV/c, polar angle θ in degrees.

	$20 < \theta < 30$					$30 < \theta < 40$				
p_T	$\langle p_\mathrm{T}\rangle$	$\langle\theta\rangle$	$\mathrm{d}^2\sigma/\mathrm{d}p\mathrm{d}\Omega$			$\langle p_\mathrm{T}\rangle$	$\langle\theta\rangle$	$\mathrm{d}^2\sigma/\mathrm{d}p\mathrm{d}\Omega$		
0.10–0.13	0.116	25.1	313.85 ± 12.72	±	24.22	0.116	35.0	298.42 ± 11.92	±	22.16
0.13–0.16	0.146	24.7	349.23 ± 12.00	±	20.59	0.145	34.8	318.57 ± 11.41	±	19.22
0.16–0.20	0.180	25.0	406.36 ± 11.11	±	20.71	0.179	34.8	300.07 ± 9.16	±	14.93
0.20–0.24	0.220	24.9	394.38 ± 10.76	±	17.36	0.220	34.9	333.44 ± 9.86	±	14.69
0.24–0.30	0.269	24.9	383.84 ± 8.62	±	13.95	0.269	34.8	300.98 ± 7.51	±	10.63
0.30–0.36	0.327	24.9	306.95 ± 7.68	±	9.90	0.327	34.8	256.97 ± 6.94	±	7.95
0.36–0.42	0.388	24.9	252.76 ± 7.01	±	8.87	0.387	34.8	218.04 ± 6.45	±	6.60
0.42–0.50	0.456	24.9	177.66 ± 5.00	±	7.06	0.456	34.8	170.10 ± 5.02	±	6.55
0.50–0.60	0.543	25.0	109.03 ± 3.32	±	5.75	0.544	34.9	98.68 ± 3.18	±	4.72
0.60–0.72	0.651	25.1	56.51 ± 2.06	±	4.48	0.649	34.8	62.27 ± 2.28	±	4.53
0.72–0.90						0.786	34.9	23.62 ± 0.99	±	2.65

	$40 < \theta < 50$					$50 < \theta < 60$				
p_T	$\langle p_\mathrm{T}\rangle$	$\langle\theta\rangle$	$\mathrm{d}^2\sigma/\mathrm{d}p\mathrm{d}\Omega$			$\langle p_\mathrm{T}\rangle$	$\langle\theta\rangle$	$\mathrm{d}^2\sigma/\mathrm{d}p\mathrm{d}\Omega$		
0.10–0.13	0.116	44.9	260.88 ± 11.27	±	19.88					
0.13–0.16	0.145	44.7	283.00 ± 10.49	±	16.90	0.145	55.1	281.39 ± 10.79	±	17.41
0.16–0.20	0.180	44.9	265.33 ± 8.54	±	13.36	0.179	55.0	281.22 ± 9.02	±	13.96
0.20–0.24	0.220	44.9	264.87 ± 8.67	±	11.60	0.220	54.9	239.73 ± 8.05	±	10.28
0.24–0.30	0.269	44.8	239.58 ± 6.65	±	8.52	0.269	54.8	203.56 ± 6.21	±	7.16
0.30–0.36	0.329	44.9	219.40 ± 6.54	±	7.11	0.330	54.9	175.84 ± 5.97	±	6.37
0.36–0.42	0.389	44.9	197.56 ± 6.34	±	7.02	0.390	54.7	148.60 ± 5.45	±	5.25
0.42–0.50	0.459	44.8	136.23 ± 4.45	±	4.82	0.458	54.7	112.75 ± 4.08	±	4.46
0.50–0.60	0.547	44.6	96.27 ± 3.28	±	4.50	0.546	54.6	70.04 ± 2.84	±	3.62
0.60–0.72	0.654	44.7	53.86 ± 2.23	±	3.77	0.656	54.8	49.79 ± 2.18	±	3.62
0.72–0.90	0.796	44.6	23.71 ± 1.09	±	2.40	0.794	54.6	18.83 ± 1.02	±	1.93
0.90–1.25						1.027	54.5	4.73 ± 0.31	±	0.77

	$60 < \theta < 75$					$75 < \theta < 90$				
p_T	$\langle p_\mathrm{T}\rangle$	$\langle\theta\rangle$	$\mathrm{d}^2\sigma/\mathrm{d}p\mathrm{d}\Omega$			$\langle p_\mathrm{T}\rangle$	$\langle\theta\rangle$	$\mathrm{d}^2\sigma/\mathrm{d}p\mathrm{d}\Omega$		
0.13–0.16	0.146	67.0	243.21 ± 9.40	±	15.54					
0.16–0.20	0.179	67.3	259.65 ± 7.25	±	12.68	0.180	81.6	219.18 ± 8.00	±	16.11
0.20–0.24	0.219	67.2	200.53 ± 6.17	±	8.21	0.219	81.8	203.21 ± 7.00	±	11.55
0.24–0.30	0.269	67.1	179.42 ± 4.89	±	6.56	0.267	81.8	133.86 ± 4.44	±	5.65
0.30–0.36	0.328	67.1	131.64 ± 4.29	±	5.32	0.328	82.0	89.71 ± 3.64	±	4.34
0.36–0.42	0.389	66.9	104.86 ± 3.79	±	4.35	0.390	81.9	69.22 ± 3.16	±	3.53
0.42–0.50	0.457	66.9	81.09 ± 2.91	±	4.08	0.459	81.9	52.00 ± 2.38	±	3.31
0.50–0.60	0.546	66.9	55.27 ± 2.12	±	3.53	0.544	81.5	34.02 ± 1.67	±	2.61
0.60–0.72	0.657	66.4	34.87 ± 1.56	±	3.19	0.650	81.4	15.55 ± 1.03	±	1.64
0.72–0.90	0.795	66.4	13.20 ± 0.69	±	1.56	0.792	80.8	5.89 ± 0.46	±	0.84
0.90–1.25	1.034	66.0	2.49 ± 0.17	±	0.48	1.018	81.1	0.98 ± 0.10	±	0.23

	$90 < \theta < 105$					$105 < \theta < 125$				
p_T	$\langle p_\mathrm{T}\rangle$	$\langle\theta\rangle$	$\mathrm{d}^2\sigma/\mathrm{d}p\mathrm{d}\Omega$			$\langle p_\mathrm{T}\rangle$	$\langle\theta\rangle$	$\mathrm{d}^2\sigma/\mathrm{d}p\mathrm{d}\Omega$		
0.13–0.16						0.145	114.9	197.77 ± 7.54	±	11.16
0.16–0.20	0.180	97.8	202.07 ± 7.89	±	15.60	0.179	114.4	142.94 ± 4.79	±	5.43
0.20–0.24	0.219	97.7	147.36 ± 5.77	±	6.14	0.219	113.9	96.94 ± 3.82	±	3.58
0.24–0.30	0.268	97.2	101.53 ± 3.87	±	4.21	0.267	113.8	60.06 ± 2.48	±	2.62
0.30–0.36	0.329	97.4	60.54 ± 2.93	±	2.91	0.327	114.5	36.10 ± 1.93	±	2.22
0.36–0.42	0.389	96.4	46.27 ± 2.68	±	3.39	0.388	113.2	26.72 ± 1.67	±	2.19
0.42–0.50	0.457	97.2	33.78 ± 1.88	±	2.69	0.453	112.9	13.36 ± 0.97	±	1.42
0.50–0.60	0.546	97.0	20.12 ± 1.29	±	2.15	0.545	112.8	6.10 ± 0.57	±	0.87
0.60–0.72	0.652	96.6	7.76 ± 0.68	±	1.11	0.649	112.4	1.92 ± 0.27	±	0.39
0.72–0.90	0.792	96.4	2.28 ± 0.27	±	0.46	0.783	112.5	0.34 ± 0.07	±	0.11
0.90–1.25	1.029	96.9	0.12 ± 0.02	±	0.05	1.056	115.8	0.03 ± 0.02	±	0.02

Table A.18: Double-differential inclusive cross-section $\mathrm{d}^2\sigma/\mathrm{d}p\mathrm{d}\Omega$ [mb/(GeV/c sr)] of the production of π^-'s in π^- + Ta $\rightarrow$ π^- + X interactions with -5.0 GeV/c beam momentum; the first error is statistical, the second systematic; p_T in GeV/c, polar angle θ in degrees.

	$20 < \theta < 30$			$30 < \theta < 40$		
p_T	$\langle p_\mathrm{T}\rangle$	$\langle\theta\rangle$	$\mathrm{d}^2\sigma/\mathrm{d}p\mathrm{d}\Omega$	$\langle p_\mathrm{T}\rangle$	$\langle\theta\rangle$	$\mathrm{d}^2\sigma/\mathrm{d}p\mathrm{d}\Omega$
0.10–0.13	0.116	25.0	518.05 ± 16.62 ± 38.94	0.115	35.0	538.95 ± 16.82 ± 40.64
0.13–0.16	0.145	25.0	568.86 ± 15.85 ± 33.58	0.146	35.0	472.34 ± 14.07 ± 28.25
0.16–0.20	0.180	25.0	629.37 ± 14.14 ± 31.50	0.180	34.9	512.06 ± 12.63 ± 26.09
0.20–0.24	0.221	24.9	592.76 ± 13.56 ± 24.99	0.221	34.9	483.52 ± 12.08 ± 20.37
0.24–0.30	0.271	24.9	526.38 ± 10.28 ± 17.62	0.270	34.8	463.05 ± 9.51 ± 15.59
0.30–0.36	0.329	24.8	461.27 ± 9.61 ± 13.34	0.330	34.8	388.42 ± 8.75 ± 11.20
0.36–0.42	0.390	25.0	355.99 ± 8.59 ± 11.49	0.391	34.9	338.54 ± 8.31 ± 10.41
0.42–0.50	0.459	25.1	262.23 ± 6.35 ± 9.88	0.460	34.9	244.12 ± 6.07 ± 8.76
0.50–0.60	0.549	24.9	175.95 ± 4.59 ± 9.05	0.549	34.9	156.08 ± 4.33 ± 7.76
0.60–0.72	0.659	25.1	106.30 ± 3.27 ± 7.68	0.659	34.9	90.76 ± 2.97 ± 6.35
0.72–0.90				0.803	34.9	43.68 ± 1.75 ± 4.37

	$40 < \theta < 50$			$50 < \theta < 60$		
p_T	$\langle p_\mathrm{T}\rangle$	$\langle\theta\rangle$	$\mathrm{d}^2\sigma/\mathrm{d}p\mathrm{d}\Omega$	$\langle p_\mathrm{T}\rangle$	$\langle\theta\rangle$	$\mathrm{d}^2\sigma/\mathrm{d}p\mathrm{d}\Omega$
0.10–0.13	0.115	45.0	450.25 ± 15.37 ± 34.70			
0.13–0.16	0.145	44.9	434.13 ± 13.55 ± 26.22	0.145	55.0	417.17 ± 13.64 ± 25.77
0.16–0.20	0.179	44.9	421.30 ± 11.20 ± 21.26	0.179	54.9	397.61 ± 11.20 ± 20.18
0.20–0.24	0.220	44.8	395.69 ± 10.80 ± 16.90	0.219	54.8	313.77 ± 9.43 ± 13.29
0.24–0.30	0.269	44.8	355.04 ± 8.37 ± 12.04	0.270	54.9	293.27 ± 7.70 ± 10.38
0.30–0.36	0.330	44.8	319.20 ± 8.06 ± 9.76	0.329	54.9	251.89 ± 7.17 ± 7.92
0.36–0.42	0.389	44.7	265.69 ± 7.31 ± 8.17	0.390	54.7	211.82 ± 6.65 ± 7.54
0.42–0.50	0.458	44.9	209.68 ± 5.66 ± 8.04	0.457	54.8	150.01 ± 4.71 ± 5.96
0.50–0.60	0.545	44.9	138.84 ± 4.07 ± 7.31	0.546	54.7	111.91 ± 3.70 ± 6.19
0.60–0.72	0.653	44.9	77.08 ± 2.78 ± 5.71	0.655	54.7	64.92 ± 2.61 ± 5.05
0.72–0.90	0.798	45.2	38.28 ± 1.63 ± 4.03	0.800	54.7	28.81 ± 1.42 ± 3.12
0.90–1.25				1.029	54.8	7.51 ± 0.51 ± 1.23

	$60 < \theta < 75$			$75 < \theta < 90$		
p_T	$\langle p_\mathrm{T}\rangle$	$\langle\theta\rangle$	$\mathrm{d}^2\sigma/\mathrm{d}p\mathrm{d}\Omega$	$\langle p_\mathrm{T}\rangle$	$\langle\theta\rangle$	$\mathrm{d}^2\sigma/\mathrm{d}p\mathrm{d}\Omega$
0.13–0.16	0.145	67.3	406.62 ± 11.99 ± 23.99			
0.16–0.20	0.179	67.6	339.56 ± 8.50 ± 15.68	0.180	81.6	316.96 ± 9.71 ± 20.38
0.20–0.24	0.219	67.3	290.88 ± 7.59 ± 11.24	0.219	81.9	267.18 ± 8.17 ± 15.31
0.24–0.30	0.269	67.0	229.98 ± 5.62 ± 7.98	0.269	81.8	184.89 ± 5.49 ± 10.81
0.30–0.36	0.328	66.8	190.81 ± 5.23 ± 7.25	0.327	81.6	121.19 ± 4.21 ± 5.11
0.36–0.42	0.389	66.8	140.55 ± 4.45 ± 5.52	0.388	81.7	91.30 ± 3.71 ± 4.91
0.42–0.50	0.457	67.0	111.67 ± 3.41 ± 5.24	0.457	82.0	74.83 ± 2.86 ± 4.69
0.50–0.60	0.546	67.0	77.62 ± 2.57 ± 5.05	0.546	81.5	47.07 ± 2.08 ± 4.12
0.60–0.72	0.653	67.0	43.09 ± 1.73 ± 3.75	0.654	81.8	24.97 ± 1.37 ± 2.80
0.72–0.90	0.793	66.9	21.29 ± 1.00 ± 2.56	0.794	81.1	8.56 ± 0.63 ± 1.27
0.90–1.25	1.018	66.7	3.86 ± 0.27 ± 0.70	1.020	80.7	1.48 ± 0.15 ± 0.35

	$90 < \theta < 105$			$105 < \theta < 125$		
p_T	$\langle p_\mathrm{T}\rangle$	$\langle\theta\rangle$	$\mathrm{d}^2\sigma/\mathrm{d}p\mathrm{d}\Omega$	$\langle p_\mathrm{T}\rangle$	$\langle\theta\rangle$	$\mathrm{d}^2\sigma/\mathrm{d}p\mathrm{d}\Omega$
0.13–0.16				0.144	114.4	320.17 ± 12.37 ± 15.58
0.16–0.20	0.179	97.9	313.20 ± 10.58 ± 29.43	0.178	114.1	198.04 ± 5.76 ± 7.12
0.20–0.24	0.219	97.9	207.86 ± 7.24 ± 11.35	0.218	113.9	122.68 ± 4.39 ± 4.53
0.24–0.30	0.268	97.5	135.87 ± 4.72 ± 7.77	0.267	114.2	74.82 ± 2.76 ± 3.54
0.30–0.36	0.327	97.3	86.72 ± 3.71 ± 5.43	0.329	113.6	48.23 ± 2.25 ± 3.26
0.36–0.42	0.389	97.2	63.46 ± 3.14 ± 4.66	0.388	113.4	33.70 ± 1.93 ± 3.14
0.42–0.50	0.458	97.5	47.15 ± 2.35 ± 4.36	0.456	113.2	19.67 ± 1.24 ± 2.33
0.50–0.60	0.545	96.6	27.80 ± 1.59 ± 3.31	0.540	111.1	7.36 ± 0.66 ± 1.16
0.60–0.72	0.653	96.4	10.78 ± 0.85 ± 1.66	0.645	113.1	1.97 ± 0.27 ± 0.44
0.72–0.90	0.794	97.0	2.71 ± 0.31 ± 0.59	0.788	111.0	0.43 ± 0.09 ± 0.15
0.90–1.25	1.017	97.1	0.25 ± 0.05 ± 0.10	1.007	112.7	0.05 ± 0.02 ± 0.04

Table A.19: Double-differential inclusive cross-section $\mathrm{d}^2\sigma/\mathrm{d}p\mathrm{d}\Omega$ [mb/(GeV/c sr)] of the production of protons in p + Ta $\rightarrow$ p + X interactions with $+8.0$ GeV/c beam momentum; the first error is statistical, the second systematic; p_T in GeV/c, polar angle θ in degrees.

	$20 < \theta < 30$					$30 < \theta < 40$				
p_T	$\langle p_\mathrm{T}\rangle$	$\langle\theta\rangle$	$\mathrm{d}^2\sigma/\mathrm{d}p\mathrm{d}\Omega$			$\langle p_\mathrm{T}\rangle$	$\langle\theta\rangle$	$\mathrm{d}^2\sigma/\mathrm{d}p\mathrm{d}\Omega$		
0.20–0.24	0.220	25.2	1519.76	± 21.36	± 81.33					
0.24–0.30	0.269	25.3	1362.58	± 16.11	± 65.81	0.271	34.9	1550.36	± 16.95	± 67.55
0.30–0.36	0.329	25.3	1060.74	± 14.66	± 52.11	0.329	35.1	1392.31	± 15.61	± 51.92
0.36–0.42	0.389	25.3	845.75	± 13.37	± 43.97	0.389	35.1	1074.18	± 14.25	± 41.04
0.42–0.50	0.458	25.3	634.25	± 10.03	± 34.16	0.458	35.2	821.25	± 11.23	± 37.04
0.50–0.60	0.547	25.3	432.51	± 7.35	± 25.95	0.547	35.2	607.41	± 8.86	± 32.26
0.60–0.72	0.656	25.3	299.28	± 5.71	± 21.12	0.654	35.2	380.83	± 6.44	± 24.63
0.72–0.90						0.798	35.1	206.23	± 3.91	± 17.98

	$40 < \theta < 50$					$50 < \theta < 60$				
p_T	$\langle p_\mathrm{T}\rangle$	$\langle\theta\rangle$	$\mathrm{d}^2\sigma/\mathrm{d}p\mathrm{d}\Omega$			$\langle p_\mathrm{T}\rangle$	$\langle\theta\rangle$	$\mathrm{d}^2\sigma/\mathrm{d}p\mathrm{d}\Omega$		
0.30–0.36	0.331	45.2	1541.91	± 37.40	± 51.85					
0.36–0.42	0.392	45.1	1293.58	± 14.89	± 36.30	0.392	55.1	1328.38	± 14.38	± 43.34
0.42–0.50	0.462	45.1	973.51	± 11.76	± 33.69	0.462	55.0	1051.25	± 11.54	± 29.04
0.50–0.60	0.553	45.1	665.33	± 9.20	± 36.03	0.553	55.0	736.72	± 9.09	± 29.27
0.60–0.72	0.664	45.1	430.18	± 6.98	± 29.42	0.663	55.0	456.40	± 7.02	± 28.89
0.72–0.90	0.812	45.1	220.14	± 4.18	± 20.88	0.811	54.9	226.57	± 4.19	± 20.26
0.90–1.25	1.054	45.0	64.47	± 1.66	± 9.07	1.056	54.9	61.36	± 1.62	± 8.87

	$60 < \theta < 75$					$75 < \theta < 90$				
p_T	$\langle p_\mathrm{T}\rangle$	$\langle\theta\rangle$	$\mathrm{d}^2\sigma/\mathrm{d}p\mathrm{d}\Omega$			$\langle p_\mathrm{T}\rangle$	$\langle\theta\rangle$	$\mathrm{d}^2\sigma/\mathrm{d}p\mathrm{d}\Omega$		
0.50–0.60	0.552	67.4	678.79	± 6.63	± 26.82					
0.60–0.72	0.663	67.3	422.02	± 5.20	± 25.10	0.661	81.7	312.17	± 4.13	± 22.11
0.72–0.90	0.811	67.1	198.77	± 3.17	± 19.52	0.808	81.6	125.51	± 2.34	± 12.88
0.90–1.25	1.050	66.8	52.14	± 1.22	± 8.37	1.043	81.4	26.54	± 0.88	± 4.69

	$90 < \theta < 105$					$105 < \theta < 125$				
p_T	$\langle p_\mathrm{T}\rangle$	$\langle\theta\rangle$	$\mathrm{d}^2\sigma/\mathrm{d}p\mathrm{d}\Omega$			$\langle p_\mathrm{T}\rangle$	$\langle\theta\rangle$	$\mathrm{d}^2\sigma/\mathrm{d}p\mathrm{d}\Omega$		
0.42–0.50						0.463	113.6	375.35	± 4.61	± 22.53
0.50–0.60						0.548	112.9	166.84	± 2.84	± 15.70
0.60–0.72	0.658	97.1	177.49	± 3.09	± 15.95	0.657	112.6	64.67	± 1.84	± 9.36
0.72–0.90	0.804	96.6	61.93	± 1.70	± 7.48	0.802	112.2	15.31	± 0.81	± 3.46

Table A.20: Double-differential inclusive cross-section $\mathrm{d}^2\sigma/\mathrm{d}p\mathrm{d}\Omega$ [mb/(GeV/c sr)] of the production of π^+'s in p + Ta $\rightarrow$ π^+ + X interactions with $+8.0$ GeV/c beam momentum; the first error is statistical, the second systematic; p_T in GeV/c, polar angle θ in degrees.

	$20 < \theta < 30$					$30 < \theta < 40$				
p_T	$\langle p_\mathrm{T}\rangle$	$\langle\theta\rangle$	$\mathrm{d}^2\sigma/\mathrm{d}p\mathrm{d}\Omega$			$\langle p_\mathrm{T}\rangle$	$\langle\theta\rangle$	$\mathrm{d}^2\sigma/\mathrm{d}p\mathrm{d}\Omega$		
0.10–0.13	0.115	25.1	448.06 ± 15.39	±	35.36	0.116	34.9	423.17 ± 14.15	±	31.54
0.13–0.16	0.146	24.7	490.92 ± 14.33	±	29.21	0.146	34.9	407.27 ± 12.62	±	23.35
0.16–0.20	0.180	24.8	543.60 ± 12.57	±	27.39	0.180	34.9	448.44 ± 11.25	±	21.77
0.20–0.24	0.220	25.0	545.59 ± 12.56	±	24.51	0.220	34.8	448.39 ± 11.22	±	19.02
0.24–0.30	0.269	24.9	516.19 ± 9.81	±	18.94	0.269	34.9	433.33 ± 9.03	±	15.61
0.30–0.36	0.329	25.0	422.79 ± 8.81	±	13.66	0.329	34.8	353.72 ± 8.14	±	11.14
0.36–0.42	0.389	24.9	338.21 ± 7.74	±	10.55	0.389	34.7	283.23 ± 7.22	±	8.59
0.42–0.50	0.458	24.8	239.05 ± 5.48	±	8.76	0.459	34.8	219.57 ± 5.48	±	7.76
0.50–0.60	0.547	24.9	163.48 ± 3.95	±	8.57	0.547	34.8	134.94 ± 3.63	±	6.49
0.60–0.72	0.656	24.8	100.31 ± 2.62	±	7.80	0.654	34.7	81.17 ± 2.44	±	5.75
0.72–0.90						0.795	34.7	35.78 ± 1.14	±	4.02

	$40 < \theta < 50$					$50 < \theta < 60$				
p_T	$\langle p_\mathrm{T}\rangle$	$\langle\theta\rangle$	$\mathrm{d}^2\sigma/\mathrm{d}p\mathrm{d}\Omega$			$\langle p_\mathrm{T}\rangle$	$\langle\theta\rangle$	$\mathrm{d}^2\sigma/\mathrm{d}p\mathrm{d}\Omega$		
0.10–0.13	0.116	44.9	338.16 ± 12.72	±	25.39					
0.13–0.16	0.146	45.0	366.60 ± 11.68	±	21.31	0.146	54.9	337.74 ± 11.34	±	20.49
0.16–0.20	0.180	45.0	418.30 ± 10.71	±	20.28	0.180	54.9	318.36 ± 9.11	±	15.34
0.20–0.24	0.221	44.8	369.80 ± 10.07	±	15.44	0.220	55.0	341.45 ± 9.60	±	13.88
0.24–0.30	0.271	44.7	333.15 ± 7.85	±	11.76	0.271	54.9	291.52 ± 7.33	±	10.02
0.30–0.36	0.332	44.8	284.96 ± 7.29	±	8.90	0.330	54.8	226.58 ± 6.55	±	7.50
0.36–0.42	0.391	44.9	236.61 ± 6.73	±	7.82	0.392	54.6	182.53 ± 5.87	±	6.26
0.42–0.50	0.461	44.8	171.29 ± 4.75	±	5.93	0.463	54.8	133.83 ± 4.24	±	5.02
0.50–0.60	0.553	44.8	113.24 ± 3.49	±	5.40	0.552	54.8	84.76 ± 3.00	±	4.31
0.60–0.72	0.663	44.6	62.60 ± 2.21	±	4.21	0.664	54.5	47.66 ± 1.99	±	3.41
0.72–0.90	0.807	44.7	28.79 ± 1.10	±	2.94	0.810	54.6	21.83 ± 1.01	±	2.23
0.90–1.25						1.050	54.2	4.46 ± 0.25	±	0.77

	$60 < \theta < 75$					$75 < \theta < 90$				
p_T	$\langle p_\mathrm{T}\rangle$	$\langle\theta\rangle$	$\mathrm{d}^2\sigma/\mathrm{d}p\mathrm{d}\Omega$			$\langle p_\mathrm{T}\rangle$	$\langle\theta\rangle$	$\mathrm{d}^2\sigma/\mathrm{d}p\mathrm{d}\Omega$		
0.13–0.16	0.146	67.4	274.10 ± 9.35	±	16.91					
0.16–0.20	0.180	67.3	269.25 ± 6.82	±	13.08	0.181	81.7	232.98 ± 7.52	±	13.83
0.20–0.24	0.221	67.2	264.59 ± 6.89	±	10.44	0.221	81.9	220.07 ± 6.70	±	9.62
0.24–0.30	0.270	67.1	225.88 ± 5.35	±	8.20	0.269	81.9	175.27 ± 4.94	±	8.23
0.30–0.36	0.329	66.9	165.22 ± 4.64	±	5.97	0.331	81.7	114.23 ± 4.05	±	6.16
0.36–0.42	0.392	66.9	125.61 ± 4.05	±	4.96	0.391	81.4	81.93 ± 3.41	±	4.61
0.42–0.50	0.462	66.7	90.87 ± 2.90	±	3.93	0.460	81.8	53.71 ± 2.30	±	3.08
0.50–0.60	0.552	66.7	57.64 ± 2.06	±	3.48	0.551	81.6	31.81 ± 1.57	±	2.42
0.60–0.72	0.662	66.5	31.07 ± 1.32	±	2.61	0.662	81.4	15.43 ± 0.94	±	1.58
0.72–0.90	0.805	66.5	11.81 ± 0.60	±	1.42	0.804	81.2	5.19 ± 0.41	±	0.74
0.90–1.25	1.039	66.3	3.00 ± 0.18	±	0.57	1.042	81.4	0.92 ± 0.09	±	0.21

	$90 < \theta < 105$					$105 < \theta < 125$				
p_T	$\langle p_\mathrm{T}\rangle$	$\langle\theta\rangle$	$\mathrm{d}^2\sigma/\mathrm{d}p\mathrm{d}\Omega$			$\langle p_\mathrm{T}\rangle$	$\langle\theta\rangle$	$\mathrm{d}^2\sigma/\mathrm{d}p\mathrm{d}\Omega$		
0.13–0.16						0.145	114.5	180.90 ± 6.12	±	10.08
0.16–0.20	0.181	97.8	213.16 ± 7.24	±	11.14	0.180	114.1	155.70 ± 4.47	±	6.43
0.20–0.24	0.220	97.7	175.98 ± 5.99	±	6.94	0.220	113.7	112.03 ± 3.90	±	3.84
0.24–0.30	0.269	97.3	116.79 ± 4.05	±	5.58	0.268	113.5	70.10 ± 2.64	±	3.08
0.30–0.36	0.330	97.3	77.52 ± 3.34	±	4.45	0.329	113.4	35.54 ± 1.83	±	2.14
0.36–0.42	0.390	96.6	47.57 ± 2.53	±	2.93	0.391	113.5	25.11 ± 1.54	±	2.06
0.42–0.50	0.463	97.0	32.35 ± 1.81	±	2.64	0.458	112.8	12.35 ± 0.90	±	1.33
0.50–0.60	0.551	96.4	16.07 ± 1.08	±	1.71	0.554	113.1	4.61 ± 0.48	±	0.66
0.60–0.72	0.658	96.0	7.19 ± 0.63	±	1.03	0.652	111.7	1.43 ± 0.24	±	0.27
0.72–0.90	0.809	96.4	2.55 ± 0.29	±	0.49	0.812	111.4	0.37 ± 0.08	±	0.10
0.90–1.25	1.049	95.4	0.35 ± 0.06	±	0.11	1.080	113.4	0.05 ± 0.02	±	0.02

Table A.21: Double-differential inclusive cross-section $\mathrm{d}^2\sigma/\mathrm{d}p\mathrm{d}\Omega$ [mb/(GeV/c sr)] of the production of π^-'s in p + Ta $\rightarrow \pi^-$ + X interactions with $+8.0$ GeV/c beam momentum; the first error is statistical, the second systematic; p_T in GeV/c, polar angle θ in degrees.

	$20 < \theta < 30$					$30 < \theta < 40$				
p_T	$\langle p_\mathrm{T}\rangle$	$\langle\theta\rangle$	$\mathrm{d}^2\sigma/\mathrm{d}p\mathrm{d}\Omega$			$\langle p_\mathrm{T}\rangle$	$\langle\theta\rangle$	$\mathrm{d}^2\sigma/\mathrm{d}p\mathrm{d}\Omega$		
0.10–0.13	0.115	25.0	570.39 ± 16.61	±	43.49	0.116	34.9	558.31 ± 16.27	±	42.88
0.13–0.16	0.146	25.0	574.52 ± 15.37	±	35.56	0.145	34.9	520.42 ± 14.11	±	30.65
0.16–0.20	0.180	25.0	579.63 ± 12.76	±	28.74	0.180	34.9	499.76 ± 11.64	±	24.53
0.20–0.24	0.220	25.0	552.67 ± 12.21	±	22.70	0.220	34.9	490.87 ± 11.51	±	20.25
0.24–0.30	0.269	24.9	462.98 ± 9.17	±	16.31	0.269	34.9	411.29 ± 8.59	±	13.73
0.30–0.36	0.328	25.1	326.07 ± 7.57	±	9.39	0.329	34.9	327.85 ± 7.70	±	9.53
0.36–0.42	0.388	25.1	256.17 ± 6.73	±	7.71	0.388	34.9	244.79 ± 6.60	±	7.23
0.42–0.50	0.457	25.1	174.01 ± 4.83	±	6.61	0.456	34.9	168.06 ± 4.67	±	6.06
0.50–0.60	0.546	25.0	111.06 ± 3.37	±	5.76	0.544	35.0	108.38 ± 3.36	±	5.42
0.60–0.72	0.651	25.2	60.66 ± 2.26	±	4.43	0.653	35.1	51.21 ± 2.05	±	3.62
0.72–0.90						0.796	35.0	26.15 ± 1.19	±	2.63

	$40 < \theta < 50$					$50 < \theta < 60$				
p_T	$\langle p_\mathrm{T}\rangle$	$\langle\theta\rangle$	$\mathrm{d}^2\sigma/\mathrm{d}p\mathrm{d}\Omega$			$\langle p_\mathrm{T}\rangle$	$\langle\theta\rangle$	$\mathrm{d}^2\sigma/\mathrm{d}p\mathrm{d}\Omega$		
0.10–0.13	0.115	45.1	468.86 ± 15.09	±	36.02					
0.13–0.16	0.144	45.0	480.35 ± 13.46	±	28.69	0.144	55.0	445.60 ± 13.06	±	27.47
0.16–0.20	0.179	44.9	442.03 ± 10.88	±	21.86	0.179	55.0	395.64 ± 10.24	±	19.41
0.20–0.24	0.219	44.9	389.50 ± 10.20	±	16.28	0.218	54.8	326.01 ± 9.31	±	13.31
0.24–0.30	0.268	44.8	350.19 ± 8.00	±	12.22	0.267	54.9	283.32 ± 7.22	±	9.83
0.30–0.36	0.326	44.8	275.10 ± 7.12	±	8.51	0.326	54.8	229.76 ± 6.57	±	7.60
0.36–0.42	0.384	44.9	212.14 ± 6.24	±	6.71	0.386	54.6	165.91 ± 5.53	±	5.60
0.42–0.50	0.454	44.9	145.75 ± 4.36	±	5.54	0.454	54.7	132.75 ± 4.24	±	5.33
0.50–0.60	0.539	44.7	93.08 ± 3.08	±	4.93	0.540	55.0	77.91 ± 2.85	±	4.33
0.60–0.72	0.643	44.9	50.20 ± 2.05	±	3.75	0.645	54.9	36.32 ± 1.70	±	2.85
0.72–0.90	0.785	44.5	22.93 ± 1.11	±	2.43	0.783	54.4	12.38 ± 0.80	±	1.37
0.90–1.25						1.008	54.9	3.68 ± 0.30	±	0.62

	$60 < \theta < 75$					$75 < \theta < 90$				
p_T	$\langle p_\mathrm{T}\rangle$	$\langle\theta\rangle$	$\mathrm{d}^2\sigma/\mathrm{d}p\mathrm{d}\Omega$			$\langle p_\mathrm{T}\rangle$	$\langle\theta\rangle$	$\mathrm{d}^2\sigma/\mathrm{d}p\mathrm{d}\Omega$		
0.13–0.16	0.145	67.1	394.68 ± 11.07	±	23.19					
0.16–0.20	0.179	67.1	336.55 ± 7.78	±	15.41	0.179	81.9	295.98 ± 8.67	±	16.71
0.20–0.24	0.218	67.4	287.71 ± 7.32	±	11.16	0.218	82.0	232.96 ± 7.00	±	10.89
0.24–0.30	0.267	67.1	230.93 ± 5.43	±	8.38	0.266	81.7	174.66 ± 5.02	±	9.44
0.30–0.36	0.327	67.0	173.61 ± 4.74	±	6.49	0.325	81.6	112.47 ± 3.97	±	5.81
0.36–0.42	0.385	66.8	120.36 ± 3.91	±	4.70	0.385	81.7	79.31 ± 3.28	±	4.28
0.42–0.50	0.453	67.0	86.57 ± 2.79	±	3.95	0.452	81.6	53.97 ± 2.29	±	3.41
0.50–0.60	0.540	66.8	48.78 ± 1.87	±	3.09	0.539	81.7	30.13 ± 1.48	±	2.46
0.60–0.72	0.644	66.6	24.83 ± 1.18	±	2.16	0.638	81.8	12.84 ± 0.83	±	1.44
0.72–0.90	0.775	66.6	9.58 ± 0.57	±	1.17	0.780	81.3	4.80 ± 0.43	±	0.73
0.90–1.25	1.012	66.2	1.88 ± 0.16	±	0.36	1.022	80.7	0.67 ± 0.10	±	0.15

	$90 < \theta < 105$					$105 < \theta < 125$				
p_T	$\langle p_\mathrm{T}\rangle$	$\langle\theta\rangle$	$\mathrm{d}^2\sigma/\mathrm{d}p\mathrm{d}\Omega$			$\langle p_\mathrm{T}\rangle$	$\langle\theta\rangle$	$\mathrm{d}^2\sigma/\mathrm{d}p\mathrm{d}\Omega$		
0.13–0.16						0.144	114.5	241.80 ± 7.53	±	12.15
0.16–0.20	0.176	97.8	281.67 ± 47.43	±	13.69	0.178	113.9	171.68 ± 4.85	±	6.24
0.20–0.24	0.218	97.5	198.72 ± 6.48	±	8.77	0.217	114.0	112.64 ± 4.00	±	4.11
0.24–0.30	0.267	97.3	124.02 ± 4.20	±	6.15	0.266	113.7	67.68 ± 2.56	±	3.31
0.30–0.36	0.325	97.3	75.25 ± 3.23	±	4.24	0.325	113.6	34.44 ± 1.79	±	2.37
0.36–0.42	0.384	97.4	51.07 ± 2.61	±	3.47	0.386	113.2	23.10 ± 1.43	±	2.16
0.42–0.50	0.452	97.0	27.99 ± 1.61	±	2.41	0.451	113.3	12.86 ± 0.92	±	1.57
0.50–0.60	0.540	97.0	16.87 ± 1.10	±	1.98	0.533	113.3	5.70 ± 0.53	±	0.92
0.60–0.72	0.641	96.8	6.13 ± 0.60	±	0.97	0.638	111.7	1.32 ± 0.22	±	0.28
0.72–0.90	0.792	96.4	1.50 ± 0.22	±	0.33	0.779	112.4	0.45 ± 0.10	±	0.13
0.90–1.25	1.010	96.6	0.16 ± 0.04	±	0.05					

Table A.22: Double-differential inclusive cross-section $\mathrm{d}^2\sigma/\mathrm{d}p\mathrm{d}\Omega$ [mb/(GeV/c sr)] of the production of protons in π^+ + Ta $\rightarrow$ p + X interactions with $+8.0$ GeV/c beam momentum; the first error is statistical, the second systematic; p_T in GeV/c, polar angle θ in degrees.

	$20 < \theta < 30$			$30 < \theta < 40$		
p_T	$\langle p_\mathrm{T}\rangle$	$\langle\theta\rangle$	$\mathrm{d}^2\sigma/\mathrm{d}p\mathrm{d}\Omega$	$\langle p_\mathrm{T}\rangle$	$\langle\theta\rangle$	$\mathrm{d}^2\sigma/\mathrm{d}p\mathrm{d}\Omega$
0.20–0.24	0.221	25.2	1292.78 ± 28.16 ± 69.78			
0.24–0.30	0.269	25.3	1178.60 ± 21.40 ± 57.45	0.271	34.9	1361.67 ± 22.56 ± 60.11
0.30–0.36	0.329	25.3	918.74 ± 19.54 ± 45.76	0.329	35.1	1186.40 ± 20.67 ± 45.03
0.36–0.42	0.388	25.4	707.36 ± 17.51 ± 37.52	0.389	35.1	959.76 ± 19.32 ± 37.35
0.42–0.50	0.458	25.4	534.25 ± 13.15 ± 29.22	0.459	35.2	735.96 ± 15.24 ± 33.75
0.50–0.60	0.545	25.4	357.84 ± 9.50 ± 21.71	0.547	35.1	516.19 ± 11.63 ± 27.71
0.60–0.72	0.656	25.3	236.63 ± 7.15 ± 16.78	0.654	35.2	321.32 ± 8.42 ± 20.94
0.72–0.90				0.799	35.1	162.29 ± 4.90 ± 14.20

	$40 < \theta < 50$			$50 < \theta < 60$		
p_T	$\langle p_\mathrm{T}\rangle$	$\langle\theta\rangle$	$\mathrm{d}^2\sigma/\mathrm{d}p\mathrm{d}\Omega$	$\langle p_\mathrm{T}\rangle$	$\langle\theta\rangle$	$\mathrm{d}^2\sigma/\mathrm{d}p\mathrm{d}\Omega$
0.30–0.36	0.331	45.1	1340.16 ± 21.28 ± 45.69			
0.36–0.42	0.392	45.1	1103.60 ± 19.71 ± 31.92	0.392	55.2	1151.84 ± 19.18 ± 39.17
0.42–0.50	0.462	45.1	843.12 ± 15.67 ± 29.72	0.463	55.1	936.01 ± 15.59 ± 26.88
0.50–0.60	0.554	45.1	569.98 ± 12.18 ± 31.18	0.553	55.1	615.56 ± 11.90 ± 24.88
0.60–0.72	0.663	45.1	354.33 ± 9.05 ± 24.37	0.664	55.0	387.53 ± 9.27 ± 24.84
0.72–0.90	0.813	45.1	185.56 ± 5.47 ± 17.67	0.811	54.9	189.44 ± 5.48 ± 17.07
0.90–1.25	1.055	45.0	53.49 ± 2.14 ± 7.53	1.051	54.9	49.07 ± 2.07 ± 7.11

	$60 < \theta < 75$			$75 < \theta < 90$		
p_T	$\langle p_\mathrm{T}\rangle$	$\langle\theta\rangle$	$\mathrm{d}^2\sigma/\mathrm{d}p\mathrm{d}\Omega$	$\langle p_\mathrm{T}\rangle$	$\langle\theta\rangle$	$\mathrm{d}^2\sigma/\mathrm{d}p\mathrm{d}\Omega$
0.50–0.60	0.552	67.5	606.81 ± 8.99 ± 24.45			
0.60–0.72	0.663	67.2	367.21 ± 6.96 ± 22.07	0.660	81.7	282.39 ± 5.64 ± 20.08
0.72–0.90	0.813	67.1	167.26 ± 4.18 ± 16.56	0.808	81.6	114.81 ± 3.22 ± 11.81
0.90–1.25	1.053	66.8	42.50 ± 1.58 ± 6.85	1.054	81.4	25.01 ± 1.23 ± 4.41

	$90 < \theta < 105$			$105 < \theta < 125$		
p_T	$\langle p_\mathrm{T}\rangle$	$\langle\theta\rangle$	$\mathrm{d}^2\sigma/\mathrm{d}p\mathrm{d}\Omega$	$\langle p_\mathrm{T}\rangle$	$\langle\theta\rangle$	$\mathrm{d}^2\sigma/\mathrm{d}p\mathrm{d}\Omega$
0.42–0.50				0.463	113.4	367.03 ± 6.81 ± 21.91
0.50–0.60				0.549	113.0	173.37 ± 4.17 ± 16.33
0.60–0.72	0.659	97.2	162.84 ± 4.25 ± 14.64	0.659	112.8	70.06 ± 2.73 ± 10.15
0.72–0.90	0.804	96.6	57.68 ± 2.35 ± 6.95	0.800	112.4	15.90 ± 1.18 ± 3.58

Table A.23: Double-differential inclusive cross-section $\mathrm{d}^2\sigma/\mathrm{d}p\mathrm{d}\Omega$ [mb/(GeV/c sr)] of the production of π^+'s in π^+ + Ta $\rightarrow \pi^+$ + X interactions with $+8.0$ GeV/c beam momentum; the first error is statistical, the second systematic; p_T in GeV/c, polar angle θ in degrees.

	$20 < \theta < 30$			$30 < \theta < 40$		
p_T	$\langle p_\mathrm{T}\rangle$	$\langle\theta\rangle$	$\mathrm{d}^2\sigma/\mathrm{d}p\mathrm{d}\Omega$	$\langle p_\mathrm{T}\rangle$	$\langle\theta\rangle$	$\mathrm{d}^2\sigma/\mathrm{d}p\mathrm{d}\Omega$
0.10–0.13	0.116	25.0	521.85 ± 23.45 ± 41.39	0.115	35.0	497.71 ± 22.04 ± 37.08
0.13–0.16	0.146	24.8	557.41 ± 21.88 ± 33.06	0.145	34.8	522.86 ± 20.32 ± 29.96
0.16–0.20	0.180	24.9	659.58 ± 19.81 ± 33.27	0.180	34.9	521.51 ± 17.34 ± 25.40
0.20–0.24	0.220	24.7	691.15 ± 20.19 ± 31.15	0.220	34.9	546.47 ± 17.74 ± 23.26
0.24–0.30	0.270	24.9	667.49 ± 16.01 ± 24.74	0.270	34.8	547.80 ± 14.58 ± 19.92
0.30–0.36	0.329	24.8	571.14 ± 14.69 ± 18.63	0.329	34.8	466.76 ± 13.43 ± 14.84
0.36–0.42	0.389	24.8	489.31 ± 13.41 ± 15.34	0.389	34.7	386.13 ± 12.10 ± 11.72
0.42–0.50	0.459	24.8	354.99 ± 9.68 ± 13.01	0.458	34.8	297.97 ± 9.17 ± 10.54
0.50–0.60	0.547	24.8	251.66 ± 7.16 ± 13.18	0.546	34.9	200.92 ± 6.42 ± 9.63
0.60–0.72	0.655	24.8	148.60 ± 4.75 ± 11.52	0.654	34.6	111.82 ± 4.17 ± 7.89
0.72–0.90				0.799	34.7	51.76 ± 2.08 ± 5.80

	$40 < \theta < 50$			$50 < \theta < 60$		
p_T	$\langle p_\mathrm{T}\rangle$	$\langle\theta\rangle$	$\mathrm{d}^2\sigma/\mathrm{d}p\mathrm{d}\Omega$	$\langle p_\mathrm{T}\rangle$	$\langle\theta\rangle$	$\mathrm{d}^2\sigma/\mathrm{d}p\mathrm{d}\Omega$
0.10–0.13	0.116	45.0	392.41 ± 20.00 ± 29.58			
0.13–0.16	0.146	44.7	463.57 ± 18.84 ± 26.91	0.146	54.8	366.07 ± 16.89 ± 22.16
0.16–0.20	0.180	45.0	466.86 ± 16.23 ± 22.69	0.181	54.9	350.19 ± 13.73 ± 16.91
0.20–0.24	0.221	44.8	460.20 ± 16.13 ± 19.34	0.221	55.0	360.15 ± 14.18 ± 14.72
0.24–0.30	0.271	44.7	396.13 ± 12.29 ± 14.21	0.270	54.7	318.55 ± 11.03 ± 11.25
0.30–0.36	0.332	44.8	393.41 ± 12.32 ± 12.44	0.331	54.7	275.96 ± 10.39 ± 9.31
0.36–0.42	0.392	44.7	286.18 ± 10.62 ± 9.48	0.392	54.8	241.93 ± 9.74 ± 8.31
0.42–0.50	0.463	44.7	219.58 ± 7.72 ± 7.57	0.462	54.6	163.31 ± 6.71 ± 6.08
0.50–0.60	0.552	44.7	154.51 ± 5.89 ± 7.33	0.554	54.6	112.25 ± 4.97 ± 5.66
0.60–0.72	0.666	44.6	90.21 ± 3.86 ± 6.03	0.664	54.6	63.22 ± 3.32 ± 4.48
0.72–0.90	0.810	44.5	40.67 ± 1.94 ± 4.12	0.806	54.6	31.31 ± 1.78 ± 3.17
0.90–1.25				1.046	54.6	5.99 ± 0.44 ± 1.03

	$60 < \theta < 75$			$75 < \theta < 90$		
p_T	$\langle p_\mathrm{T}\rangle$	$\langle\theta\rangle$	$\mathrm{d}^2\sigma/\mathrm{d}p\mathrm{d}\Omega$	$\langle p_\mathrm{T}\rangle$	$\langle\theta\rangle$	$\mathrm{d}^2\sigma/\mathrm{d}p\mathrm{d}\Omega$
0.13–0.16	0.146	66.7	318.03 ± 14.85 ± 20.80	0.152	81.1	192.23 ± 19.03 ± 48.43
0.16–0.20	0.180	67.1	300.20 ± 10.41 ± 14.53	0.181	81.8	281.09 ± 12.20 ± 18.72
0.20–0.24	0.221	67.3	304.84 ± 10.71 ± 12.15	0.221	81.8	242.81 ± 10.15 ± 11.06
0.24–0.30	0.270	67.0	255.23 ± 8.22 ± 9.75	0.271	81.7	196.12 ± 7.56 ± 9.84
0.30–0.36	0.331	66.8	204.59 ± 7.44 ± 7.62	0.331	81.8	143.35 ± 6.56 ± 8.01
0.36–0.42	0.392	66.8	165.41 ± 6.68 ± 6.57	0.391	81.6	93.43 ± 5.23 ± 5.28
0.42–0.50	0.461	66.8	105.47 ± 4.49 ± 4.54	0.462	82.1	68.20 ± 3.72 ± 3.86
0.50–0.60	0.553	66.7	74.85 ± 3.36 ± 4.49	0.554	81.6	45.45 ± 2.68 ± 3.42
0.60–0.72	0.660	67.0	45.88 ± 2.32 ± 3.83	0.664	81.8	26.23 ± 1.79 ± 2.66
0.72–0.90	0.805	66.6	17.33 ± 1.08 ± 2.07	0.800	81.9	7.59 ± 0.72 ± 1.07
0.90–1.25	1.053	66.5	3.58 ± 0.29 ± 0.68	1.040	80.3	1.17 ± 0.15 ± 0.27

	$90 < \theta < 105$			$105 < \theta < 125$		
p_T	$\langle p_\mathrm{T}\rangle$	$\langle\theta\rangle$	$\mathrm{d}^2\sigma/\mathrm{d}p\mathrm{d}\Omega$	$\langle p_\mathrm{T}\rangle$	$\langle\theta\rangle$	$\mathrm{d}^2\sigma/\mathrm{d}p\mathrm{d}\Omega$
0.13–0.16	0.152	99.4	163.56 ± 16.38 ± 28.88	0.142	112.8	265.81 ± 62.98 ± 13.54
0.16–0.20	0.181	97.9	227.08 ± 11.10 ± 13.92	0.179	114.3	170.87 ± 6.83 ± 6.57
0.20–0.24	0.221	97.6	199.17 ± 9.18 ± 8.23	0.219	114.5	119.92 ± 5.81 ± 4.10
0.24–0.30	0.269	97.8	152.62 ± 6.68 ± 7.56	0.268	114.3	78.17 ± 4.00 ± 3.44
0.30–0.36	0.331	97.2	92.43 ± 5.21 ± 5.26	0.330	114.1	47.17 ± 3.01 ± 2.78
0.36–0.42	0.394	96.9	62.62 ± 4.15 ± 3.78	0.391	113.4	32.75 ± 2.51 ± 2.63
0.42–0.50	0.461	97.1	42.37 ± 2.98 ± 3.40	0.460	113.5	16.75 ± 1.50 ± 1.77
0.50–0.60	0.553	96.7	23.13 ± 1.86 ± 2.43	0.547	113.1	5.97 ± 0.78 ± 0.84
0.60–0.72	0.664	96.4	10.36 ± 1.09 ± 1.46	0.646	112.6	3.29 ± 0.52 ± 0.61
0.72–0.90	0.803	95.1	3.25 ± 0.48 ± 0.62	0.794	114.8	0.28 ± 0.09 ± 0.07
0.90–1.25	1.081	95.6	0.48 ± 0.10 ± 0.14	1.019	109.4	0.08 ± 0.03 ± 0.03

Table A.24: Double-differential inclusive cross-section $\mathrm{d}^2\sigma/\mathrm{d}p\mathrm{d}\Omega$ [mb/(GeV/c sr)] of the production of π^-'s in π^+ + Ta $\rightarrow$ π^- + X interactions with $+8.0$ GeV/c beam momentum; the first error is statistical, the second systematic; p_T in GeV/c, polar angle θ in degrees.

	$20 < \theta < 30$					$30 < \theta < 40$				
p_T	$\langle p_\mathrm{T}\rangle$	$\langle\theta\rangle$	$\mathrm{d}^2\sigma/\mathrm{d}p\mathrm{d}\Omega$			$\langle p_\mathrm{T}\rangle$	$\langle\theta\rangle$	$\mathrm{d}^2\sigma/\mathrm{d}p\mathrm{d}\Omega$		
0.10–0.13	0.115	25.0	657.44 ± 25.83	±	52.07	0.115	34.9	546.53 ± 23.11	±	43.38
0.13–0.16	0.145	25.0	636.56 ± 23.23	±	40.08	0.145	34.9	549.07 ± 20.79	±	32.45
0.16–0.20	0.180	24.8	614.08 ± 18.61	±	30.83	0.179	34.9	565.22 ± 17.69	±	27.91
0.20–0.24	0.220	24.9	644.76 ± 18.81	±	26.77	0.219	34.7	516.70 ± 16.87	±	21.46
0.24–0.30	0.269	24.9	551.35 ± 14.29	±	19.84	0.269	34.8	455.26 ± 12.95	±	15.41
0.30–0.36	0.330	24.7	424.38 ± 12.30	±	12.29	0.329	34.8	389.93 ± 12.03	±	11.58
0.36–0.42	0.388	25.0	343.60 ± 11.16	±	10.28	0.387	34.9	296.79 ± 10.40	±	8.77
0.42–0.50	0.458	24.8	238.79 ± 8.05	±	9.04	0.458	34.9	213.16 ± 7.54	±	7.65
0.50–0.60	0.544	24.8	149.71 ± 5.59	±	7.70	0.545	35.0	133.80 ± 5.34	±	6.64
0.60–0.72	0.654	24.9	76.81 ± 3.64	±	5.55	0.655	34.9	67.95 ± 3.37	±	4.75
0.72–0.90						0.802	34.9	35.22 ± 1.98	±	3.51

	$40 < \theta < 50$					$50 < \theta < 60$				
p_T	$\langle p_\mathrm{T}\rangle$	$\langle\theta\rangle$	$\mathrm{d}^2\sigma/\mathrm{d}p\mathrm{d}\Omega$			$\langle p_\mathrm{T}\rangle$	$\langle\theta\rangle$	$\mathrm{d}^2\sigma/\mathrm{d}p\mathrm{d}\Omega$		
0.10–0.13	0.115	44.9	511.68 ± 22.83	±	39.41					
0.13–0.16	0.145	45.1	489.71 ± 19.54	±	29.35	0.145	54.8	433.97 ± 18.40	±	26.75
0.16–0.20	0.180	44.9	445.26 ± 15.54	±	22.13	0.179	54.8	397.34 ± 14.65	±	19.59
0.20–0.24	0.218	44.8	418.80 ± 15.11	±	17.62	0.218	54.7	331.02 ± 13.39	±	13.59
0.24–0.30	0.268	44.8	383.66 ± 12.01	±	13.70	0.268	54.6	301.98 ± 10.64	±	10.66
0.30–0.36	0.326	44.7	334.91 ± 11.28	±	10.61	0.327	54.8	257.32 ± 9.99	±	8.64
0.36–0.42	0.386	44.8	269.36 ± 10.10	±	8.62	0.385	54.8	204.32 ± 8.80	±	6.92
0.42–0.50	0.454	44.7	168.15 ± 6.71	±	6.37	0.453	54.6	146.16 ± 6.39	±	5.84
0.50–0.60	0.538	44.8	117.12 ± 4.98	±	6.17	0.540	54.8	88.13 ± 4.35	±	4.87
0.60–0.72	0.648	44.9	59.27 ± 3.19	±	4.40	0.645	54.8	46.35 ± 2.75	±	3.60
0.72–0.90	0.786	44.6	27.50 ± 1.75	±	2.89	0.790	54.5	19.45 ± 1.43	±	2.13
0.90–1.25						1.004	55.1	5.11 ± 0.51	±	0.86

	$60 < \theta < 75$					$75 < \theta < 90$				
p_T	$\langle p_\mathrm{T}\rangle$	$\langle\theta\rangle$	$\mathrm{d}^2\sigma/\mathrm{d}p\mathrm{d}\Omega$			$\langle p_\mathrm{T}\rangle$	$\langle\theta\rangle$	$\mathrm{d}^2\sigma/\mathrm{d}p\mathrm{d}\Omega$		
0.13–0.16	0.145	67.2	392.51 ± 15.98	±	23.14	0.150	80.7	263.46 ± 24.52	±	79.38
0.16–0.20	0.179	67.4	353.14 ± 11.41	±	16.29	0.179	81.8	321.26 ± 13.12	±	19.24
0.20–0.24	0.218	67.0	303.94 ± 10.74	±	11.92	0.218	81.9	257.40 ± 10.54	±	12.40
0.24–0.30	0.266	67.0	259.45 ± 8.27	±	9.61	0.266	81.8	179.33 ± 7.35	±	10.19
0.30–0.36	0.327	66.9	187.22 ± 7.06	±	7.09	0.327	81.6	129.79 ± 6.14	±	6.97
0.36–0.42	0.386	67.0	141.61 ± 6.08	±	5.54	0.386	81.8	98.91 ± 5.27	±	5.39
0.42–0.50	0.454	66.7	100.19 ± 4.30	±	4.55	0.456	81.7	62.34 ± 3.53	±	3.90
0.50–0.60	0.539	66.6	63.00 ± 3.04	±	3.96	0.537	81.9	41.56 ± 2.50	±	3.35
0.60–0.72	0.643	66.9	33.40 ± 1.96	±	2.89	0.642	81.0	16.40 ± 1.34	±	1.80
0.72–0.90	0.783	66.4	12.65 ± 0.94	±	1.53	0.783	80.5	5.68 ± 0.67	±	0.85
0.90–1.25	1.006	66.4	2.45 ± 0.26	±	0.46	1.009	80.8	1.03 ± 0.17	±	0.23

	$90 < \theta < 105$					$105 < \theta < 125$				
p_T	$\langle p_\mathrm{T}\rangle$	$\langle\theta\rangle$	$\mathrm{d}^2\sigma/\mathrm{d}p\mathrm{d}\Omega$			$\langle p_\mathrm{T}\rangle$	$\langle\theta\rangle$	$\mathrm{d}^2\sigma/\mathrm{d}p\mathrm{d}\Omega$		
0.13–0.16						0.144	114.4	249.63 ± 11.13	±	12.41
0.16–0.20	0.178	97.8	254.26 ± 11.58	±	13.00	0.177	114.1	170.81 ± 7.00	±	6.24
0.20–0.24	0.218	97.4	191.71 ± 9.20	±	9.06	0.218	114.1	115.70 ± 5.86	±	4.30
0.24–0.30	0.265	97.4	141.58 ± 6.49	±	7.49	0.266	113.8	74.16 ± 3.83	±	3.60
0.30–0.36	0.327	97.3	88.62 ± 5.07	±	5.17	0.327	113.9	44.74 ± 2.92	±	3.03
0.36–0.42	0.385	97.3	59.72 ± 4.06	±	4.04	0.388	114.3	27.12 ± 2.22	±	2.49
0.42–0.50	0.449	97.1	35.93 ± 2.63	±	3.06	0.450	112.1	16.62 ± 1.51	±	1.99
0.50–0.60	0.539	97.3	19.67 ± 1.70	±	2.27	0.533	112.2	6.56 ± 0.83	±	1.04
0.60–0.72	0.645	96.1	9.35 ± 1.07	±	1.45	0.653	111.1	1.72 ± 0.37	±	0.36
0.72–0.90	0.772	96.9	2.73 ± 0.43	±	0.58	0.760	111.0	0.34 ± 0.12	±	0.10
0.90–1.25	1.037	94.7	0.44 ± 0.10	±	0.14	0.986	110.6	0.04 ± 0.02	±	0.02

Table A.25: Double-differential inclusive cross-section $\mathrm{d}^2\sigma/\mathrm{d}p\mathrm{d}\Omega$ [mb/(GeV/c sr)] of the production of protons in π^- + Ta $\rightarrow$ p + X interactions with -8.0 GeV/c beam momentum; the first error is statistical, the second systematic; p_T in GeV/c, polar angle θ in degrees.

	$20 < \theta < 30$					$30 < \theta < 40$				
p_T	$\langle p_\mathrm{T}\rangle$	$\langle\theta\rangle$	$\mathrm{d}^2\sigma/\mathrm{d}p\mathrm{d}\Omega$			$\langle p_\mathrm{T}\rangle$	$\langle\theta\rangle$	$\mathrm{d}^2\sigma/\mathrm{d}p\mathrm{d}\Omega$		
0.20–0.24	0.220	25.1	1255.33 ± 28.72	±	67.81					
0.24–0.30	0.269	25.2	1110.74 ± 21.49	±	54.34	0.270	34.9	1269.46 ± 22.86	±	56.06
0.30–0.36	0.329	25.3	858.36 ± 19.51	±	42.45	0.329	35.1	1079.55 ± 20.40	±	41.38
0.36–0.42	0.389	25.3	640.13 ± 17.18	±	34.45	0.388	35.1	858.65 ± 18.81	±	33.06
0.42–0.50	0.457	25.4	457.88 ± 12.49	±	25.67	0.458	35.2	633.26 ± 14.54	±	29.40
0.50–0.60	0.546	25.5	310.01 ± 9.47	±	21.15	0.547	35.2	455.19 ± 11.31	±	25.67
0.60–0.72	0.655	25.5	191.74 ± 6.75	±	15.40	0.654	35.2	289.32 ± 8.34	±	19.57
0.72–0.90						0.799	35.3	139.47 ± 4.80	±	13.41

	$40 < \theta < 50$					$50 < \theta < 60$				
p_T	$\langle p_\mathrm{T}\rangle$	$\langle\theta\rangle$	$\mathrm{d}^2\sigma/\mathrm{d}p\mathrm{d}\Omega$			$\langle p_\mathrm{T}\rangle$	$\langle\theta\rangle$	$\mathrm{d}^2\sigma/\mathrm{d}p\mathrm{d}\Omega$		
0.30–0.36	0.329	45.1	1182.50 ± 20.65	±	40.20					
0.36–0.42	0.389	45.1	1025.38 ± 19.56	±	30.00	0.389	55.1	1024.73 ± 18.53	±	36.40
0.42–0.50	0.458	45.1	744.26 ± 15.12	±	25.58	0.457	55.0	833.99 ± 15.11	±	24.16
0.50–0.60	0.546	45.2	523.53 ± 12.17	±	28.98	0.547	55.0	566.48 ± 11.93	±	23.59
0.60–0.72	0.655	45.1	336.67 ± 9.17	±	24.66	0.655	54.9	342.88 ± 9.03	±	23.28
0.72–0.90	0.800	45.1	167.37 ± 5.47	±	17.23	0.797	55.0	166.65 ± 5.46	±	16.11
0.90–1.25						1.037	55.1	45.24 ± 2.05	±	6.80

	$60 < \theta < 75$					$75 < \theta < 90$				
p_T	$\langle p_\mathrm{T}\rangle$	$\langle\theta\rangle$	$\mathrm{d}^2\sigma/\mathrm{d}p\mathrm{d}\Omega$			$\langle p_\mathrm{T}\rangle$	$\langle\theta\rangle$	$\mathrm{d}^2\sigma/\mathrm{d}p\mathrm{d}\Omega$		
0.50–0.60	0.546	67.4	567.96 ± 9.05	±	22.44					
0.60–0.72	0.653	67.2	336.37 ± 6.88	±	20.38	0.652	81.8	269.40 ± 5.62	±	19.37
0.72–0.90	0.798	67.2	156.34 ± 4.21	±	15.91	0.793	81.7	109.69 ± 3.25	±	11.38
0.90–1.25	1.027	66.9	40.89 ± 1.62	±	6.77	1.021	81.4	21.26 ± 1.18	±	3.83

	$90 < \theta < 105$					$105 < \theta < 125$				
p_T	$\langle p_\mathrm{T}\rangle$	$\langle\theta\rangle$	$\mathrm{d}^2\sigma/\mathrm{d}p\mathrm{d}\Omega$			$\langle p_\mathrm{T}\rangle$	$\langle\theta\rangle$	$\mathrm{d}^2\sigma/\mathrm{d}p\mathrm{d}\Omega$		
0.42–0.50						0.459	113.9	329.96 ± 6.77	±	20.19
0.50–0.60						0.542	112.9	172.81 ± 4.29	±	16.29
0.60–0.72	0.650	97.3	170.46 ± 4.42	±	15.56	0.649	112.7	59.07 ± 2.59	±	8.73
0.72–0.90	0.789	96.6	54.77 ± 2.34	±	6.62	0.793	112.3	13.43 ± 1.14	±	3.15

Table A.26: Double-differential inclusive cross-section $\mathrm{d}^2\sigma/\mathrm{d}p\mathrm{d}\Omega$ [mb/(GeV/c sr)] of the production of π^+'s in π^- + Ta $\rightarrow$ π^+ + X interactions with -8.0 GeV/c beam momentum; the first error is statistical, the second systematic; p_T in GeV/c, polar angle θ in degrees.

	$20 < \theta < 30$			$30 < \theta < 40$		
p_T	$\langle p_\mathrm{T}\rangle$	$\langle\theta\rangle$	$\mathrm{d}^2\sigma/\mathrm{d}p\mathrm{d}\Omega$	$\langle p_\mathrm{T}\rangle$	$\langle\theta\rangle$	$\mathrm{d}^2\sigma/\mathrm{d}p\mathrm{d}\Omega$
0.10–0.13	0.115	24.8	479.33 ± 22.64 ± 39.70	0.116	34.9	402.49 ± 19.83 ± 29.60
0.13–0.16	0.146	24.8	471.13 ± 19.79 ± 27.39	0.145	34.9	424.25 ± 18.12 ± 24.31
0.16–0.20	0.180	25.0	561.90 ± 18.19 ± 28.21	0.179	34.8	461.03 ± 16.27 ± 22.32
0.20–0.24	0.220	25.0	572.42 ± 18.15 ± 24.70	0.220	35.0	465.31 ± 16.49 ± 19.66
0.24–0.30	0.269	24.9	561.20 ± 14.61 ± 20.60	0.269	34.8	447.22 ± 13.18 ± 16.35
0.30–0.36	0.329	24.8	461.38 ± 13.23 ± 14.83	0.329	34.9	377.39 ± 12.09 ± 11.41
0.36–0.42	0.389	24.9	360.13 ± 11.37 ± 10.77	0.389	34.9	318.78 ± 11.15 ± 9.83
0.42–0.50	0.458	24.9	256.44 ± 8.20 ± 9.27	0.458	34.7	216.03 ± 7.56 ± 7.13
0.50–0.60	0.547	25.1	171.26 ± 5.82 ± 8.83	0.547	34.9	147.34 ± 5.53 ± 6.88
0.60–0.72	0.658	24.8	105.22 ± 3.97 ± 8.14	0.654	34.5	91.74 ± 3.79 ± 6.43
0.72–0.90				0.793	34.9	36.77 ± 1.70 ± 4.14

	$40 < \theta < 50$			$50 < \theta < 60$		
p_T	$\langle p_\mathrm{T}\rangle$	$\langle\theta\rangle$	$\mathrm{d}^2\sigma/\mathrm{d}p\mathrm{d}\Omega$	$\langle p_\mathrm{T}\rangle$	$\langle\theta\rangle$	$\mathrm{d}^2\sigma/\mathrm{d}p\mathrm{d}\Omega$
0.10–0.13	0.116	44.9	370.96 ± 20.55 ± 29.75			
0.13–0.16	0.144	44.9	384.96 ± 17.74 ± 22.35	0.145	54.8	328.54 ± 16.26 ± 19.86
0.16–0.20	0.180	45.1	376.26 ± 14.73 ± 18.35	0.180	55.1	370.47 ± 14.57 ± 17.93
0.20–0.24	0.221	44.8	375.35 ± 14.73 ± 16.09	0.219	55.1	303.45 ± 13.04 ± 12.42
0.24–0.30	0.269	44.8	358.13 ± 11.82 ± 12.74	0.270	54.8	284.85 ± 10.65 ± 10.46
0.30–0.36	0.329	44.7	298.66 ± 10.79 ± 9.25	0.330	54.9	234.18 ± 9.63 ± 7.60
0.36–0.42	0.389	44.7	221.59 ± 9.11 ± 6.48	0.389	54.7	198.30 ± 8.83 ± 6.54
0.42–0.50	0.458	44.6	171.26 ± 6.96 ± 5.75	0.457	54.7	134.53 ± 6.09 ± 4.93
0.50–0.60	0.547	44.7	117.19 ± 5.07 ± 5.34	0.549	54.7	92.53 ± 4.56 ± 4.60
0.60–0.72	0.655	44.8	67.14 ± 3.30 ± 4.41	0.651	54.8	53.65 ± 3.04 ± 3.76
0.72–0.90	0.792	44.9	26.46 ± 1.53 ± 2.67	0.791	54.4	21.95 ± 1.43 ± 2.28
0.90–1.25				1.023	54.4	5.80 ± 0.43 ± 0.99

	$60 < \theta < 75$			$75 < \theta < 90$		
p_T	$\langle p_\mathrm{T}\rangle$	$\langle\theta\rangle$	$\mathrm{d}^2\sigma/\mathrm{d}p\mathrm{d}\Omega$	$\langle p_\mathrm{T}\rangle$	$\langle\theta\rangle$	$\mathrm{d}^2\sigma/\mathrm{d}p\mathrm{d}\Omega$
0.13–0.16	0.146	66.8	289.14 ± 14.95 ± 21.73	0.149	81.4	145.40 ± 28.52 ± 19.73
0.16–0.20	0.179	67.1	270.03 ± 9.98 ± 13.20	0.181	81.9	236.39 ± 11.98 ± 19.32
0.20–0.24	0.219	67.3	256.54 ± 9.94 ± 10.21	0.219	81.9	214.06 ± 9.64 ± 9.22
0.24–0.30	0.269	67.3	237.29 ± 8.03 ± 8.73	0.268	82.0	178.43 ± 7.41 ± 9.31
0.30–0.36	0.329	67.1	176.20 ± 7.01 ± 6.75	0.327	81.6	114.84 ± 5.94 ± 6.42
0.36–0.42	0.387	66.5	124.07 ± 5.74 ± 4.43	0.390	81.8	81.99 ± 4.92 ± 4.42
0.42–0.50	0.458	67.0	96.41 ± 4.34 ± 4.15	0.455	82.2	60.10 ± 3.53 ± 3.49
0.50–0.60	0.547	66.4	62.98 ± 3.06 ± 3.73	0.543	81.1	38.31 ± 2.44 ± 2.85
0.60–0.72	0.653	66.5	36.89 ± 2.09 ± 3.06	0.651	81.5	18.01 ± 1.45 ± 1.81
0.72–0.90	0.790	66.8	13.93 ± 0.95 ± 1.67	0.783	81.9	6.17 ± 0.65 ± 0.87
0.90–1.25	1.027	66.3	2.62 ± 0.24 ± 0.51	1.040	80.8	1.41 ± 0.18 ± 0.32

	$90 < \theta < 105$			$105 < \theta < 125$		
p_T	$\langle p_\mathrm{T}\rangle$	$\langle\theta\rangle$	$\mathrm{d}^2\sigma/\mathrm{d}p\mathrm{d}\Omega$	$\langle p_\mathrm{T}\rangle$	$\langle\theta\rangle$	$\mathrm{d}^2\sigma/\mathrm{d}p\mathrm{d}\Omega$
0.13–0.16	0.150	99.2	159.61 ± 17.44 ± 33.42	0.145	115.2	289.66 ± 15.70 ± 35.45
0.16–0.20	0.180	98.2	246.74 ± 12.21 ± 19.64	0.179	114.7	175.67 ± 7.62 ± 6.60
0.20–0.24	0.219	97.6	200.02 ± 9.75 ± 10.56	0.218	113.4	113.15 ± 5.92 ± 3.94
0.24–0.30	0.266	97.0	129.40 ± 6.42 ± 7.40	0.268	114.0	65.37 ± 3.61 ± 2.70
0.30–0.36	0.329	97.2	90.32 ± 5.33 ± 5.60	0.326	114.3	45.71 ± 3.06 ± 2.78
0.36–0.42	0.389	97.3	54.80 ± 4.01 ± 3.61	0.386	113.9	24.35 ± 2.20 ± 1.97
0.42–0.50	0.457	97.3	35.26 ± 2.68 ± 2.77	0.456	113.2	11.38 ± 1.22 ± 1.21
0.50–0.60	0.544	96.5	18.65 ± 1.66 ± 1.97	0.537	113.3	6.09 ± 0.80 ± 0.86
0.60–0.72	0.652	96.8	6.55 ± 0.87 ± 0.92	0.664	109.4	1.05 ± 0.29 ± 0.20
0.72–0.90	0.786	96.3	3.11 ± 0.45 ± 0.60	0.812	114.3	0.38 ± 0.12 ± 0.10
0.90–1.25	1.061	95.1	0.28 ± 0.07 ± 0.09			

Table A.27: Double-differential inclusive cross-section $\mathrm{d}^2\sigma/\mathrm{d}p\mathrm{d}\Omega$ [mb/(GeV/c sr)] of the production of π^-'s in π^- + Ta $\rightarrow \pi^-$ + X interactions with -8.0 GeV/c beam momentum; the first error is statistical, the second systematic; p_T in GeV/c, polar angle θ in degrees.

	$20 < \theta < 30$					$30 < \theta < 40$				
p_T	$\langle p_\mathrm{T}\rangle$	$\langle\theta\rangle$	$\mathrm{d}^2\sigma/\mathrm{d}p\mathrm{d}\Omega$			$\langle p_\mathrm{T}\rangle$	$\langle\theta\rangle$	$\mathrm{d}^2\sigma/\mathrm{d}p\mathrm{d}\Omega$		
0.10–0.13	0.116	24.8	680.46 ± 27.46	±	55.16	0.116	34.8	618.38 ± 25.28	±	46.80
0.13–0.16	0.145	24.9	734.83 ± 25.30	±	43.12	0.146	34.9	639.11 ± 23.25	±	37.51
0.16–0.20	0.181	25.0	794.68 ± 22.22	±	39.56	0.180	34.9	666.99 ± 19.93	±	32.72
0.20–0.24	0.219	24.9	796.99 ± 21.80	±	33.02	0.220	34.8	663.29 ± 19.94	±	27.44
0.24–0.30	0.269	24.9	749.03 ± 17.25	±	25.49	0.269	34.7	614.31 ± 15.71	±	21.48
0.30–0.36	0.329	24.9	636.70 ± 15.89	±	19.14	0.329	34.8	509.17 ± 14.27	±	14.95
0.36–0.42	0.389	24.9	465.02 ± 13.30	±	13.61	0.389	34.7	390.27 ± 12.40	±	11.24
0.42–0.50	0.458	24.8	374.73 ± 10.47	±	13.92	0.459	34.8	286.05 ± 9.08	±	10.08
0.50–0.60	0.546	24.9	241.39 ± 7.45	±	12.26	0.546	34.7	180.23 ± 6.43	±	8.83
0.60–0.72	0.653	24.7	144.51 ± 5.14	±	10.35	0.653	34.8	117.53 ± 4.67	±	8.13
0.72–0.90						0.798	34.8	50.51 ± 2.44	±	4.97

	$40 < \theta < 50$					$50 < \theta < 60$				
p_T	$\langle p_\mathrm{T}\rangle$	$\langle\theta\rangle$	$\mathrm{d}^2\sigma/\mathrm{d}p\mathrm{d}\Omega$			$\langle p_\mathrm{T}\rangle$	$\langle\theta\rangle$	$\mathrm{d}^2\sigma/\mathrm{d}p\mathrm{d}\Omega$		
0.10–0.13	0.115	45.1	550.47 ± 24.95	±	42.68					
0.13–0.16	0.145	45.2	557.95 ± 21.52	±	33.22	0.146	54.9	515.20 ± 21.00	±	31.51
0.16–0.20	0.180	44.8	529.46 ± 17.74	±	26.16	0.179	54.9	475.32 ± 16.75	±	23.30
0.20–0.24	0.219	44.6	571.79 ± 18.73	±	24.97	0.220	55.0	434.29 ± 16.29	±	18.21
0.24–0.30	0.269	44.9	458.59 ± 13.60	±	16.01	0.268	54.8	367.12 ± 12.20	±	12.97
0.30–0.36	0.329	44.7	401.73 ± 12.71	±	12.20	0.329	54.9	293.61 ± 10.96	±	9.39
0.36–0.42	0.388	44.7	326.67 ± 11.35	±	9.74	0.388	54.7	234.21 ± 9.62	±	7.38
0.42–0.50	0.458	44.9	230.04 ± 8.17	±	8.55	0.458	54.8	189.00 ± 7.52	±	7.48
0.50–0.60	0.546	44.8	158.31 ± 6.04	±	8.24	0.545	54.7	118.27 ± 5.20	±	6.44
0.60–0.72	0.655	44.7	83.15 ± 3.91	±	6.11	0.654	54.8	65.24 ± 3.52	±	4.95
0.72–0.90	0.796	45.0	42.72 ± 2.22	±	4.49	0.798	54.9	24.94 ± 1.65	±	2.73
0.90–1.25						1.032	54.8	6.15 ± 0.53	±	1.07

	$60 < \theta < 75$					$75 < \theta < 90$				
p_T	$\langle p_\mathrm{T}\rangle$	$\langle\theta\rangle$	$\mathrm{d}^2\sigma/\mathrm{d}p\mathrm{d}\Omega$			$\langle p_\mathrm{T}\rangle$	$\langle\theta\rangle$	$\mathrm{d}^2\sigma/\mathrm{d}p\mathrm{d}\Omega$		
0.13–0.16	0.146	67.2	462.28 ± 18.20	±	27.15	0.148	80.2	323.30 ± 30.87	±	72.32
0.16–0.20	0.179	67.1	377.05 ± 12.35	±	17.29	0.180	81.9	408.05 ± 30.93	±	29.23
0.20–0.24	0.219	67.0	350.86 ± 12.02	±	13.96	0.219	82.0	271.94 ± 11.28	±	13.33
0.24–0.30	0.268	67.0	275.19 ± 8.85	±	10.74	0.269	81.8	210.58 ± 8.17	±	11.15
0.30–0.36	0.329	67.1	223.36 ± 7.93	±	8.18	0.329	81.9	159.16 ± 7.08	±	9.05
0.36–0.42	0.388	66.8	163.00 ± 6.71	±	6.19	0.388	81.9	99.58 ± 5.48	±	5.61
0.42–0.50	0.458	66.7	131.40 ± 5.18	±	6.19	0.459	81.6	73.35 ± 3.99	±	4.69
0.50–0.60	0.544	66.7	77.73 ± 3.47	±	4.84	0.548	81.3	49.56 ± 2.82	±	3.96
0.60–0.72	0.653	66.7	42.32 ± 2.31	±	3.63	0.651	81.3	21.65 ± 1.67	±	2.34
0.72–0.90	0.794	66.7	18.21 ± 1.17	±	2.20	0.795	82.4	6.98 ± 0.73	±	1.03
0.90–1.25	1.015	66.7	3.29 ± 0.32	±	0.61	1.028	81.3	1.50 ± 0.23	±	0.33

	$90 < \theta < 105$					$105 < \theta < 125$				
p_T	$\langle p_\mathrm{T}\rangle$	$\langle\theta\rangle$	$\mathrm{d}^2\sigma/\mathrm{d}p\mathrm{d}\Omega$			$\langle p_\mathrm{T}\rangle$	$\langle\theta\rangle$	$\mathrm{d}^2\sigma/\mathrm{d}p\mathrm{d}\Omega$		
0.13–0.16	0.148	98.8	282.32 ± 33.52	±	67.61	0.145	113.7	300.22 ± 12.73	±	14.54
0.16–0.20	0.179	98.1	319.07 ± 13.77	±	21.94	0.178	113.7	201.76 ± 7.97	±	7.23
0.20–0.24	0.219	97.2	225.75 ± 10.36	±	10.70	0.219	113.9	133.79 ± 6.48	±	4.79
0.24–0.30	0.268	96.8	152.53 ± 6.93	±	7.85	0.266	114.2	83.72 ± 4.17	±	3.92
0.30–0.36	0.328	97.1	99.00 ± 5.53	±	5.69	0.329	114.0	52.70 ± 3.34	±	3.61
0.36–0.42	0.388	96.5	64.97 ± 4.41	±	4.47	0.390	113.4	36.04 ± 2.66	±	3.26
0.42–0.50	0.457	96.9	42.49 ± 2.94	±	3.56	0.458	113.5	21.92 ± 1.82	±	2.59
0.50–0.60	0.542	96.9	25.89 ± 2.03	±	2.95	0.551	111.9	11.45 ± 1.11	±	1.78
0.60–0.72	0.651	95.9	9.82 ± 1.11	±	1.50	0.644	111.5	4.31 ± 0.63	±	0.87
0.72–0.90	0.786	96.3	3.72 ± 0.52	±	0.77	0.799	112.6	0.48 ± 0.13	±	0.14
0.90–1.25	1.029	96.4	0.46 ± 0.11	±	0.14	0.986	115.1	0.04 ± 0.02	±	0.02

Table A.28: Double-differential inclusive cross-section $\mathrm{d}^2\sigma/\mathrm{d}p\mathrm{d}\Omega$ [mb/(GeV/c sr)] of the production of protons in p + Ta $\rightarrow$ p + X interactions with $+12.0$ GeV/c beam momentum; the first error is statistical, the second systematic; p_T in GeV/c, polar angle θ in degrees.

	$20 < \theta < 30$					$30 < \theta < 40$				
p_T	$\langle p_\mathrm{T}\rangle$	$\langle\theta\rangle$	$\mathrm{d}^2\sigma/\mathrm{d}p\mathrm{d}\Omega$			$\langle p_\mathrm{T}\rangle$	$\langle\theta\rangle$	$\mathrm{d}^2\sigma/\mathrm{d}p\mathrm{d}\Omega$		
0.20–0.24	0.221	25.2	1697.60	± 32.16	± 91.13					
0.24–0.30	0.269	25.1	1499.10	± 23.75	± 72.10	0.271	34.8	1591.89	± 24.06	± 69.38
0.30–0.36	0.329	25.2	1199.17	± 21.94	± 58.35	0.330	35.1	1439.86	± 22.48	± 53.99
0.36–0.42	0.389	25.4	947.24	± 20.00	± 49.36	0.389	35.0	1230.85	± 21.72	± 45.75
0.42–0.50	0.458	25.3	747.63	± 15.51	± 41.26	0.458	35.2	930.98	± 16.79	± 40.63
0.50–0.60	0.547	25.3	532.26	± 11.78	± 33.80	0.547	35.1	699.89	± 13.42	± 36.80
0.60–0.72	0.655	25.3	347.90	± 8.77	± 27.90	0.655	35.2	459.74	± 10.05	± 30.73
0.72–0.90						0.803	35.1	261.89	± 6.28	± 23.38

	$40 < \theta < 50$					$50 < \theta < 60$				
p_T	$\langle p_\mathrm{T}\rangle$	$\langle\theta\rangle$	$\mathrm{d}^2\sigma/\mathrm{d}p\mathrm{d}\Omega$			$\langle p_\mathrm{T}\rangle$	$\langle\theta\rangle$	$\mathrm{d}^2\sigma/\mathrm{d}p\mathrm{d}\Omega$		
0.30–0.36	0.329	45.2	1596.25	± 23.02	± 54.21					
0.36–0.42	0.390	45.1	1402.18	± 22.09	± 39.61	0.389	55.1	1433.61	± 21.04	± 49.26
0.42–0.50	0.459	45.2	1052.93	± 17.25	± 36.36	0.458	55.1	1150.44	± 17.22	± 32.24
0.50–0.60	0.547	45.1	786.95	± 14.12	± 39.95	0.547	55.0	795.23	± 13.47	± 33.13
0.60–0.72	0.656	44.9	490.40	± 10.57	± 34.30	0.654	54.9	509.73	± 10.58	± 32.49
0.72–0.90	0.801	44.9	270.28	± 6.59	± 25.70	0.800	54.9	258.44	± 6.41	± 23.54
0.90–1.25	1.040	44.8	82.80	± 2.64	± 12.33	1.034	54.9	73.63	± 2.46	± 10.17

	$60 < \theta < 75$					$75 < \theta < 90$				
p_T	$\langle p_\mathrm{T}\rangle$	$\langle\theta\rangle$	$\mathrm{d}^2\sigma/\mathrm{d}p\mathrm{d}\Omega$			$\langle p_\mathrm{T}\rangle$	$\langle\theta\rangle$	$\mathrm{d}^2\sigma/\mathrm{d}p\mathrm{d}\Omega$		
0.50–0.60	0.549	67.3	742.82	± 9.84	± 29.30					
0.60–0.72	0.659	67.2	463.44	± 7.68	± 27.40	0.657	81.9	363.39	± 6.28	± 25.82
0.72–0.90	0.803	67.3	229.21	± 4.84	± 22.54	0.804	81.6	153.01	± 3.70	± 15.72
0.90–1.25	1.043	66.8	62.08	± 1.90	± 10.04	1.039	81.4	35.59	± 1.42	± 6.10

	$90 < \theta < 105$					$105 < \theta < 125$				
p_T	$\langle p_\mathrm{T}\rangle$	$\langle\theta\rangle$	$\mathrm{d}^2\sigma/\mathrm{d}p\mathrm{d}\Omega$			$\langle p_\mathrm{T}\rangle$	$\langle\theta\rangle$	$\mathrm{d}^2\sigma/\mathrm{d}p\mathrm{d}\Omega$		
0.42–0.50						0.461	113.9	411.27	± 6.83	± 24.63
0.50–0.60						0.546	113.1	209.18	± 4.49	± 19.70
0.60–0.72	0.655	97.2	216.23	± 4.81	± 19.44	0.655	112.6	80.31	± 2.87	± 11.61
0.72–0.90	0.798	97.1	75.58	± 2.65	± 9.14	0.793	112.5	24.21	± 1.45	± 5.48

Table A.29: Double-differential inclusive cross-section $\mathrm{d}^2\sigma/\mathrm{d}p\mathrm{d}\Omega$ [mb/(GeV/c sr)] of the production of π^+'s in p + Ta $\rightarrow \pi^+$ + X interactions with $+12.0$ GeV/c beam momentum; the first error is statistical, the second systematic; p_T in GeV/c, polar angle θ in degrees.

	$20 < \theta < 30$					$30 < \theta < 40$				
p_T	$\langle p_\mathrm{T}\rangle$	$\langle\theta\rangle$	$\mathrm{d}^2\sigma/\mathrm{d}p\mathrm{d}\Omega$			$\langle p_\mathrm{T}\rangle$	$\langle\theta\rangle$	$\mathrm{d}^2\sigma/\mathrm{d}p\mathrm{d}\Omega$		
0.10–0.13	0.115	25.0	568.88 ± 24.38	±	45.72	0.115	35.0	523.05 ± 22.20	±	38.61
0.13–0.16	0.145	24.8	693.68 ± 24.37	±	42.03	0.146	34.8	556.08 ± 20.45	±	31.73
0.16–0.20	0.179	25.0	751.11 ± 20.99	±	38.09	0.180	35.0	585.96 ± 18.18	±	28.31
0.20–0.24	0.220	24.9	786.68 ± 21.02	±	34.17	0.220	34.7	633.44 ± 18.86	±	27.23
0.24–0.30	0.269	24.8	741.20 ± 16.50	±	26.75	0.269	34.8	593.76 ± 14.82	±	20.78
0.30–0.36	0.329	24.8	633.29 ± 15.20	±	20.47	0.329	34.8	509.45 ± 13.88	±	16.19
0.36–0.42	0.389	24.8	498.22 ± 13.30	±	15.78	0.389	34.7	403.09 ± 12.12	±	11.88
0.42–0.50	0.458	24.8	358.74 ± 9.42	±	12.97	0.459	34.8	302.18 ± 8.95	±	10.28
0.50–0.60	0.548	24.8	252.84 ± 6.97	±	13.09	0.548	34.8	195.08 ± 6.20	±	9.33
0.60–0.72	0.656	24.9	156.08 ± 4.69	±	12.10	0.656	34.9	119.51 ± 4.24	±	8.48
0.72–0.90						0.799	34.5	53.02 ± 1.98	±	5.96

	$40 < \theta < 50$					$50 < \theta < 60$				
p_T	$\langle p_\mathrm{T}\rangle$	$\langle\theta\rangle$	$\mathrm{d}^2\sigma/\mathrm{d}p\mathrm{d}\Omega$			$\langle p_\mathrm{T}\rangle$	$\langle\theta\rangle$	$\mathrm{d}^2\sigma/\mathrm{d}p\mathrm{d}\Omega$		
0.10–0.13	0.116	45.1	459.23 ± 21.12	±	34.44					
0.13–0.16	0.146	44.9	492.69 ± 19.30	±	28.50	0.145	55.0	403.89 ± 17.51	±	24.42
0.16–0.20	0.180	44.9	516.21 ± 16.65	±	24.95	0.181	54.8	416.75 ± 14.60	±	19.99
0.20–0.24	0.220	44.9	480.56 ± 16.28	±	20.11	0.220	55.0	397.35 ± 14.54	±	16.08
0.24–0.30	0.269	44.8	431.09 ± 12.56	±	14.98	0.268	54.8	356.36 ± 11.66	±	12.95
0.30–0.36	0.330	44.7	395.74 ± 12.19	±	12.46	0.329	54.8	287.73 ± 10.40	±	9.30
0.36–0.42	0.389	44.7	315.76 ± 10.81	±	9.51	0.389	54.7	245.08 ± 9.55	±	7.95
0.42–0.50	0.457	44.7	221.87 ± 7.75	±	7.69	0.459	54.7	178.02 ± 7.01	±	6.63
0.50–0.60	0.546	44.7	156.00 ± 5.72	±	7.29	0.546	54.7	118.64 ± 5.00	±	5.98
0.60–0.72	0.657	44.5	88.56 ± 3.82	±	5.85	0.654	54.5	68.94 ± 3.38	±	4.88
0.72–0.90	0.799	44.6	43.30 ± 1.88	±	4.49	0.796	54.7	31.98 ± 1.77	±	3.27
0.90–1.25						1.042	54.8	7.67 ± 0.48	±	1.33

	$60 < \theta < 75$					$75 < \theta < 90$				
p_T	$\langle p_\mathrm{T}\rangle$	$\langle\theta\rangle$	$\mathrm{d}^2\sigma/\mathrm{d}p\mathrm{d}\Omega$			$\langle p_\mathrm{T}\rangle$	$\langle\theta\rangle$	$\mathrm{d}^2\sigma/\mathrm{d}p\mathrm{d}\Omega$		
0.13–0.16	0.146	67.1	358.83 ± 14.72	±	22.10					
0.16–0.20	0.180	67.1	354.17 ± 11.16	±	17.02	0.182	81.6	286.19 ± 11.49	±	15.68
0.20–0.24	0.220	66.9	354.03 ± 11.23	±	13.93	0.220	81.8	242.81 ± 9.72	±	9.58
0.24–0.30	0.269	66.8	306.46 ± 8.93	±	11.81	0.269	81.5	214.04 ± 7.80	±	10.84
0.30–0.36	0.330	67.0	201.84 ± 7.27	±	7.55	0.330	81.6	137.42 ± 6.30	±	7.57
0.36–0.42	0.390	67.1	169.45 ± 6.65	±	6.78	0.390	82.0	95.30 ± 5.20	±	5.14
0.42–0.50	0.460	66.7	128.64 ± 4.91	±	5.59	0.462	82.0	75.41 ± 3.91	±	4.53
0.50–0.60	0.550	66.5	77.80 ± 3.37	±	4.65	0.549	81.7	44.31 ± 2.62	±	3.35
0.60–0.72	0.660	66.6	41.47 ± 2.15	±	3.49	0.656	80.9	25.35 ± 1.75	±	2.59
0.72–0.90	0.801	66.8	16.97 ± 1.04	±	2.04	0.794	81.4	7.66 ± 0.71	±	1.09
0.90–1.25	1.051	66.0	3.68 ± 0.29	±	0.70	1.043	81.2	1.45 ± 0.17	±	0.33

	$90 < \theta < 105$					$105 < \theta < 125$				
p_T	$\langle p_\mathrm{T}\rangle$	$\langle\theta\rangle$	$\mathrm{d}^2\sigma/\mathrm{d}p\mathrm{d}\Omega$			$\langle p_\mathrm{T}\rangle$	$\langle\theta\rangle$	$\mathrm{d}^2\sigma/\mathrm{d}p\mathrm{d}\Omega$		
0.13–0.16						0.145	114.6	196.16 ± 9.11	±	10.89
0.16–0.20	0.180	97.9	250.00 ± 10.75	±	12.16	0.179	114.5	179.82 ± 6.78	±	7.50
0.20–0.24	0.220	97.6	206.30 ± 9.02	±	7.62	0.219	114.4	145.78 ± 6.36	±	5.01
0.24–0.30	0.269	97.2	152.62 ± 6.55	±	7.36	0.268	113.7	79.60 ± 3.93	±	3.38
0.30–0.36	0.328	97.4	87.73 ± 4.95	±	4.66	0.327	113.6	41.05 ± 2.82	±	2.50
0.36–0.42	0.389	97.7	55.72 ± 3.90	±	3.52	0.388	113.2	25.00 ± 2.18	±	2.05
0.42–0.50	0.463	96.6	37.49 ± 2.67	±	2.92	0.461	113.3	16.21 ± 1.47	±	1.74
0.50–0.60	0.549	97.4	19.33 ± 1.69	±	2.05	0.545	112.1	7.85 ± 0.87	±	1.13
0.60–0.72	0.658	96.7	9.98 ± 1.06	±	1.42	0.657	111.4	2.17 ± 0.41	±	0.41
0.72–0.90	0.796	96.4	3.19 ± 0.45	±	0.62	0.787	109.5	0.68 ± 0.17	±	0.18
0.90–1.25	1.016	96.1	0.49 ± 0.09	±	0.15	1.062	109.1	0.05 ± 0.02	±	0.02

Table A.30: Double-differential inclusive cross-section $\mathrm{d}^2\sigma/\mathrm{d}p\mathrm{d}\Omega$ [mb/(GeV/c sr)] of the production of π^-'s in p + Ta $\rightarrow \pi^-$ + X interactions with $+12.0$ GeV/c beam momentum; the first error is statistical, the second systematic; p_T in GeV/c, polar angle θ in degrees.

	$20 < \theta < 30$					$30 < \theta < 40$				
p_T	$\langle p_\mathrm{T}\rangle$	$\langle\theta\rangle$	$\mathrm{d}^2\sigma/\mathrm{d}p\mathrm{d}\Omega$			$\langle p_\mathrm{T}\rangle$	$\langle\theta\rangle$	$\mathrm{d}^2\sigma/\mathrm{d}p\mathrm{d}\Omega$		
0.10–0.13	0.116	25.0	801.53 ± 27.91	±	62.35	0.116	34.9	759.61 ± 26.50	±	57.83
0.13–0.16	0.145	25.1	857.05 ± 26.32	±	51.92	0.145	35.0	740.44 ± 23.67	±	43.37
0.16–0.20	0.180	25.0	852.65 ± 21.69	±	41.77	0.180	34.9	745.58 ± 19.95	±	36.36
0.20–0.24	0.220	25.0	795.64 ± 20.69	±	32.70	0.219	35.0	680.48 ± 19.01	±	27.82
0.24–0.30	0.269	25.0	700.51 ± 15.79	±	23.25	0.269	34.8	593.72 ± 14.63	±	19.90
0.30–0.36	0.329	24.9	514.65 ± 13.43	±	14.50	0.328	34.8	486.77 ± 13.28	±	14.29
0.36–0.42	0.389	24.9	404.53 ± 11.96	±	12.11	0.388	34.9	387.29 ± 11.70	±	11.18
0.42–0.50	0.457	24.8	298.50 ± 8.87	±	10.85	0.458	34.9	264.14 ± 8.25	±	9.34
0.50–0.60	0.546	24.8	183.56 ± 6.02	±	9.37	0.547	34.7	160.82 ± 5.71	±	7.93
0.60–0.72	0.653	25.0	95.06 ± 3.89	±	6.89	0.656	34.8	79.91 ± 3.50	±	5.72
0.72–0.90						0.799	34.5	38.94 ± 1.97	±	3.95

	$40 < \theta < 50$					$50 < \theta < 60$				
p_T	$\langle p_\mathrm{T}\rangle$	$\langle\theta\rangle$	$\mathrm{d}^2\sigma/\mathrm{d}p\mathrm{d}\Omega$			$\langle p_\mathrm{T}\rangle$	$\langle\theta\rangle$	$\mathrm{d}^2\sigma/\mathrm{d}p\mathrm{d}\Omega$		
0.10–0.13	0.116	45.0	624.00 ± 24.81	±	47.95					
0.13–0.16	0.145	44.8	615.04 ± 21.48	±	36.58	0.145	55.0	554.87 ± 20.52	±	33.99
0.16–0.20	0.179	44.8	615.17 ± 18.11	±	30.24	0.179	55.0	534.06 ± 17.10	±	26.05
0.20–0.24	0.219	44.7	587.27 ± 17.68	±	24.32	0.219	54.8	461.13 ± 15.52	±	18.66
0.24–0.30	0.269	44.8	482.80 ± 13.24	±	16.38	0.269	54.7	378.92 ± 11.83	±	13.34
0.30–0.36	0.329	44.8	405.83 ± 12.09	±	11.53	0.328	54.8	289.39 ± 10.33	±	9.02
0.36–0.42	0.387	45.0	302.36 ± 10.48	±	9.13	0.389	54.8	238.70 ± 9.35	±	7.74
0.42–0.50	0.458	44.8	207.67 ± 7.30	±	7.77	0.457	54.6	161.93 ± 6.54	±	6.41
0.50–0.60	0.547	44.7	127.64 ± 5.01	±	6.73	0.547	54.7	103.54 ± 4.62	±	5.70
0.60–0.72	0.654	45.0	73.07 ± 3.59	±	5.41	0.654	54.7	60.83 ± 3.21	±	4.67
0.72–0.90	0.791	45.2	28.18 ± 1.67	±	3.05	0.797	54.9	21.16 ± 1.42	±	2.38
0.90–1.25						1.018	54.3	5.34 ± 0.46	±	0.95

	$60 < \theta < 75$					$75 < \theta < 90$				
p_T	$\langle p_\mathrm{T}\rangle$	$\langle\theta\rangle$	$\mathrm{d}^2\sigma/\mathrm{d}p\mathrm{d}\Omega$			$\langle p_\mathrm{T}\rangle$	$\langle\theta\rangle$	$\mathrm{d}^2\sigma/\mathrm{d}p\mathrm{d}\Omega$		
0.13–0.16	0.145	67.3	463.20 ± 16.84	±	27.17					
0.16–0.20	0.179	67.7	419.64 ± 12.30	±	19.16	0.180	81.8	370.72 ± 13.20	±	19.31
0.20–0.24	0.219	67.0	378.99 ± 11.71	±	14.18	0.219	82.1	291.27 ± 10.90	±	12.64
0.24–0.30	0.268	67.4	303.11 ± 8.80	±	10.97	0.267	81.8	238.50 ± 8.30	±	12.84
0.30–0.36	0.327	66.8	218.10 ± 7.44	±	7.69	0.327	81.7	149.58 ± 6.49	±	7.57
0.36–0.42	0.387	66.6	170.68 ± 6.66	±	7.16	0.387	81.7	104.98 ± 5.38	±	5.83
0.42–0.50	0.456	67.1	112.55 ± 4.51	±	5.11	0.456	81.6	72.51 ± 3.70	±	4.37
0.50–0.60	0.541	66.8	74.07 ± 3.20	±	4.66	0.541	81.8	40.41 ± 2.40	±	3.28
0.60–0.72	0.650	66.4	40.69 ± 2.18	±	3.52	0.646	81.4	16.96 ± 1.42	±	1.86
0.72–0.90	0.790	66.0	13.72 ± 0.97	±	1.67	0.778	82.0	4.25 ± 0.53	±	0.65
0.90–1.25	1.009	66.1	2.30 ± 0.25	±	0.44	1.012	82.7	0.97 ± 0.16	±	0.23

	$90 < \theta < 105$					$105 < \theta < 125$				
p_T	$\langle p_\mathrm{T}\rangle$	$\langle\theta\rangle$	$\mathrm{d}^2\sigma/\mathrm{d}p\mathrm{d}\Omega$			$\langle p_\mathrm{T}\rangle$	$\langle\theta\rangle$	$\mathrm{d}^2\sigma/\mathrm{d}p\mathrm{d}\Omega$		
0.13–0.16	0.146	98.0	534.10 ± 54.13	±	165.09	0.144	114.2	315.63 ± 13.57	±	16.88
0.16–0.20	0.180	97.9	301.97 ± 11.83	±	13.43	0.178	114.1	221.40 ± 7.74	±	8.11
0.20–0.24	0.218	97.7	249.65 ± 10.21	±	10.47	0.216	113.8	137.30 ± 6.21	±	4.96
0.24–0.30	0.267	97.2	167.66 ± 7.03	±	9.25	0.267	113.1	82.54 ± 3.99	±	3.94
0.30–0.36	0.327	96.9	101.26 ± 5.31	±	5.69	0.326	113.1	43.22 ± 2.83	±	2.96
0.36–0.42	0.387	97.4	65.66 ± 4.14	±	4.30	0.383	113.1	28.41 ± 2.27	±	2.65
0.42–0.50	0.456	96.5	44.05 ± 2.86	±	3.76	0.454	112.8	14.12 ± 1.36	±	1.72
0.50–0.60	0.540	97.0	20.54 ± 1.70	±	2.39	0.544	110.9	5.11 ± 0.73	±	0.82
0.60–0.72	0.648	96.1	7.82 ± 0.94	±	1.22	0.638	112.0	2.31 ± 0.42	±	0.50
0.72–0.90	0.773	96.0	2.27 ± 0.40	±	0.48	0.778	111.4	0.17 ± 0.08	±	0.05
0.90–1.25	1.027	95.8	0.19 ± 0.07	±	0.06	1.071	114.3	0.04 ± 0.02	±	0.02

Table A.31: Double-differential inclusive cross-section $\mathrm{d}^2\sigma/\mathrm{d}p\mathrm{d}\Omega$ [mb/(GeV/c sr)] of the production of protons in π^+ + Ta $\rightarrow$ p + X interactions with $+12.0$ GeV/c beam momentum; the first error is statistical, the second systematic; p_T in GeV/c, polar angle θ in degrees.

	$20 < \theta < 30$					$30 < \theta < 40$				
p_T	$\langle p_\mathrm{T}\rangle$	$\langle\theta\rangle$	$\mathrm{d}^2\sigma/\mathrm{d}p\mathrm{d}\Omega$			$\langle p_\mathrm{T}\rangle$	$\langle\theta\rangle$	$\mathrm{d}^2\sigma/\mathrm{d}p\mathrm{d}\Omega$		
0.20–0.24	0.220	25.0	1316.70 ± 94.07	±	71.37					
0.24–0.30	0.270	25.1	1218.70 ± 72.92	±	59.48	0.271	34.9	1256.09 ± 73.12	±	55.69
0.30–0.36	0.331	25.2	959.99 ± 66.74	±	47.19	0.329	35.0	1141.91 ± 68.05	±	43.82
0.36–0.42	0.386	25.5	716.87 ± 59.00	±	37.75	0.388	35.2	1036.49 ± 67.65	±	39.36
0.42–0.50	0.458	25.3	644.94 ± 48.59	±	36.08	0.458	35.0	728.83 ± 50.32	±	32.53
0.50–0.60	0.545	25.2	414.41 ± 34.75	±	26.60	0.547	35.4	553.05 ± 40.46	±	29.72
0.60–0.72	0.656	25.3	286.46 ± 26.56	±	23.16	0.651	35.2	386.45 ± 31.13	±	26.24
0.72–0.90						0.804	34.8	172.07 ± 17.01	±	15.44

	$40 < \theta < 50$					$50 < \theta < 60$				
p_T	$\langle p_\mathrm{T}\rangle$	$\langle\theta\rangle$	$\mathrm{d}^2\sigma/\mathrm{d}p\mathrm{d}\Omega$			$\langle p_\mathrm{T}\rangle$	$\langle\theta\rangle$	$\mathrm{d}^2\sigma/\mathrm{d}p\mathrm{d}\Omega$		
0.30–0.36	0.330	45.1	1372.15 ± 71.60	±	49.15					
0.36–0.42	0.388	45.0	1127.92 ± 66.98	±	33.14	0.387	54.9	1252.67 ± 65.89	±	48.94
0.42–0.50	0.458	45.0	864.59 ± 53.15	±	31.05	0.457	55.1	950.77 ± 53.29	±	27.80
0.50–0.60	0.547	45.3	577.40 ± 41.27	±	30.43	0.545	54.8	625.03 ± 40.65	±	26.92
0.60–0.72	0.655	44.9	413.34 ± 32.92	±	29.48	0.659	55.1	395.68 ± 31.79	±	25.74
0.72–0.90	0.800	45.0	222.67 ± 20.42	±	21.32	0.797	55.0	204.13 ± 19.39	±	18.68
0.90–1.25	1.028	45.1	65.46 ± 7.99	±	9.74	1.015	54.9	54.94 ± 7.20	±	7.61

	$60 < \theta < 75$					$75 < \theta < 90$				
p_T	$\langle p_\mathrm{T}\rangle$	$\langle\theta\rangle$	$\mathrm{d}^2\sigma/\mathrm{d}p\mathrm{d}\Omega$			$\langle p_\mathrm{T}\rangle$	$\langle\theta\rangle$	$\mathrm{d}^2\sigma/\mathrm{d}p\mathrm{d}\Omega$		
0.50–0.60	0.548	68.0	665.79 ± 31.85	±	26.65					
0.60–0.72	0.658	67.1	398.71 ± 24.26	±	23.87	0.659	81.9	293.80 ± 19.20	±	21.02
0.72–0.90	0.804	66.9	176.42 ± 14.39	±	17.42	0.814	81.3	126.03 ± 11.39	±	12.99
0.90–1.25	1.032	66.5	52.21 ± 5.90	±	8.45	1.050	82.1	28.26 ± 4.30	±	4.88

	$90 < \theta < 105$					$105 < \theta < 125$				
p_T	$\langle p_\mathrm{T}\rangle$	$\langle\theta\rangle$	$\mathrm{d}^2\sigma/\mathrm{d}p\mathrm{d}\Omega$			$\langle p_\mathrm{T}\rangle$	$\langle\theta\rangle$	$\mathrm{d}^2\sigma/\mathrm{d}p\mathrm{d}\Omega$		
0.42–0.50						0.462	114.2	402.56 ± 22.91	±	24.41
0.50–0.60						0.545	113.2	177.56 ± 14.16	±	16.73
0.60–0.72	0.657	97.0	211.73 ± 16.18	±	19.13	0.649	113.5	77.66 ± 9.64	±	11.35
0.72–0.90	0.795	97.1	53.43 ± 7.58	±	6.48	0.790	113.1	19.97 ± 4.49	±	4.55

Table A.32: Double-differential inclusive cross-section $\mathrm{d}^2\sigma/\mathrm{d}p\mathrm{d}\Omega$ [mb/(GeV/c sr)] of the production of π^+'s in π^+ + Ta $\rightarrow \pi^+$ + X interactions with $+12.0$ GeV/c beam momentum; the first error is statistical, the second systematic; p_T in GeV/c, polar angle θ in degrees.

	$20 < \theta < 30$			$30 < \theta < 40$		
p_T	$\langle p_\mathrm{T}\rangle$	$\langle\theta\rangle$	$\mathrm{d}^2\sigma/\mathrm{d}p\mathrm{d}\Omega$	$\langle p_\mathrm{T}\rangle$	$\langle\theta\rangle$	$\mathrm{d}^2\sigma/\mathrm{d}p\mathrm{d}\Omega$
0.10–0.13	0.116	24.9	797.96 ± 100.72 ± 67.08	0.115	34.3	657.50 ± 86.06 ± 50.72
0.13–0.16	0.145	24.3	657.76 ± 82.40 ± 45.06	0.144	34.9	676.80 ± 80.42 ± 41.06
0.16–0.20	0.181	25.0	989.79 ± 83.79 ± 51.41	0.180	34.8	617.97 ± 63.67 ± 30.19
0.20–0.24	0.221	24.6	876.84 ± 76.19 ± 38.53	0.220	34.6	634.80 ± 64.45 ± 27.41
0.24–0.30	0.270	24.9	856.68 ± 60.96 ± 31.53	0.269	34.5	701.95 ± 54.96 ± 25.15
0.30–0.36	0.329	24.7	793.02 ± 58.33 ± 26.32	0.329	34.8	456.48 ± 44.76 ± 15.00
0.36–0.42	0.389	24.8	581.27 ± 49.38 ± 18.88	0.389	34.6	457.58 ± 44.02 ± 13.81
0.42–0.50	0.458	24.8	475.32 ± 37.27 ± 17.45	0.458	34.8	283.68 ± 29.75 ± 9.82
0.50–0.60	0.549	25.1	318.45 ± 27.03 ± 16.61	0.545	34.0	222.41 ± 22.54 ± 10.71
0.60–0.72	0.657	25.0	193.54 ± 17.90 ± 15.03	0.662	34.8	132.32 ± 15.27 ± 9.40
0.72–0.90				0.793	34.9	58.55 ± 7.39 ± 6.57

	$40 < \theta < 50$			$50 < \theta < 60$		
p_T	$\langle p_\mathrm{T}\rangle$	$\langle\theta\rangle$	$\mathrm{d}^2\sigma/\mathrm{d}p\mathrm{d}\Omega$	$\langle p_\mathrm{T}\rangle$	$\langle\theta\rangle$	$\mathrm{d}^2\sigma/\mathrm{d}p\mathrm{d}\Omega$
0.10–0.13	0.119	45.5	291.13 ± 55.90 ± 22.07			
0.13–0.16	0.147	44.3	506.24 ± 68.79 ± 31.11	0.146	54.9	403.02 ± 63.74 ± 25.23
0.16–0.20	0.181	44.7	496.60 ± 55.29 ± 24.22	0.180	54.9	474.10 ± 53.02 ± 22.98
0.20–0.24	0.219	45.0	504.88 ± 57.99 ± 21.26	0.220	54.7	402.94 ± 49.62 ± 16.46
0.24–0.30	0.269	44.4	466.10 ± 44.76 ± 16.54	0.275	54.6	419.13 ± 43.25 ± 15.56
0.30–0.36	0.329	44.9	348.88 ± 39.03 ± 11.38	0.328	54.6	383.94 ± 41.42 ± 12.85
0.36–0.42	0.390	44.8	375.55 ± 40.73 ± 11.58	0.388	54.4	238.98 ± 32.41 ± 7.95
0.42–0.50	0.460	44.6	214.65 ± 26.03 ± 7.57	0.461	54.7	191.98 ± 24.93 ± 7.23
0.50–0.60	0.547	44.5	163.75 ± 20.07 ± 7.71	0.548	55.2	127.40 ± 17.75 ± 6.45
0.60–0.72	0.654	43.9	113.99 ± 14.82 ± 7.55	0.658	55.2	59.66 ± 10.66 ± 4.23
0.72–0.90	0.786	44.9	45.42 ± 6.82 ± 4.70	0.789	54.7	30.19 ± 5.91 ± 3.08
0.90–1.25				1.043	53.1	8.61 ± 1.78 ± 1.49

	$60 < \theta < 75$			$75 < \theta < 90$		
p_T	$\langle p_\mathrm{T}\rangle$	$\langle\theta\rangle$	$\mathrm{d}^2\sigma/\mathrm{d}p\mathrm{d}\Omega$	$\langle p_\mathrm{T}\rangle$	$\langle\theta\rangle$	$\mathrm{d}^2\sigma/\mathrm{d}p\mathrm{d}\Omega$
0.13–0.16	0.147	67.5	471.53 ± 62.94 ± 35.67			
0.16–0.20	0.180	66.6	392.10 ± 39.70 ± 19.01	0.183	81.1	343.99 ± 46.18 ± 26.87
0.20–0.24	0.221	67.9	406.58 ± 41.59 ± 16.20	0.220	81.0	244.11 ± 33.12 ± 9.68
0.24–0.30	0.269	66.9	331.62 ± 31.89 ± 13.08	0.269	81.3	184.49 ± 24.77 ± 9.52
0.30–0.36	0.332	67.3	217.61 ± 25.79 ± 8.43	0.329	81.6	179.23 ± 24.87 ± 10.39
0.36–0.42	0.389	66.8	171.59 ± 23.12 ± 7.02	0.394	81.3	96.47 ± 17.88 ± 5.41
0.42–0.50	0.461	66.4	148.73 ± 18.03 ± 6.53	0.465	81.2	72.32 ± 13.04 ± 4.38
0.50–0.60	0.554	67.4	88.95 ± 12.32 ± 5.33	0.545	82.5	58.30 ± 10.31 ± 4.38
0.60–0.72	0.658	67.4	47.70 ± 8.02 ± 4.01	0.666	81.8	22.71 ± 5.65 ± 2.30
0.72–0.90	0.797	67.6	23.12 ± 4.23 ± 2.78	0.778	82.4	8.15 ± 2.56 ± 1.15
0.90–1.25	1.028	67.7	4.41 ± 1.09 ± 0.84	1.042	80.7	1.49 ± 0.54 ± 0.34

	$90 < \theta < 105$			$105 < \theta < 125$		
p_T	$\langle p_\mathrm{T}\rangle$	$\langle\theta\rangle$	$\mathrm{d}^2\sigma/\mathrm{d}p\mathrm{d}\Omega$	$\langle p_\mathrm{T}\rangle$	$\langle\theta\rangle$	$\mathrm{d}^2\sigma/\mathrm{d}p\mathrm{d}\Omega$
0.13–0.16	0.148	98.3	250.21 ± 80.22 ± 87.33	0.145	112.4	171.14 ± 27.51 ± 10.88
0.16–0.20	0.180	97.7	268.21 ± 40.02 ± 18.44	0.180	114.5	217.71 ± 27.13 ± 8.26
0.20–0.24	0.221	98.6	231.59 ± 33.26 ± 9.90	0.222	114.2	146.12 ± 21.89 ± 5.21
0.24–0.30	0.267	97.1	158.79 ± 23.14 ± 8.48	0.270	115.6	67.36 ± 12.32 ± 3.04
0.30–0.36	0.333	96.9	87.15 ± 17.20 ± 5.15	0.335	113.5	56.84 ± 11.59 ± 3.57
0.36–0.42	0.389	97.1	66.26 ± 14.60 ± 4.38	0.396	112.6	41.00 ± 9.75 ± 3.36
0.42–0.50	0.460	99.2	22.63 ± 7.16 ± 1.77	0.464	113.0	17.11 ± 5.20 ± 1.82
0.50–0.60	0.555	96.3	28.33 ± 6.89 ± 2.97	0.553	110.9	10.92 ± 3.64 ± 1.54
0.60–0.72	0.661	93.8	9.84 ± 3.61 ± 1.39	0.647	110.4	2.31 ± 1.35 ± 0.43
0.72–0.90	0.846	97.5	3.94 ± 1.72 ± 0.76			
0.90–1.25	1.082	96.6	0.34 ± 0.15 ± 0.10	1.096	111.6	0.10 ± 0.08 ± 0.04

Table A.33: Double-differential inclusive cross-section $\mathrm{d}^2\sigma/\mathrm{d}p\mathrm{d}\Omega$ [mb/(GeV/c sr)] of the production of π^-'s in π^+ + Ta $\rightarrow \pi^-$ + X interactions with $+12.0$ GeV/c beam momentum; the first error is statistical, the second systematic; p_T in GeV/c, polar angle θ in degrees.

	$20 < \theta < 30$			$30 < \theta < 40$		
p_T	$\langle p_\mathrm{T}\rangle$	$\langle\theta\rangle$	$\mathrm{d}^2\sigma/\mathrm{d}p\mathrm{d}\Omega$	$\langle p_\mathrm{T}\rangle$	$\langle\theta\rangle$	$\mathrm{d}^2\sigma/\mathrm{d}p\mathrm{d}\Omega$
0.10–0.13	0.115	24.7	762.56 ± 90.06 ± 59.06	0.117	35.0	867.45 ± 99.64 ± 68.23
0.13–0.16	0.144	25.0	728.36 ± 82.52 ± 45.83	0.145	35.0	710.58 ± 81.50 ± 42.22
0.16–0.20	0.180	25.2	804.99 ± 71.94 ± 40.11	0.178	34.9	669.40 ± 64.45 ± 33.03
0.20–0.24	0.218	24.9	834.54 ± 72.03 ± 35.04	0.219	35.0	752.88 ± 68.84 ± 31.27
0.24–0.30	0.269	25.0	825.07 ± 58.64 ± 28.27	0.269	34.9	612.90 ± 50.81 ± 21.20
0.30–0.36	0.326	24.8	600.86 ± 49.61 ± 17.43	0.327	34.8	483.18 ± 45.12 ± 14.66
0.36–0.42	0.391	25.0	443.74 ± 42.82 ± 13.71	0.389	34.5	330.93 ± 36.63 ± 9.79
0.42–0.50	0.457	24.6	279.71 ± 29.16 ± 10.32	0.456	34.4	232.57 ± 26.23 ± 8.35
0.50–0.60	0.543	25.1	213.41 ± 22.43 ± 10.94	0.545	34.8	190.27 ± 21.20 ± 9.44
0.60–0.72	0.642	24.4	130.02 ± 15.35 ± 9.42	0.651	34.8	114.58 ± 14.33 ± 8.20
0.72–0.90				0.789	34.5	42.13 ± 6.98 ± 4.26

	$40 < \theta < 50$			$50 < \theta < 60$		
p_T	$\langle p_\mathrm{T}\rangle$	$\langle\theta\rangle$	$\mathrm{d}^2\sigma/\mathrm{d}p\mathrm{d}\Omega$	$\langle p_\mathrm{T}\rangle$	$\langle\theta\rangle$	$\mathrm{d}^2\sigma/\mathrm{d}p\mathrm{d}\Omega$
0.10–0.13	0.115	44.7	691.34 ± 95.10 ± 58.38			
0.13–0.16	0.147	45.0	593.53 ± 74.24 ± 35.64	0.144	55.8	560.33 ± 75.55 ± 34.88
0.16–0.20	0.179	44.6	625.56 ± 61.92 ± 31.11	0.179	55.3	461.94 ± 54.06 ± 22.83
0.20–0.24	0.218	45.1	401.41 ± 49.83 ± 16.88	0.218	54.7	491.97 ± 54.54 ± 20.22
0.24–0.30	0.269	44.5	548.47 ± 48.29 ± 19.10	0.271	55.2	395.66 ± 41.43 ± 14.23
0.30–0.36	0.327	44.6	471.75 ± 44.37 ± 13.83	0.331	54.8	285.27 ± 34.91 ± 9.09
0.36–0.42	0.387	44.9	325.31 ± 37.17 ± 10.05	0.387	54.9	215.08 ± 30.26 ± 7.11
0.42–0.50	0.459	44.6	252.11 ± 27.38 ± 9.56	0.458	54.1	122.61 ± 19.26 ± 4.91
0.50–0.60	0.547	44.6	127.15 ± 17.00 ± 6.74	0.543	55.5	106.30 ± 16.04 ± 5.88
0.60–0.72	0.657	45.0	79.73 ± 12.64 ± 5.91	0.647	56.4	46.05 ± 9.61 ± 3.54
0.72–0.90	0.766	45.1	33.42 ± 6.21 ± 3.62	0.803	54.1	27.66 ± 5.54 ± 3.10
0.90–1.25				0.987	52.7	4.90 ± 1.47 ± 0.87

	$60 < \theta < 75$			$75 < \theta < 90$		
p_T	$\langle p_\mathrm{T}\rangle$	$\langle\theta\rangle$	$\mathrm{d}^2\sigma/\mathrm{d}p\mathrm{d}\Omega$	$\langle p_\mathrm{T}\rangle$	$\langle\theta\rangle$	$\mathrm{d}^2\sigma/\mathrm{d}p\mathrm{d}\Omega$
0.13–0.16	0.145	66.5	427.09 ± 54.60 ± 25.21	0.149	80.8	399.37 ± 97.92 ± 101.54
0.16–0.20	0.178	66.7	380.94 ± 40.31 ± 17.69	0.178	81.6	299.72 ± 40.60 ± 15.29
0.20–0.24	0.219	67.1	378.23 ± 39.94 ± 14.48	0.219	81.8	272.83 ± 37.57 ± 15.33
0.24–0.30	0.268	67.2	276.98 ± 28.53 ± 10.24	0.262	81.7	234.77 ± 28.58 ± 14.59
0.30–0.36	0.328	67.2	208.62 ± 24.98 ± 7.49	0.326	81.5	163.02 ± 23.32 ± 8.89
0.36–0.42	0.384	66.4	142.84 ± 20.57 ± 6.08	0.383	80.2	108.30 ± 18.63 ± 6.25
0.42–0.50	0.462	67.2	102.21 ± 14.61 ± 4.68	0.449	81.2	60.32 ± 11.61 ± 3.68
0.50–0.60	0.541	65.4	77.04 ± 11.12 ± 4.86	0.538	81.2	38.06 ± 7.95 ± 3.08
0.60–0.72	0.651	66.5	43.98 ± 7.71 ± 3.81	0.661	82.4	19.42 ± 5.19 ± 2.12
0.72–0.90	0.795	64.9	10.02 ± 2.80 ± 1.21	0.789	81.1	4.66 ± 1.90 ± 0.71
0.90–1.25	0.983	65.2	3.45 ± 1.04 ± 0.66	1.067	82.7	1.45 ± 0.65 ± 0.34

	$90 < \theta < 105$			$105 < \theta < 125$		
p_T	$\langle p_\mathrm{T}\rangle$	$\langle\theta\rangle$	$\mathrm{d}^2\sigma/\mathrm{d}p\mathrm{d}\Omega$	$\langle p_\mathrm{T}\rangle$	$\langle\theta\rangle$	$\mathrm{d}^2\sigma/\mathrm{d}p\mathrm{d}\Omega$
0.13–0.16	0.146	100.1	416.02 ± 93.83 ± 117.46	0.144	114.9	341.69 ± 42.54 ± 16.62
0.16–0.20	0.178	98.3	330.79 ± 41.06 ± 14.17	0.180	115.5	204.30 ± 25.70 ± 7.40
0.20–0.24	0.218	97.8	272.18 ± 37.56 ± 15.19	0.219	114.3	132.07 ± 20.85 ± 4.80
0.24–0.30	0.267	96.7	148.94 ± 23.30 ± 10.36	0.266	112.5	70.17 ± 12.86 ± 3.64
0.30–0.36	0.324	97.5	95.84 ± 18.12 ± 6.29	0.326	114.4	58.83 ± 11.54 ± 4.16
0.36–0.42	0.391	98.2	81.50 ± 15.99 ± 5.61	0.383	115.6	19.44 ± 6.48 ± 1.81
0.42–0.50	0.457	95.9	36.87 ± 8.97 ± 3.17	0.452	113.9	16.64 ± 5.04 ± 2.00
0.50–0.60	0.546	97.8	21.60 ± 5.99 ± 2.49	0.549	119.6	4.66 ± 2.33 ± 0.73
0.60–0.72	0.617	93.5	2.70 ± 1.91 ± 0.42			
0.72–0.90	0.779	97.9	3.55 ± 1.62 ± 0.74			

Table A.34: Double-differential inclusive cross-section $\mathrm{d}^2\sigma/\mathrm{d}p\mathrm{d}\Omega$ [mb/(GeV/c sr)] of the production of protons in π^- + Ta $\rightarrow$ p + X interactions with -12.0 GeV/c beam momentum; the first error is statistical, the second systematic; p_T in GeV/c, polar angle θ in degrees.

	$20 < \theta < 30$						$30 < \theta < 40$					
p_T	$\langle p_\mathrm{T}\rangle$	$\langle\theta\rangle$	$\mathrm{d}^2\sigma/\mathrm{d}p\mathrm{d}\Omega$				$\langle p_\mathrm{T}\rangle$	$\langle\theta\rangle$	$\mathrm{d}^2\sigma/\mathrm{d}p\mathrm{d}\Omega$			
0.20–0.24	0.221	25.2	1322.62	± 24.91	±	71.69						
0.24–0.30	0.269	25.3	1162.60	± 18.51	±	56.76	0.271	34.9	1361.65	± 19.82	±	60.37
0.30–0.36	0.329	25.3	887.87	± 16.65	±	44.96	0.329	35.1	1180.65	± 17.94	±	44.98
0.36–0.42	0.388	25.3	703.76	± 15.06	±	36.34	0.389	35.1	921.18	± 16.53	±	36.47
0.42–0.50	0.458	25.3	541.17	± 11.67	±	33.21	0.458	35.1	700.83	± 12.89	±	32.92
0.50–0.60	0.547	25.4	355.62	± 8.29	±	22.98	0.546	35.3	472.36	± 9.63	±	26.46
0.60–0.72	0.655	25.3	221.48	± 6.01	±	17.33	0.656	35.3	297.71	± 7.22	±	21.85
0.72–0.90							0.796	35.2	150.10	± 4.15	±	14.11

	$40 < \theta < 50$						$50 < \theta < 60$					
p_T	$\langle p_\mathrm{T}\rangle$	$\langle\theta\rangle$	$\mathrm{d}^2\sigma/\mathrm{d}p\mathrm{d}\Omega$				$\langle p_\mathrm{T}\rangle$	$\langle\theta\rangle$	$\mathrm{d}^2\sigma/\mathrm{d}p\mathrm{d}\Omega$			
0.30–0.36	0.329	45.1	1280.68	± 18.48	±	45.00						
0.36–0.42	0.389	45.1	1052.41	± 16.82	±	30.90	0.389	55.2	1073.63	± 15.99	±	39.41
0.42–0.50	0.458	45.0	808.64	± 13.40	±	28.64	0.458	55.1	871.11	± 13.18	±	25.25
0.50–0.60	0.546	45.1	532.68	± 10.32	±	30.67	0.547	55.0	589.45	± 10.26	±	25.16
0.60–0.72	0.655	45.2	339.45	± 7.76	±	24.71	0.657	55.0	370.09	± 7.94	±	24.41
0.72–0.90	0.798	45.1	164.66	± 4.60	±	17.27	0.797	54.9	181.22	± 4.71	±	17.24
0.90–1.25							1.030	54.9	47.78	± 1.80	±	7.30

	$60 < \theta < 75$						$75 < \theta < 90$					
p_T	$\langle p_\mathrm{T}\rangle$	$\langle\theta\rangle$	$\mathrm{d}^2\sigma/\mathrm{d}p\mathrm{d}\Omega$				$\langle p_\mathrm{T}\rangle$	$\langle\theta\rangle$	$\mathrm{d}^2\sigma/\mathrm{d}p\mathrm{d}\Omega$			
0.50–0.60	0.546	67.5	604.94	± 7.93	±	23.59						
0.60–0.72	0.655	67.4	344.00	± 5.88	±	20.56	0.653	81.8	270.90	± 4.77	±	19.58
0.72–0.90	0.797	67.1	157.69	± 3.54	±	15.67	0.795	81.5	114.11	± 2.79	±	11.70
0.90–1.25	1.035	66.8	41.15	± 1.36	±	6.78	1.023	81.6	23.68	± 1.03	±	4.17

	$90 < \theta < 105$						$105 < \theta < 125$					
p_T	$\langle p_\mathrm{T}\rangle$	$\langle\theta\rangle$	$\mathrm{d}^2\sigma/\mathrm{d}p\mathrm{d}\Omega$				$\langle p_\mathrm{T}\rangle$	$\langle\theta\rangle$	$\mathrm{d}^2\sigma/\mathrm{d}p\mathrm{d}\Omega$			
0.42–0.50							0.458	113.8	334.63	± 5.49	±	19.52
0.50–0.60							0.543	113.1	169.19	± 3.56	±	15.93
0.60–0.72	0.649	97.2	171.74	± 3.74	±	15.60	0.649	113.1	68.18	± 2.32	±	9.82
0.72–0.90	0.793	96.9	62.79	± 2.11	±	7.53	0.789	112.9	22.08	± 1.22	±	4.96

Table A.35: Double-differential inclusive cross-section $\mathrm{d}^2\sigma/\mathrm{d}p\mathrm{d}\Omega$ [mb/(GeV/c sr)] of the production of π^+'s in π^- + Ta $\rightarrow \pi^+$ + X interactions with -12.0 GeV/c beam momentum; the first error is statistical, the second systematic; p_T in GeV/c, polar angle θ in degrees.

	$20 < \theta < 30$					$30 < \theta < 40$				
p_T	$\langle p_\mathrm{T}\rangle$	$\langle\theta\rangle$	$\mathrm{d}^2\sigma/\mathrm{d}p\mathrm{d}\Omega$			$\langle p_\mathrm{T}\rangle$	$\langle\theta\rangle$	$\mathrm{d}^2\sigma/\mathrm{d}p\mathrm{d}\Omega$		
0.10–0.13	0.116	24.9	589.66 ± 21.32	±	48.49	0.116	34.9	556.76 ± 20.52	±	44.61
0.13–0.16	0.145	24.9	668.62 ± 20.23	±	39.98	0.145	34.8	560.39 ± 18.01	±	32.03
0.16–0.20	0.180	25.0	734.34 ± 17.59	±	36.60	0.180	34.8	595.83 ± 15.60	±	28.66
0.20–0.24	0.219	25.0	769.94 ± 17.89	±	33.65	0.220	34.8	571.35 ± 15.08	±	23.58
0.24–0.30	0.269	24.9	713.32 ± 13.93	±	25.87	0.269	34.9	567.07 ± 12.60	±	20.39
0.30–0.36	0.329	24.7	612.34 ± 12.77	±	19.22	0.329	34.8	512.39 ± 11.93	±	15.63
0.36–0.42	0.388	24.9	471.71 ± 10.91	±	14.08	0.389	34.7	397.34 ± 10.32	±	11.37
0.42–0.50	0.457	24.9	366.60 ± 8.36	±	13.33	0.458	34.8	289.05 ± 7.41	±	9.50
0.50–0.60	0.548	24.7	217.29 ± 5.37	±	11.17	0.548	34.8	193.21 ± 5.29	±	8.98
0.60–0.72	0.655	24.8	139.23 ± 3.81	±	10.75	0.656	34.8	107.44 ± 3.33	±	7.53
0.72–0.90						0.795	34.6	53.45 ± 1.79	±	5.91

	$40 < \theta < 50$					$50 < \theta < 60$				
p_T	$\langle p_\mathrm{T}\rangle$	$\langle\theta\rangle$	$\mathrm{d}^2\sigma/\mathrm{d}p\mathrm{d}\Omega$			$\langle p_\mathrm{T}\rangle$	$\langle\theta\rangle$	$\mathrm{d}^2\sigma/\mathrm{d}p\mathrm{d}\Omega$		
0.10–0.13	0.115	45.0	456.24 ± 19.78	±	37.47					
0.13–0.16	0.145	45.0	454.18 ± 16.07	±	26.37	0.145	55.1	346.96 ± 14.29	±	21.00
0.16–0.20	0.180	44.9	466.39 ± 13.73	±	22.66	0.179	54.9	387.48 ± 12.38	±	18.73
0.20–0.24	0.220	44.8	475.45 ± 13.94	±	19.78	0.220	54.8	409.97 ± 12.97	±	16.69
0.24–0.30	0.269	44.8	455.68 ± 11.26	±	16.15	0.269	54.8	327.77 ± 9.48	±	11.33
0.30–0.36	0.330	44.7	358.19 ± 9.97	±	11.10	0.329	54.5	276.81 ± 8.84	±	8.96
0.36–0.42	0.388	44.8	304.34 ± 9.10	±	8.89	0.389	54.7	242.51 ± 8.29	±	8.05
0.42–0.50	0.458	44.6	235.68 ± 6.86	±	7.88	0.457	54.8	167.77 ± 5.80	±	6.15
0.50–0.60	0.548	44.8	144.53 ± 4.62	±	6.54	0.548	54.7	105.55 ± 4.03	±	5.22
0.60–0.72	0.656	44.6	92.17 ± 3.31	±	6.00	0.656	54.5	64.61 ± 2.79	±	4.50
0.72–0.90	0.793	44.7	37.43 ± 1.51	±	3.84	0.794	54.5	27.55 ± 1.41	±	2.78
0.90–1.25						1.024	54.5	5.47 ± 0.32	±	0.99

	$60 < \theta < 75$					$75 < \theta < 90$				
p_T	$\langle p_\mathrm{T}\rangle$	$\langle\theta\rangle$	$\mathrm{d}^2\sigma/\mathrm{d}p\mathrm{d}\Omega$			$\langle p_\mathrm{T}\rangle$	$\langle\theta\rangle$	$\mathrm{d}^2\sigma/\mathrm{d}p\mathrm{d}\Omega$		
0.13–0.16	0.145	67.4	333.75 ± 18.54	±	20.53	0.150	80.6	317.10 ± 28.80	±	138.19
0.16–0.20	0.180	66.9	317.21 ± 9.15	±	15.38	0.176	81.6	336.48 ± 70.12	±	20.40
0.20–0.24	0.220	67.4	292.90 ± 8.87	±	11.65	0.220	81.9	244.48 ± 8.69	±	10.43
0.24–0.30	0.269	67.1	260.93 ± 7.02	±	8.90	0.268	81.7	186.74 ± 6.34	±	9.12
0.30–0.36	0.328	66.8	211.44 ± 6.45	±	7.65	0.329	81.9	132.03 ± 5.37	±	7.06
0.36–0.42	0.388	66.6	150.67 ± 5.37	±	5.60	0.389	81.9	86.00 ± 4.24	±	4.45
0.42–0.50	0.458	66.7	109.23 ± 3.91	±	4.75	0.456	81.6	66.55 ± 3.15	±	3.87
0.50–0.60	0.546	66.6	78.75 ± 2.94	±	4.68	0.546	82.0	40.30 ± 2.13	±	3.00
0.60–0.72	0.656	66.6	43.16 ± 1.92	±	3.57	0.650	81.5	22.49 ± 1.38	±	2.26
0.72–0.90	0.793	66.1	13.97 ± 0.80	±	1.68	0.793	81.4	8.18 ± 0.62	±	1.15
0.90–1.25	1.040	66.0	3.62 ± 0.23	±	0.70	1.030	80.1	1.44 ± 0.14	±	0.32

	$90 < \theta < 105$					$105 < \theta < 125$				
p_T	$\langle p_\mathrm{T}\rangle$	$\langle\theta\rangle$	$\mathrm{d}^2\sigma/\mathrm{d}p\mathrm{d}\Omega$			$\langle p_\mathrm{T}\rangle$	$\langle\theta\rangle$	$\mathrm{d}^2\sigma/\mathrm{d}p\mathrm{d}\Omega$		
0.13–0.16						0.145	114.9	198.22 ± 7.90	±	10.62
0.16–0.20	0.175	98.1	289.20 ± 70.80	±	14.25	0.179	114.0	160.81 ± 5.68	±	6.49
0.20–0.24	0.220	97.7	187.68 ± 7.84	±	8.54	0.219	114.0	125.21 ± 5.24	±	4.32
0.24–0.30	0.267	97.3	148.09 ± 5.72	±	7.57	0.267	113.6	69.56 ± 3.18	±	2.88
0.30–0.36	0.328	97.3	86.80 ± 4.39	±	5.24	0.327	113.6	41.01 ± 2.43	±	2.45
0.36–0.42	0.389	96.7	57.95 ± 3.42	±	3.52	0.390	113.3	32.01 ± 2.13	±	2.57
0.42–0.50	0.458	96.6	41.78 ± 2.48	±	3.31	0.455	113.7	17.77 ± 1.34	±	1.86
0.50–0.60	0.544	97.0	23.43 ± 1.61	±	2.46	0.547	114.0	8.76 ± 0.80	±	1.23
0.60–0.72	0.654	97.0	9.11 ± 0.85	±	1.29	0.651	112.5	2.94 ± 0.42	±	0.54
0.72–0.90	0.799	96.8	3.81 ± 0.45	±	0.72	0.791	110.0	0.32 ± 0.09	±	0.08
0.90–1.25	1.038	96.4	0.47 ± 0.08	±	0.14	1.040	112.3	0.07 ± 0.02	±	0.03

Table A.36: Double-differential inclusive cross-section $\mathrm{d}^2\sigma/\mathrm{d}p\mathrm{d}\Omega$ [mb/(GeV/c sr)] of the production of π^-'s in π^- + Ta $\rightarrow \pi^-$ + X interactions with -12.0 GeV/c beam momentum; the first error is statistical, the second systematic; p_T in GeV/c, polar angle θ in degrees.

	$20 < \theta < 30$			$30 < \theta < 40$		
p_T	$\langle p_\mathrm{T}\rangle$	$\langle\theta\rangle$	$\mathrm{d}^2\sigma/\mathrm{d}p\mathrm{d}\Omega$	$\langle p_\mathrm{T}\rangle$	$\langle\theta\rangle$	$\mathrm{d}^2\sigma/\mathrm{d}p\mathrm{d}\Omega$
0.10–0.13	0.115	24.9	817.83 ± 24.86 ± 61.65	0.115	35.0	698.97 ± 22.54 ± 52.29
0.13–0.16	0.145	24.8	853.86 ± 22.99 ± 50.13	0.146	34.9	725.61 ± 21.08 ± 42.98
0.16–0.20	0.180	24.8	967.40 ± 20.48 ± 47.75	0.180	34.8	769.59 ± 18.13 ± 37.77
0.20–0.24	0.220	24.8	977.94 ± 20.50 ± 41.24	0.220	34.8	759.47 ± 17.87 ± 31.29
0.24–0.30	0.269	24.8	869.74 ± 15.61 ± 29.54	0.270	34.8	712.17 ± 14.19 ± 24.10
0.30–0.36	0.329	24.8	724.21 ± 14.11 ± 20.68	0.329	34.8	567.23 ± 12.66 ± 16.52
0.36–0.42	0.389	24.9	594.19 ± 12.82 ± 17.40	0.389	34.8	482.53 ± 11.61 ± 13.99
0.42–0.50	0.458	24.7	457.87 ± 9.76 ± 16.79	0.457	34.7	345.69 ± 8.38 ± 12.22
0.50–0.60	0.546	24.8	292.27 ± 6.84 ± 14.83	0.547	34.7	208.85 ± 5.81 ± 10.25
0.60–0.72	0.654	24.7	171.81 ± 4.76 ± 12.28	0.656	34.7	130.46 ± 4.10 ± 9.01
0.72–0.90				0.798	34.7	65.40 ± 2.34 ± 6.42

	$40 < \theta < 50$			$50 < \theta < 60$		
p_T	$\langle p_\mathrm{T}\rangle$	$\langle\theta\rangle$	$\mathrm{d}^2\sigma/\mathrm{d}p\mathrm{d}\Omega$	$\langle p_\mathrm{T}\rangle$	$\langle\theta\rangle$	$\mathrm{d}^2\sigma/\mathrm{d}p\mathrm{d}\Omega$
0.10–0.13	0.115	45.2	606.00 ± 21.74 ± 46.49			
0.13–0.16	0.146	44.9	630.25 ± 19.50 ± 37.60	0.144	55.1	601.44 ± 19.29 ± 36.89
0.16–0.20	0.180	44.9	616.98 ± 16.14 ± 30.50	0.179	55.0	508.48 ± 14.54 ± 24.95
0.20–0.24	0.219	44.9	587.13 ± 15.82 ± 24.92	0.220	55.0	463.08 ± 13.87 ± 18.82
0.24–0.30	0.269	44.8	545.69 ± 12.48 ± 18.94	0.268	54.8	422.32 ± 11.01 ± 14.84
0.30–0.36	0.328	44.8	451.86 ± 11.45 ± 14.35	0.329	54.8	345.47 ± 9.99 ± 10.89
0.36–0.42	0.389	44.8	344.27 ± 9.71 ± 10.37	0.388	54.8	269.79 ± 8.83 ± 9.05
0.42–0.50	0.458	44.7	259.08 ± 7.37 ± 9.69	0.458	54.6	192.85 ± 6.34 ± 7.60
0.50–0.60	0.546	44.8	165.16 ± 5.17 ± 8.62	0.544	54.9	131.73 ± 4.69 ± 7.18
0.60–0.72	0.653	44.9	97.66 ± 3.57 ± 7.17	0.655	54.7	72.78 ± 3.10 ± 5.52
0.72–0.90	0.796	44.8	43.20 ± 1.89 ± 4.52	0.795	54.4	30.90 ± 1.60 ± 3.32
0.90–1.25				1.023	55.0	6.32 ± 0.45 ± 1.10

	$60 < \theta < 75$			$75 < \theta < 90$		
p_T	$\langle p_\mathrm{T}\rangle$	$\langle\theta\rangle$	$\mathrm{d}^2\sigma/\mathrm{d}p\mathrm{d}\Omega$	$\langle p_\mathrm{T}\rangle$	$\langle\theta\rangle$	$\mathrm{d}^2\sigma/\mathrm{d}p\mathrm{d}\Omega$
0.13–0.16	0.145	67.1	453.47 ± 21.11 ± 26.70			
0.16–0.20	0.179	67.3	416.18 ± 10.75 ± 19.13	0.180	81.7	342.63 ± 11.34 ± 18.30
0.20–0.24	0.219	67.4	380.65 ± 10.52 ± 14.73	0.219	81.9	279.62 ± 9.58 ± 13.05
0.24–0.30	0.269	67.0	316.87 ± 7.97 ± 11.67	0.268	81.9	235.60 ± 7.24 ± 11.97
0.30–0.36	0.329	67.0	241.12 ± 7.05 ± 9.69	0.329	81.6	168.11 ± 6.22 ± 10.19
0.36–0.42	0.389	66.8	191.93 ± 6.23 ± 8.00	0.388	82.1	111.38 ± 4.83 ± 5.80
0.42–0.50	0.458	67.0	128.61 ± 4.27 ± 5.79	0.458	81.7	79.57 ± 3.46 ± 4.83
0.50–0.60	0.545	66.8	90.06 ± 3.17 ± 5.61	0.545	81.8	50.34 ± 2.42 ± 4.05
0.60–0.72	0.653	67.1	44.70 ± 1.97 ± 3.83	0.649	81.5	24.09 ± 1.48 ± 2.61
0.72–0.90	0.791	66.7	18.67 ± 1.01 ± 2.24	0.787	81.6	7.98 ± 0.65 ± 1.19
0.90–1.25	1.038	66.2	3.25 ± 0.27 ± 0.61	1.010	80.7	1.64 ± 0.19 ± 0.37

	$90 < \theta < 105$			$105 < \theta < 125$		
p_T	$\langle p_\mathrm{T}\rangle$	$\langle\theta\rangle$	$\mathrm{d}^2\sigma/\mathrm{d}p\mathrm{d}\Omega$	$\langle p_\mathrm{T}\rangle$	$\langle\theta\rangle$	$\mathrm{d}^2\sigma/\mathrm{d}p\mathrm{d}\Omega$
0.13–0.16				0.144	114.5	268.93 ± 9.51 ± 16.04
0.16–0.20	0.180	97.8	278.04 ± 10.35 ± 14.09	0.179	113.6	212.93 ± 6.80 ± 7.71
0.20–0.24	0.219	97.5	255.22 ± 9.52 ± 14.13	0.218	113.8	138.27 ± 5.61 ± 5.07
0.24–0.30	0.268	97.4	171.61 ± 6.30 ± 9.79	0.267	113.8	78.68 ± 3.46 ± 3.80
0.30–0.36	0.328	97.3	101.22 ± 4.74 ± 6.02	0.330	113.6	48.66 ± 2.68 ± 3.29
0.36–0.42	0.389	97.0	77.35 ± 4.02 ± 5.19	0.387	113.0	37.83 ± 2.34 ± 3.44
0.42–0.50	0.458	96.9	50.47 ± 2.80 ± 4.45	0.456	112.8	19.20 ± 1.39 ± 2.28
0.50–0.60	0.543	96.6	25.48 ± 1.68 ± 2.93	0.544	113.0	8.16 ± 0.81 ± 1.27
0.60–0.72	0.654	96.7	8.96 ± 0.88 ± 1.38	0.646	112.2	2.94 ± 0.42 ± 0.60
0.72–0.90	0.781	96.2	2.54 ± 0.37 ± 0.53	0.790	112.5	0.56 ± 0.14 ± 0.15
0.90–1.25	0.954	97.2	0.31 ± 0.08 ± 0.10			

Table A.37: Double-differential inclusive cross-section $\mathrm{d}^2\sigma/\mathrm{d}p\mathrm{d}\Omega$ [mb/(GeV/c sr)] of the production of protons in p + Ta $\rightarrow$ p + X interactions with $+15.0$ GeV/c beam momentum; the first error is statistical, the second systematic; p_T in GeV/c, polar angle θ in degrees.

	$20 < \theta < 30$					$30 < \theta < 40$				
p_T	$\langle p_\mathrm{T}\rangle$	$\langle\theta\rangle$	$\mathrm{d}^2\sigma/\mathrm{d}p\mathrm{d}\Omega$			$\langle p_\mathrm{T}\rangle$	$\langle\theta\rangle$	$\mathrm{d}^2\sigma/\mathrm{d}p\mathrm{d}\Omega$		
0.20–0.24	0.220	25.2	1644.71 ± 50.11	±	158.22					
0.24–0.30	0.268	25.2	1534.96 ± 38.08	±	126.93	0.270	34.9	1756.13 ± 41.18	±	130.89
0.30–0.36	0.328	25.2	1292.93 ± 36.35	±	91.71	0.328	35.1	1635.18 ± 38.71	±	95.89
0.36–0.42	0.388	25.1	1033.10 ± 32.85	±	62.73	0.388	35.2	1313.09 ± 35.73	±	62.87
0.42–0.50	0.455	25.3	753.22 ± 24.78	±	43.20	0.456	35.2	1038.17 ± 28.46	±	46.33
0.50–0.60	0.545	25.3	524.34 ± 18.35	±	33.25	0.543	35.1	721.33 ± 21.81	±	39.71
0.60–0.72	0.651	25.4	381.21 ± 14.37	±	30.17	0.651	35.1	472.54 ± 16.38	±	38.31
0.72–0.90						0.793	35.0	261.44 ± 9.94	±	31.04

	$40 < \theta < 50$					$50 < \theta < 60$				
p_T	$\langle p_\mathrm{T}\rangle$	$\langle\theta\rangle$	$\mathrm{d}^2\sigma/\mathrm{d}p\mathrm{d}\Omega$			$\langle p_\mathrm{T}\rangle$	$\langle\theta\rangle$	$\mathrm{d}^2\sigma/\mathrm{d}p\mathrm{d}\Omega$		
0.30–0.36	0.329	45.0	1671.83 ± 37.63	±	74.07					
0.36–0.42	0.389	44.9	1401.04 ± 35.17	±	45.24	0.389	55.1	1408.12 ± 33.38	±	48.59
0.42–0.50	0.458	45.0	1114.11 ± 28.28	±	36.18	0.458	55.2	1153.27 ± 27.34	±	35.49
0.50–0.60	0.546	45.0	788.32 ± 22.45	±	43.96	0.546	54.9	800.01 ± 21.45	±	42.12
0.60–0.72	0.655	45.1	532.32 ± 17.54	±	43.79	0.654	54.9	513.97 ± 16.73	±	44.52
0.72–0.90	0.800	44.9	277.64 ± 10.70	±	35.82	0.800	54.9	278.42 ± 10.58	±	36.20
0.90–1.25	1.044	45.0	80.93 ± 4.17	±	16.76	1.037	54.9	75.86 ± 4.02	±	15.88

	$60 < \theta < 75$					$75 < \theta < 90$				
p_T	$\langle p_\mathrm{T}\rangle$	$\langle\theta\rangle$	$\mathrm{d}^2\sigma/\mathrm{d}p\mathrm{d}\Omega$			$\langle p_\mathrm{T}\rangle$	$\langle\theta\rangle$	$\mathrm{d}^2\sigma/\mathrm{d}p\mathrm{d}\Omega$		
0.50–0.60	0.545	67.5	793.04 ± 16.34	±	46.50					
0.60–0.72	0.655	67.1	470.67 ± 12.51	±	47.37	0.651	81.6	371.28 ± 10.07	±	49.58
0.72–0.90	0.797	67.0	213.74 ± 7.46	±	35.23	0.791	81.7	142.81 ± 5.68	±	27.63
0.90–1.25	1.033	66.5	57.06 ± 2.89	±	15.61	1.023	81.6	27.82 ± 2.08	±	8.65

	$90 < \theta < 105$					$105 < \theta < 125$				
p_T	$\langle p_\mathrm{T}\rangle$	$\langle\theta\rangle$	$\mathrm{d}^2\sigma/\mathrm{d}p\mathrm{d}\Omega$			$\langle p_\mathrm{T}\rangle$	$\langle\theta\rangle$	$\mathrm{d}^2\sigma/\mathrm{d}p\mathrm{d}\Omega$		
0.42–0.50						0.458	113.7	449.36 ± 12.24	±	43.63
0.50–0.60						0.541	112.9	213.36 ± 7.34	±	37.33
0.60–0.72	0.650	97.1	227.68 ± 7.85	±	38.80	0.651	112.5	78.07 ± 4.50	±	21.48
0.72–0.90	0.791	97.1	72.97 ± 4.14	±	16.39	0.788	112.6	18.03 ± 1.99	±	7.54

Table A.38: Double-differential inclusive cross-section $\mathrm{d}^2\sigma/\mathrm{d}p\mathrm{d}\Omega$ [mb/(GeV/c sr)] of the production of π^+'s in p + Ta $\rightarrow \pi^+$ + X interactions with $+15.0$ GeV/c beam momentum; the first error is statistical, the second systematic; p_T in GeV/c, polar angle θ in degrees.

	$20 < \theta < 30$					$30 < \theta < 40$				
p_T	$\langle p_\mathrm{T}\rangle$	$\langle\theta\rangle$	$\mathrm{d}^2\sigma/\mathrm{d}p\mathrm{d}\Omega$			$\langle p_\mathrm{T}\rangle$	$\langle\theta\rangle$	$\mathrm{d}^2\sigma/\mathrm{d}p\mathrm{d}\Omega$		
0.10–0.13	0.116	25.0	717.50 ± 44.18	±	84.40	0.116	34.8	611.54 ± 38.50	±	66.86
0.13–0.16	0.145	24.9	816.60 ± 41.95	±	76.44	0.145	35.0	645.26 ± 35.30	±	58.27
0.16–0.20	0.180	24.9	936.93 ± 37.56	±	75.02	0.180	34.7	726.47 ± 32.23	±	55.72
0.20–0.24	0.219	24.8	941.65 ± 36.89	±	62.71	0.220	34.9	736.98 ± 32.28	±	46.59
0.24–0.30	0.268	24.9	848.94 ± 28.09	±	42.52	0.268	34.8	665.63 ± 25.42	±	32.42
0.30–0.36	0.327	24.8	761.21 ± 26.45	±	26.93	0.329	34.8	558.14 ± 22.88	±	18.65
0.36–0.42	0.388	24.6	584.61 ± 22.86	±	17.74	0.387	34.7	447.73 ± 20.29	±	13.21
0.42–0.50	0.455	24.8	460.98 ± 17.33	±	19.34	0.456	34.8	319.99 ± 14.54	±	13.49
0.50–0.60	0.545	24.8	300.98 ± 12.18	±	21.33	0.543	34.9	215.14 ± 10.43	±	15.14
0.60–0.72	0.652	24.8	209.96 ± 8.86	±	23.57	0.651	34.7	127.39 ± 6.82	±	14.09
0.72–0.90						0.791	34.7	73.64 ± 3.83	±	12.60

	$40 < \theta < 50$					$50 < \theta < 60$				
p_T	$\langle p_\mathrm{T}\rangle$	$\langle\theta\rangle$	$\mathrm{d}^2\sigma/\mathrm{d}p\mathrm{d}\Omega$			$\langle p_\mathrm{T}\rangle$	$\langle\theta\rangle$	$\mathrm{d}^2\sigma/\mathrm{d}p\mathrm{d}\Omega$		
0.10–0.13	0.116	45.0	608.74 ± 39.50	±	66.90					
0.13–0.16	0.145	45.4	656.32 ± 35.94	±	59.59	0.146	55.1	517.86 ± 32.31	±	46.62
0.16–0.20	0.179	44.9	616.45 ± 29.17	±	47.06	0.180	54.6	494.57 ± 25.48	±	36.20
0.20–0.24	0.219	44.7	524.63 ± 26.95	±	32.82	0.220	54.7	506.67 ± 26.75	±	29.75
0.24–0.30	0.269	44.8	535.14 ± 22.59	±	25.26	0.268	54.8	394.18 ± 19.24	±	16.75
0.30–0.36	0.330	44.8	416.66 ± 20.05	±	14.26	0.328	54.8	336.76 ± 18.07	±	11.00
0.36–0.42	0.391	44.6	369.11 ± 18.67	±	11.38	0.390	55.0	260.79 ± 15.67	±	8.94
0.42–0.50	0.458	44.8	270.79 ± 13.82	±	12.19	0.455	54.8	208.76 ± 12.21	±	11.00
0.50–0.60	0.549	44.7	174.02 ± 9.71	±	12.84	0.548	54.6	121.94 ± 8.16	±	10.20
0.60–0.72	0.652	44.6	106.58 ± 6.50	±	12.06	0.656	54.8	74.20 ± 5.64	±	9.31
0.72–0.90	0.793	44.9	46.29 ± 3.20	±	7.95	0.805	54.3	29.98 ± 2.59	±	5.56
0.90–1.25						1.015	54.2	8.14 ± 0.81	±	2.42

	$60 < \theta < 75$					$75 < \theta < 90$				
p_T	$\langle p_\mathrm{T}\rangle$	$\langle\theta\rangle$	$\mathrm{d}^2\sigma/\mathrm{d}p\mathrm{d}\Omega$			$\langle p_\mathrm{T}\rangle$	$\langle\theta\rangle$	$\mathrm{d}^2\sigma/\mathrm{d}p\mathrm{d}\Omega$		
0.13–0.16	0.146	66.9	417.53 ± 25.78	±	39.09					
0.16–0.20	0.180	67.4	393.46 ± 18.81	±	29.18	0.181	81.6	360.84 ± 21.27	±	27.67
0.20–0.24	0.220	67.1	374.62 ± 18.34	±	21.24	0.218	82.3	285.28 ± 17.02	±	14.30
0.24–0.30	0.268	66.9	333.70 ± 14.74	±	14.02	0.267	81.9	235.53 ± 12.86	±	10.57
0.30–0.36	0.329	66.9	237.38 ± 12.66	±	9.25	0.327	81.4	177.00 ± 11.48	±	10.18
0.36–0.42	0.391	67.2	184.23 ± 11.05	±	8.34	0.390	81.0	104.29 ± 8.68	±	7.43
0.42–0.50	0.458	66.7	138.57 ± 8.21	±	9.57	0.458	81.8	84.85 ± 6.56	±	8.04
0.50–0.60	0.544	66.7	84.04 ± 5.54	±	8.91	0.541	82.0	42.15 ± 3.91	±	5.75
0.60–0.72	0.654	66.6	39.36 ± 3.38	±	6.12	0.654	81.6	23.56 ± 2.63	±	4.52
0.72–0.90	0.794	66.3	18.05 ± 1.68	±	4.05	0.794	81.8	7.97 ± 1.12	±	2.15
0.90–1.25	1.031	66.5	3.74 ± 0.45	±	1.32	1.004	81.3	1.08 ± 0.24	±	0.45

	$90 < \theta < 105$					$105 < \theta < 125$				
p_T	$\langle p_\mathrm{T}\rangle$	$\langle\theta\rangle$	$\mathrm{d}^2\sigma/\mathrm{d}p\mathrm{d}\Omega$			$\langle p_\mathrm{T}\rangle$	$\langle\theta\rangle$	$\mathrm{d}^2\sigma/\mathrm{d}p\mathrm{d}\Omega$		
0.13–0.16						0.145	114.8	247.29 ± 16.45	±	15.32
0.16–0.20	0.180	97.9	294.95 ± 19.68	±	19.65	0.178	114.3	189.57 ± 11.03	±	8.64
0.20–0.24	0.218	97.1	241.02 ± 15.69	±	9.92	0.217	113.8	137.04 ± 9.85	±	5.13
0.24–0.30	0.268	97.2	170.73 ± 11.09	±	8.38	0.266	113.5	91.40 ± 6.78	±	5.67
0.30–0.36	0.328	97.1	107.20 ± 8.90	±	7.90	0.328	114.9	45.03 ± 4.67	±	4.65
0.36–0.42	0.390	97.3	76.59 ± 7.40	±	7.87	0.386	113.5	27.92 ± 3.66	±	4.10
0.42–0.50	0.455	96.4	40.97 ± 4.49	±	5.82	0.458	112.7	18.78 ± 2.53	±	3.74
0.50–0.60	0.547	96.3	21.68 ± 2.87	±	4.31	0.546	112.5	6.10 ± 1.24	±	1.63
0.60–0.72	0.655	96.0	12.76 ± 1.90	±	3.45	0.656	112.5	2.06 ± 0.62	±	0.73
0.72–0.90	0.780	96.5	2.60 ± 0.61	±	0.96	0.763	111.7	0.56 ± 0.26	±	0.27
0.90–1.25	1.010	94.6	0.38 ± 0.13	±	0.21					

Table A.39: Double-differential inclusive cross-section $\mathrm{d}^2\sigma/\mathrm{d}p\mathrm{d}\Omega$ [mb/(GeV/c sr)] of the production of π^-'s in p + Ta $\rightarrow \pi^-$ + X interactions with $+15.0$ GeV/c beam momentum; the first error is statistical, the second systematic; p_T in GeV/c, polar angle θ in degrees.

	$20 < \theta < 30$						$30 < \theta < 40$					
p_T	$\langle p_\mathrm{T}\rangle$	$\langle\theta\rangle$	$\mathrm{d}^2\sigma/\mathrm{d}p\mathrm{d}\Omega$				$\langle p_\mathrm{T}\rangle$	$\langle\theta\rangle$	$\mathrm{d}^2\sigma/\mathrm{d}p\mathrm{d}\Omega$			
0.10–0.13	0.116	24.8	878.26	± 47.60	±	104.73	0.116	34.9	739.55	± 43.13	±	85.86
0.13–0.16	0.145	24.8	864.06	± 42.25	±	82.61	0.145	34.8	736.66	± 37.49	±	69.49
0.16–0.20	0.180	25.0	991.65	± 37.69	±	78.18	0.180	34.8	839.75	± 34.00	±	65.94
0.20–0.24	0.220	24.8	954.45	± 36.22	±	59.47	0.220	34.8	835.56	± 33.97	±	52.25
0.24–0.30	0.270	24.8	803.73	± 27.14	±	35.58	0.270	34.8	701.99	± 25.37	±	31.13
0.30–0.36	0.330	25.0	668.50	± 24.48	±	19.24	0.330	34.8	539.50	± 22.08	±	15.70
0.36–0.42	0.390	25.0	561.48	± 22.50	±	18.18	0.390	34.9	474.45	± 21.14	±	15.51
0.42–0.50	0.460	25.0	361.84	± 15.63	±	19.59	0.461	34.6	303.64	± 14.16	±	15.59
0.50–0.60	0.549	24.9	216.86	± 10.62	±	19.32	0.547	35.1	205.97	± 10.48	±	17.50
0.60–0.72	0.661	24.8	150.46	± 8.15	±	20.20	0.658	35.0	94.01	± 5.96	±	12.36
0.72–0.90							0.794	34.7	54.57	± 3.76	±	10.39

	$40 < \theta < 50$						$50 < \theta < 60$					
p_T	$\langle p_\mathrm{T}\rangle$	$\langle\theta\rangle$	$\mathrm{d}^2\sigma/\mathrm{d}p\mathrm{d}\Omega$				$\langle p_\mathrm{T}\rangle$	$\langle\theta\rangle$	$\mathrm{d}^2\sigma/\mathrm{d}p\mathrm{d}\Omega$			
0.10–0.13	0.115	45.3	664.75	± 40.33	±	76.41						
0.13–0.16	0.146	45.0	693.22	± 36.58	±	66.13	0.144	55.0	510.27	± 31.49	±	47.58
0.16–0.20	0.180	44.9	644.62	± 29.65	±	50.80	0.179	54.9	537.37	± 26.98	±	40.48
0.20–0.24	0.220	44.9	572.06	± 27.97	±	35.71	0.218	54.7	533.24	± 27.26	±	31.36
0.24–0.30	0.269	44.9	552.21	± 22.77	±	24.43	0.269	54.7	410.05	± 19.60	±	17.09
0.30–0.36	0.330	44.6	397.43	± 19.15	±	11.57	0.329	54.9	373.33	± 18.68	±	11.12
0.36–0.42	0.389	45.1	351.54	± 17.92	±	11.83	0.387	54.7	275.33	± 16.11	±	10.56
0.42–0.50	0.457	45.0	245.79	± 12.90	±	13.76	0.458	54.8	206.50	± 11.87	±	12.52
0.50–0.60	0.543	45.0	163.69	± 9.34	±	14.99	0.543	54.7	114.18	± 7.61	±	11.01
0.60–0.72	0.651	45.2	83.60	± 5.97	±	11.50	0.653	54.4	68.48	± 5.49	±	9.75
0.72–0.90	0.802	44.8	35.08	± 3.00	±	7.09	0.792	55.2	19.82	± 2.22	±	4.13
0.90–1.25							1.033	54.2	4.79	± 0.70	±	1.56

	$60 < \theta < 75$						$75 < \theta < 90$					
p_T	$\langle p_\mathrm{T}\rangle$	$\langle\theta\rangle$	$\mathrm{d}^2\sigma/\mathrm{d}p\mathrm{d}\Omega$				$\langle p_\mathrm{T}\rangle$	$\langle\theta\rangle$	$\mathrm{d}^2\sigma/\mathrm{d}p\mathrm{d}\Omega$			
0.13–0.16	0.146	67.5	554.18	± 30.49	±	48.78	0.150	81.0	260.01	± 30.36	±	43.86
0.16–0.20	0.179	66.9	422.56	± 19.84	±	28.71	0.181	81.9	433.37	± 25.05	±	39.42
0.20–0.24	0.220	66.8	386.36	± 18.74	±	19.67	0.219	81.4	298.72	± 17.72	±	15.26
0.24–0.30	0.268	66.5	342.18	± 14.75	±	12.77	0.268	81.5	227.20	± 12.91	±	11.60
0.30–0.36	0.329	66.6	247.03	± 12.74	±	9.14	0.327	81.5	171.48	± 11.36	±	11.02
0.36–0.42	0.390	66.3	182.82	± 10.89	±	9.22	0.388	81.7	119.67	± 9.16	±	9.12
0.42–0.50	0.456	66.4	142.50	± 8.20	±	10.71	0.458	82.0	74.35	± 5.98	±	7.75
0.50–0.60	0.544	67.0	80.78	± 5.32	±	9.20	0.546	81.6	43.16	± 4.01	±	6.48
0.60–0.72	0.655	66.7	46.56	± 3.73	±	7.59	0.655	81.6	21.75	± 2.43	±	4.54
0.72–0.90	0.790	66.2	18.34	± 1.78	±	4.25	0.785	81.0	6.04	± 1.06	±	1.74
0.90–1.25	1.015	67.1	3.00	± 0.44	±	1.08	1.015	82.5	1.27	± 0.27	±	0.56

	$90 < \theta < 105$						$105 < \theta < 125$					
p_T	$\langle p_\mathrm{T}\rangle$	$\langle\theta\rangle$	$\mathrm{d}^2\sigma/\mathrm{d}p\mathrm{d}\Omega$				$\langle p_\mathrm{T}\rangle$	$\langle\theta\rangle$	$\mathrm{d}^2\sigma/\mathrm{d}p\mathrm{d}\Omega$			
0.13–0.16							0.145	114.2	340.65	± 20.51	±	19.53
0.16–0.20	0.181	97.8	347.76	± 23.08	±	35.06	0.177	113.7	195.83	± 11.75	±	7.20
0.20–0.24	0.218	97.3	215.86	± 15.11	±	9.06	0.218	113.6	150.69	± 10.63	±	6.54
0.24–0.30	0.268	96.9	172.70	± 11.32	±	9.53	0.269	113.4	96.21	± 6.94	±	7.33
0.30–0.36	0.329	97.0	105.57	± 8.71	±	8.26	0.330	114.4	46.93	± 4.71	±	5.72
0.36–0.42	0.387	97.2	65.23	± 6.63	±	7.28	0.391	113.6	42.27	± 4.44	±	7.22
0.42–0.50	0.462	96.1	50.85	± 4.96	±	8.02	0.458	113.3	18.43	± 2.49	±	4.19
0.50–0.60	0.551	96.5	25.37	± 3.06	±	5.58	0.547	111.4	10.41	± 1.59	±	3.15
0.60–0.72	0.651	96.5	15.04	± 2.13	±	4.47	0.635	111.5	3.20	± 0.80	±	1.26
0.72–0.90	0.800	98.3	1.66	± 0.49	±	0.67	0.791	109.5	0.53	± 0.22	±	0.28
0.90–1.25	1.015	95.4	0.37	± 0.14	±	0.22						

Table A.40: Double-differential inclusive cross-section $\mathrm{d}^2\sigma/\mathrm{d}p\mathrm{d}\Omega$ [mb/(GeV/c sr)] of the production of protons in π^+ + Ta $\rightarrow$ p + X interactions with $+15.0$ GeV/c beam momentum; the first error is statistical, the second systematic; p_T in GeV/c, polar angle θ in degrees.

	$20 < \theta < 30$			$30 < \theta < 40$		
p_T	$\langle p_\mathrm{T}\rangle$	$\langle\theta\rangle$	$\mathrm{d}^2\sigma/\mathrm{d}p\mathrm{d}\Omega$	$\langle p_\mathrm{T}\rangle$	$\langle\theta\rangle$	$\mathrm{d}^2\sigma/\mathrm{d}p\mathrm{d}\Omega$
0.50–0.60	0.548	24.7	279.11 $\pm$ 120.03 $\pm$ 19.63	0.542	35.6	300.76 $\pm$ 129.84 $\pm$ 19.00
0.60–0.72	0.659	25.3	237.06 $\pm$ 103.12 $\pm$ 20.14	0.644	36.1	283.76 $\pm$ 113.99 $\pm$ 24.59
0.72–0.90				0.814	35.5	142.40 $\pm$ 67.63 $\pm$ 17.34

	$40 < \theta < 50$			$50 < \theta < 60$		
p_T	$\langle p_\mathrm{T}\rangle$	$\langle\theta\rangle$	$\mathrm{d}^2\sigma/\mathrm{d}p\mathrm{d}\Omega$	$\langle p_\mathrm{T}\rangle$	$\langle\theta\rangle$	$\mathrm{d}^2\sigma/\mathrm{d}p\mathrm{d}\Omega$
0.50–0.60				0.552	54.8	725.51 $\pm$ 187.61 $\pm$ 43.81
0.60–0.72	0.655	44.4	582.79 $\pm$ 167.53 $\pm$ 51.30	0.661	55.9	287.15 $\pm$ 114.41 $\pm$ 26.31
0.72–0.90	0.787	46.7	202.67 $\pm$ 84.28 $\pm$ 26.85	0.802	55.6	235.15 $\pm$ 90.13 $\pm$ 31.35
0.90–1.25	1.049	44.9	43.95 $\pm$ 28.50 $\pm$ 9.20	1.071	55.1	102.54 $\pm$ 43.12 $\pm$ 21.70

	$60 < \theta < 75$			$75 < \theta < 90$		
p_T	$\langle p_\mathrm{T}\rangle$	$\langle\theta\rangle$	$\mathrm{d}^2\sigma/\mathrm{d}p\mathrm{d}\Omega$	$\langle p_\mathrm{T}\rangle$	$\langle\theta\rangle$	$\mathrm{d}^2\sigma/\mathrm{d}p\mathrm{d}\Omega$
0.50–0.60	0.541	68.9	786.30 $\pm$ 150.76 $\pm$ 50.55			
0.60–0.72	0.652	66.9	512.07 $\pm$ 118.94 $\pm$ 53.39	0.650	81.6	242.50 $\pm$ 75.57 $\pm$ 32.93
0.72–0.90	0.805	68.1	170.37 $\pm$ 60.48 $\pm$ 28.30	0.813	82.2	164.51 $\pm$ 55.70 $\pm$ 32.03
0.90–1.25	1.050	67.0	33.56 $\pm$ 20.04 $\pm$ 9.21			

	$90 < \theta < 105$			$105 < \theta < 125$		
p_T	$\langle p_\mathrm{T}\rangle$	$\langle\theta\rangle$	$\mathrm{d}^2\sigma/\mathrm{d}p\mathrm{d}\Omega$	$\langle p_\mathrm{T}\rangle$	$\langle\theta\rangle$	$\mathrm{d}^2\sigma/\mathrm{d}p\mathrm{d}\Omega$
0.42–0.50				0.459	114.8	359.78 $\pm$ 94.60 $\pm$ 35.50
0.50–0.60				0.538	112.2	184.82 $\pm$ 63.72 $\pm$ 32.54
0.60–0.72	0.680	95.2	151.46 $\pm$ 59.76 $\pm$ 26.02	0.633	113.0	30.26 $\pm$ 25.47 $\pm$ 8.33
0.72–0.90	0.797	100.1	29.29 $\pm$ 23.78 $\pm$ 6.59			

Table A.41: Double-differential inclusive cross-section $\mathrm{d}^2\sigma/\mathrm{d}p\mathrm{d}\Omega$ [mb/(GeV/c sr)] of the production of π^+'s in π^+ + Ta $\rightarrow \pi^+$ + X interactions with $+15.0$ GeV/c beam momentum; the first error is statistical, the second systematic; p_T in GeV/c, polar angle θ in degrees.

	$20 < \theta < 30$						$30 < \theta < 40$					
p_T	$\langle p_\mathrm{T}\rangle$	$\langle\theta\rangle$	$\mathrm{d}^2\sigma/\mathrm{d}p\mathrm{d}\Omega$				$\langle p_\mathrm{T}\rangle$	$\langle\theta\rangle$	$\mathrm{d}^2\sigma/\mathrm{d}p\mathrm{d}\Omega$			
0.13–0.16	0.147	26.1	121.37	$\pm$	98.97	$\pm$ 11.95						
0.36–0.42							0.374	34.6	394.59	$\pm$	171.51	$\pm$ 16.13
0.42–0.50	0.455	26.0	508.10	$\pm$	171.53	$\pm$ 25.76	0.461	35.2	380.28	$\pm$	144.80	$\pm$ 19.43
0.50–0.60	0.543	23.6	328.17	$\pm$	119.61	$\pm$ 25.11	0.563	33.7	119.43	$\pm$	72.93	$\pm$ 9.13
0.60–0.72	0.659	25.9	248.26	$\pm$	95.03	$\pm$ 28.81	0.649	33.3	138.23	$\pm$	62.99	$\pm$ 15.89
0.72–0.90							0.760	36.4	51.75	$\pm$	31.65	$\pm$ 9.02

	$40 < \theta < 50$						$50 < \theta < 60$					
p_T	$\langle p_\mathrm{T}\rangle$	$\langle\theta\rangle$	$\mathrm{d}^2\sigma/\mathrm{d}p\mathrm{d}\Omega$				$\langle p_\mathrm{T}\rangle$	$\langle\theta\rangle$	$\mathrm{d}^2\sigma/\mathrm{d}p\mathrm{d}\Omega$			
0.16–0.20							0.162	54.6	253.32	$\pm$	180.92	$\pm$ 19.77
0.24–0.30	0.266	44.4	349.86	$\pm$	156.25	$\pm$ 18.92	0.273	55.8	318.28	$\pm$	165.34	$\pm$ 15.97
0.30–0.36	0.338	42.6	296.69	$\pm$	154.21	$\pm$ 12.73	0.338	55.6	412.27	$\pm$	170.33	$\pm$ 16.98
0.36–0.42	0.405	41.8	292.88	$\pm$	148.67	$\pm$ 12.15						
0.42–0.50	0.465	43.8	213.96	$\pm$	113.30	$\pm$ 11.41	0.441	54.2	324.54	$\pm$	137.53	$\pm$ 19.37
0.50–0.60	0.531	44.9	184.18	$\pm$	87.90	$\pm$ 14.65	0.524	54.1	129.66	$\pm$	78.36	$\pm$ 11.49
0.60–0.72	0.665	47.7	44.86	$\pm$	38.62	$\pm$ 5.27	0.650	53.1	56.92	$\pm$	43.29	$\pm$ 7.36
0.72–0.90	0.811	41.3	61.88	$\pm$	35.11	$\pm$ 10.86	0.810	54.4	0.39	$\pm$	0.33	$\pm$ 0.07
0.90–1.25							1.193	56.0	1.87	$\pm$	1.20	$\pm$ 0.56

	$60 < \theta < 75$						$75 < \theta < 90$					
p_T	$\langle p_\mathrm{T}\rangle$	$\langle\theta\rangle$	$\mathrm{d}^2\sigma/\mathrm{d}p\mathrm{d}\Omega$				$\langle p_\mathrm{T}\rangle$	$\langle\theta\rangle$	$\mathrm{d}^2\sigma/\mathrm{d}p\mathrm{d}\Omega$			
0.13–0.16	0.142	67.7	250.70	$\pm$	175.85	$\pm$ 24.23						
0.20–0.24	0.232	67.0	356.07	$\pm$	162.16	$\pm$ 22.39						
0.24–0.30	0.263	67.7	445.97	$\pm$	158.07	$\pm$ 22.05						
0.30–0.36	0.337	65.1	315.26	$\pm$	133.50	$\pm$ 14.01	0.333	86.0	180.68	$\pm$	106.37	$\pm$ 10.64
0.36–0.42	0.392	66.3	461.70	$\pm$	158.46	$\pm$ 23.40						
0.42–0.50	0.446	65.0	227.02	$\pm$	96.47	$\pm$ 16.64						
0.60–0.72	0.645	65.0	99.75	$\pm$	49.92	$\pm$ 15.78						
0.72–0.90	0.749	62.9	17.93	$\pm$	15.00	$\pm$ 4.07	0.793	82.0	0.07	$\pm$	0.05	$\pm$ 0.02

	$90 < \theta < 105$						$105 < \theta < 125$					
p_T	$\langle p_\mathrm{T}\rangle$	$\langle\theta\rangle$	$\mathrm{d}^2\sigma/\mathrm{d}p\mathrm{d}\Omega$				$\langle p_\mathrm{T}\rangle$	$\langle\theta\rangle$	$\mathrm{d}^2\sigma/\mathrm{d}p\mathrm{d}\Omega$			
0.13–0.16							0.148	117.0	443.33	$\pm$	196.41	$\pm$ 29.59
0.16–0.20							0.183	117.0	67.58	$\pm$	58.70	$\pm$ 3.26
0.20–0.24	0.225	97.8	250.71	$\pm$	147.41	$\pm$ 13.55						
0.24–0.30	0.271	96.0	182.10	$\pm$	105.78	$\pm$ 9.89	0.263	115.4	78.97	$\pm$	57.19	$\pm$ 5.18
0.30–0.36	0.319	100.5	79.56	$\pm$	63.66	$\pm$ 5.88						
0.36–0.42	0.407	100.0	106.43	$\pm$	68.49	$\pm$ 11.01	0.390	120.3	104.97	$\pm$	63.90	$\pm$ 15.49
0.42–0.50							0.481	112.0	51.75	$\pm$	38.79	$\pm$ 10.29
0.50–0.60	0.549	94.9	3.27	$\pm$	2.82	$\pm$ 0.65						

Table A.42: Double-differential inclusive cross-section $\mathrm{d}^2\sigma/\mathrm{d}p\mathrm{d}\Omega$ [mb/(GeV/c sr)] of the production of π^-'s in π^+ + Ta $\rightarrow \pi^-$ + X interactions with $+15.0$ GeV/c beam momentum; the first error is statistical, the second systematic; p_T in GeV/c, polar angle θ in degrees.

	$20 < \theta < 30$			$30 < \theta < 40$		
p_T	$\langle p_\mathrm{T}\rangle$	$\langle\theta\rangle$	$\mathrm{d}^2\sigma/\mathrm{d}p\mathrm{d}\Omega$	$\langle p_\mathrm{T}\rangle$	$\langle\theta\rangle$	$\mathrm{d}^2\sigma/\mathrm{d}p\mathrm{d}\Omega$
0.36–0.42	0.395	24.8	516.82 ± 196.69 ± 22.08	0.381	36.4	463.13 ± 191.55 ± 19.64
0.42–0.50	0.460	24.9	528.31 ± 176.11 ± 32.22	0.456	34.6	280.79 ± 125.58 ± 16.49
0.50–0.60	0.552	23.6	375.65 ± 125.43 ± 35.13	0.543	34.4	353.42 ± 124.96 ± 31.77
0.60–0.72	0.636	20.0	62.71 ± 44.34 ± 8.61	0.647	33.6	92.32 ± 53.30 ± 12.51

	$40 < \theta < 50$			$50 < \theta < 60$		
p_T	$\langle p_\mathrm{T}\rangle$	$\langle\theta\rangle$	$\mathrm{d}^2\sigma/\mathrm{d}p\mathrm{d}\Omega$	$\langle p_\mathrm{T}\rangle$	$\langle\theta\rangle$	$\mathrm{d}^2\sigma/\mathrm{d}p\mathrm{d}\Omega$
0.13–0.16				0.140	52.7	231.93 ± 191.92 ± 22.47
0.24–0.30				0.272	55.1	414.63 ± 185.44 ± 20.44
0.30–0.36				0.325	55.5	431.55 ± 179.39 ± 17.12
0.36–0.42				0.396	50.7	149.85 ± 105.97 ± 6.97
0.42–0.50	0.459	46.1	176.35 ± 101.25 ± 11.08			
0.50–0.60	0.537	43.4	171.83 ± 85.93 ± 16.54	0.536	54.4	214.46 ± 95.91 ± 21.61
0.60–0.72	0.653	43.2	174.32 ± 77.96 ± 24.62			

	$60 < \theta < 75$			$75 < \theta < 90$		
p_T	$\langle p_\mathrm{T}\rangle$	$\langle\theta\rangle$	$\mathrm{d}^2\sigma/\mathrm{d}p\mathrm{d}\Omega$	$\langle p_\mathrm{T}\rangle$	$\langle\theta\rangle$	$\mathrm{d}^2\sigma/\mathrm{d}p\mathrm{d}\Omega$
0.24–0.30	0.279	69.5	222.48 ± 111.37 ± 10.24	0.262	80.9	585.44 ± 195.23 ± 36.99
0.30–0.36	0.329	66.2	168.00 ± 97.00 ± 7.43	0.327	82.3	128.34 ± 90.75 ± 8.70
0.36–0.42	0.396	68.2	163.70 ± 94.51 ± 9.13	0.380	81.4	116.79 ± 82.58 ± 9.17
0.42–0.50	0.442	69.5	120.31 ± 69.46 ± 9.58	0.444	78.3	79.30 ± 56.08 ± 8.48
0.50–0.60	0.525	69.6	147.72 ± 66.07 ± 17.32			
0.60–0.72	0.683	70.0	102.08 ± 51.04 ± 16.93	0.674	77.9	44.62 ± 31.55 ± 9.40

	$90 < \theta < 105$			$105 < \theta < 125$		
p_T	$\langle p_\mathrm{T}\rangle$	$\langle\theta\rangle$	$\mathrm{d}^2\sigma/\mathrm{d}p\mathrm{d}\Omega$	$\langle p_\mathrm{T}\rangle$	$\langle\theta\rangle$	$\mathrm{d}^2\sigma/\mathrm{d}p\mathrm{d}\Omega$
0.13–0.16				0.154	112.0	183.48 ± 129.78 ± 11.57
0.16–0.20				0.182	116.6	279.25 ± 125.98 ± 12.31
0.20–0.24	0.226	98.4	289.90 ± 165.72 ± 16.82	0.221	108.6	129.83 ± 91.82 ± 6.31
0.24–0.30	0.261	101.4	187.72 ± 108.41 ± 11.50			
0.36–0.42	0.392	97.6	266.09 ± 119.53 ± 30.09			
0.42–0.50				0.449	115.0	56.05 ± 39.63 ± 12.74

Table A.43: Double-differential inclusive cross-section $\mathrm{d}^2\sigma/\mathrm{d}p\mathrm{d}\Omega$ [mb/(GeV/c sr)] of the production of protons in π^- + Ta $\rightarrow$ p + X interactions with -15.0 GeV/c beam momentum; the first error is statistical, the second systematic; p_T in GeV/c, polar angle θ in degrees.

	$20 < \theta < 30$					$30 < \theta < 40$				
p_T	$\langle p_\mathrm{T}\rangle$	$\langle\theta\rangle$	$\mathrm{d}^2\sigma/\mathrm{d}p\mathrm{d}\Omega$			$\langle p_\mathrm{T}\rangle$	$\langle\theta\rangle$	$\mathrm{d}^2\sigma/\mathrm{d}p\mathrm{d}\Omega$		
0.20–0.24	0.221	25.1	1389.55 ± 35.87	±	85.80					
0.24–0.30	0.269	25.3	1153.71 ± 25.70	±	65.04	0.271	34.8	1242.08 ± 26.16	±	64.82
0.30–0.36	0.329	25.3	912.12 ± 23.40	±	52.24	0.329	35.1	1135.47 ± 24.63	±	53.75
0.36–0.42	0.389	25.3	746.36 ± 21.49	±	42.77	0.389	35.1	950.02 ± 23.24	±	44.48
0.42–0.50	0.458	25.3	514.11 ± 15.57	±	33.57	0.459	35.0	699.89 ± 17.95	±	37.57
0.50–0.60	0.547	25.2	366.37 ± 12.13	±	28.37	0.547	35.1	501.75 ± 13.74	±	28.92
0.60–0.72	0.656	25.3	231.70 ± 8.63	±	20.90	0.656	35.2	333.00 ± 10.27	±	23.59
0.72–0.90						0.796	35.2	168.77 ± 6.19	±	17.27

	$40 < \theta < 50$					$50 < \theta < 60$				
p_T	$\langle p_\mathrm{T}\rangle$	$\langle\theta\rangle$	$\mathrm{d}^2\sigma/\mathrm{d}p\mathrm{d}\Omega$			$\langle p_\mathrm{T}\rangle$	$\langle\theta\rangle$	$\mathrm{d}^2\sigma/\mathrm{d}p\mathrm{d}\Omega$		
0.30–0.36	0.332	45.0	1261.62 ± 25.18	±	54.43					
0.36–0.42	0.392	45.1	1053.14 ± 23.52	±	42.52	0.391	55.0	1076.12 ± 22.49	±	47.33
0.42–0.50	0.462	45.1	810.67 ± 18.42	±	36.31	0.462	54.9	864.18 ± 18.31	±	34.69
0.50–0.60	0.553	45.0	555.46 ± 14.52	±	32.76	0.553	55.0	609.01 ± 14.46	±	30.33
0.60–0.72	0.664	45.1	355.65 ± 11.00	±	27.67	0.664	55.1	380.05 ± 11.18	±	27.01
0.72–0.90	0.809	45.0	189.79 ± 6.92	±	20.35	0.810	54.9	178.37 ± 6.52	±	17.90
0.90–1.25	1.054	44.9	55.21 ± 2.63	±	8.33	1.052	55.1	50.78 ± 2.56	±	7.82

	$60 < \theta < 75$					$75 < \theta < 90$				
p_T	$\langle p_\mathrm{T}\rangle$	$\langle\theta\rangle$	$\mathrm{d}^2\sigma/\mathrm{d}p\mathrm{d}\Omega$			$\langle p_\mathrm{T}\rangle$	$\langle\theta\rangle$	$\mathrm{d}^2\sigma/\mathrm{d}p\mathrm{d}\Omega$		
0.50–0.60	0.545	67.4	580.44 ± 10.66	±	28.70					
0.60–0.72	0.654	67.4	352.36 ± 8.27	±	23.21	0.651	81.8	281.99 ± 6.70	±	21.91
0.72–0.90	0.799	66.7	162.75 ± 4.97	±	16.78	0.794	81.7	106.65 ± 3.75	±	11.42
0.90–1.25	1.032	66.5	45.40 ± 2.02	±	7.68	1.021	81.8	21.32 ± 1.38	±	3.87

	$90 < \theta < 105$					$105 < \theta < 125$				
p_T	$\langle p_\mathrm{T}\rangle$	$\langle\theta\rangle$	$\mathrm{d}^2\sigma/\mathrm{d}p\mathrm{d}\Omega$			$\langle p_\mathrm{T}\rangle$	$\langle\theta\rangle$	$\mathrm{d}^2\sigma/\mathrm{d}p\mathrm{d}\Omega$		
0.42–0.50						0.458	113.4	351.02 ± 7.78	±	23.31
0.50–0.60						0.542	112.8	166.40 ± 4.94	±	16.42
0.60–0.72	0.651	97.0	167.66 ± 5.16	±	15.88	0.649	113.0	58.85 ± 3.01	±	8.77
0.72–0.90	0.791	96.6	52.15 ± 2.72	±	6.66	0.787	111.7	14.19 ± 1.37	±	3.29

Table A.44: Double-differential inclusive cross-section $\mathrm{d}^2\sigma/\mathrm{d}p\mathrm{d}\Omega$ [mb/(GeV/c sr)] of the production of π^+'s in π^- + Ta $\rightarrow$ π^+ + X interactions with -15.0 GeV/c beam momentum; the first error is statistical, the second systematic; p_T in GeV/c, polar angle θ in degrees.

	$20 < \theta < 30$			$30 < \theta < 40$		
p_T	$\langle p_\mathrm{T}\rangle$	$\langle\theta\rangle$	$\mathrm{d}^2\sigma/\mathrm{d}p\mathrm{d}\Omega$	$\langle p_\mathrm{T}\rangle$	$\langle\theta\rangle$	$\mathrm{d}^2\sigma/\mathrm{d}p\mathrm{d}\Omega$
0.10–0.13	0.116	25.1	624.95 ± 30.00 ± 52.17	0.116	34.8	497.40 ± 25.94 ± 40.12
0.13–0.16	0.145	24.8	675.07 ± 27.86 ± 43.66	0.146	34.7	612.98 ± 26.38 ± 39.80
0.16–0.20	0.180	24.8	801.76 ± 25.45 ± 45.35	0.181	34.7	684.16 ± 23.36 ± 38.21
0.20–0.24	0.220	25.0	850.85 ± 26.11 ± 43.55	0.220	34.7	641.97 ± 22.26 ± 32.11
0.24–0.30	0.269	25.0	778.47 ± 20.43 ± 36.04	0.269	34.8	582.64 ± 17.60 ± 26.17
0.30–0.36	0.329	24.8	631.56 ± 17.80 ± 26.03	0.329	34.7	487.17 ± 16.06 ± 19.96
0.36–0.42	0.390	24.9	550.43 ± 16.83 ± 23.15	0.388	34.7	420.82 ± 14.82 ± 16.96
0.42–0.50	0.458	24.8	395.09 ± 11.81 ± 17.97	0.458	34.9	312.09 ± 10.76 ± 13.57
0.50–0.60	0.546	24.7	268.88 ± 8.61 ± 15.78	0.546	34.9	198.43 ± 7.32 ± 10.86
0.60–0.72	0.656	24.7	152.16 ± 5.63 ± 12.55	0.654	34.9	121.63 ± 5.08 ± 9.21
0.72–0.90				0.796	34.7	62.15 ± 2.66 ± 7.16

	$40 < \theta < 50$			$50 < \theta < 60$		
p_T	$\langle p_\mathrm{T}\rangle$	$\langle\theta\rangle$	$\mathrm{d}^2\sigma/\mathrm{d}p\mathrm{d}\Omega$	$\langle p_\mathrm{T}\rangle$	$\langle\theta\rangle$	$\mathrm{d}^2\sigma/\mathrm{d}p\mathrm{d}\Omega$
0.10–0.13	0.117	45.1	380.38 ± 23.28 ± 30.93			
0.13–0.16	0.146	45.0	421.58 ± 21.23 ± 27.64	0.146	54.6	432.39 ± 23.04 ± 29.62
0.16–0.20	0.181	44.8	456.89 ± 18.78 ± 25.83	0.180	54.9	403.87 ± 17.56 ± 22.81
0.20–0.24	0.221	44.8	465.12 ± 19.08 ± 23.43	0.221	54.7	376.94 ± 16.83 ± 18.88
0.24–0.30	0.270	44.8	441.96 ± 15.30 ± 19.79	0.269	54.7	361.62 ± 13.88 ± 16.02
0.30–0.36	0.331	44.7	390.23 ± 14.50 ± 16.46	0.330	54.7	290.50 ± 12.57 ± 12.80
0.36–0.42	0.392	44.8	304.53 ± 12.69 ± 12.58	0.393	54.7	243.05 ± 11.46 ± 10.60
0.42–0.50	0.461	44.7	244.08 ± 9.94 ± 11.10	0.460	54.8	172.41 ± 8.42 ± 8.46
0.50–0.60	0.552	44.8	153.50 ± 6.57 ± 8.28	0.554	54.5	111.74 ± 5.87 ± 6.47
0.60–0.72	0.659	44.7	96.81 ± 4.64 ± 6.94	0.665	54.5	67.81 ± 4.07 ± 5.17
0.72–0.90	0.808	44.6	41.01 ± 2.26 ± 4.31	0.815	54.5	26.81 ± 1.81 ± 2.93
0.90–1.25				1.059	54.5	7.31 ± 0.55 ± 1.32

	$60 < \theta < 75$			$75 < \theta < 90$		
p_T	$\langle p_\mathrm{T}\rangle$	$\langle\theta\rangle$	$\mathrm{d}^2\sigma/\mathrm{d}p\mathrm{d}\Omega$	$\langle p_\mathrm{T}\rangle$	$\langle\theta\rangle$	$\mathrm{d}^2\sigma/\mathrm{d}p\mathrm{d}\Omega$
0.13–0.16	0.145	67.3	410.61 ± 20.72 ± 30.08	0.150	81.5	142.73 ± 16.03 ± 23.01
0.16–0.20	0.180	67.1	326.99 ± 13.13 ± 18.49	0.181	81.9	257.35 ± 13.48 ± 16.66
0.20–0.24	0.220	67.2	316.07 ± 12.88 ± 15.53	0.220	81.8	244.17 ± 11.96 ± 12.34
0.24–0.30	0.269	67.2	277.42 ± 10.17 ± 12.47	0.268	81.5	200.08 ± 9.22 ± 12.12
0.30–0.36	0.329	66.8	188.39 ± 8.37 ± 8.40	0.327	82.0	142.77 ± 7.92 ± 9.73
0.36–0.42	0.390	66.8	171.30 ± 8.02 ± 8.45	0.389	81.6	101.18 ± 6.49 ± 6.43
0.42–0.50	0.459	67.0	110.98 ± 5.59 ± 6.22	0.458	81.3	65.41 ± 4.35 ± 4.35
0.50–0.60	0.546	67.0	68.68 ± 3.79 ± 4.58	0.543	81.9	42.54 ± 2.98 ± 3.44
0.60–0.72	0.655	66.4	43.67 ± 2.69 ± 3.88	0.648	80.7	19.83 ± 1.78 ± 2.13
0.72–0.90	0.796	66.1	20.82 ± 1.39 ± 2.57	0.795	81.3	7.36 ± 0.80 ± 1.10
0.90–1.25	1.036	65.5	3.61 ± 0.31 ± 0.75	1.045	81.3	1.15 ± 0.17 ± 0.27

	$90 < \theta < 105$			$105 < \theta < 125$		
p_T	$\langle p_\mathrm{T}\rangle$	$\langle\theta\rangle$	$\mathrm{d}^2\sigma/\mathrm{d}p\mathrm{d}\Omega$	$\langle p_\mathrm{T}\rangle$	$\langle\theta\rangle$	$\mathrm{d}^2\sigma/\mathrm{d}p\mathrm{d}\Omega$
0.13–0.16	0.148	97.2	171.38 ± 20.98 ± 33.68	0.144	114.5	269.55 ± 15.13 ± 19.39
0.16–0.20	0.181	97.5	269.71 ± 17.54 ± 26.48	0.180	113.8	154.41 ± 7.83 ± 7.63
0.20–0.24	0.220	97.1	196.84 ± 10.90 ± 9.71	0.219	114.1	116.70 ± 6.95 ± 5.54
0.24–0.30	0.266	97.6	126.58 ± 7.32 ± 7.30	0.265	114.1	81.18 ± 4.88 ± 4.47
0.30–0.36	0.326	97.3	72.29 ± 5.44 ± 4.50	0.329	114.5	43.79 ± 3.44 ± 3.03
0.36–0.42	0.387	97.4	67.99 ± 5.10 ± 4.61	0.385	113.9	25.26 ± 2.59 ± 2.27
0.42–0.50	0.454	96.8	38.38 ± 3.26 ± 3.24	0.458	112.0	16.88 ± 1.84 ± 1.92
0.50–0.60	0.539	97.1	24.50 ± 2.32 ± 2.72	0.540	111.9	8.16 ± 1.08 ± 1.22
0.60–0.72	0.646	97.1	11.63 ± 1.33 ± 1.72	0.654	112.4	1.82 ± 0.45 ± 0.36
0.72–0.90	0.788	96.1	3.55 ± 0.56 ± 0.70	0.803	110.6	0.93 ± 0.25 ± 0.25
0.90–1.25	1.023	96.4	0.83 ± 0.15 ± 0.26			

Table A.45: Double-differential inclusive cross-section $\mathrm{d}^2\sigma/\mathrm{d}p\mathrm{d}\Omega$ [mb/(GeV/c sr)] of the production of π^-'s in π^- + Ta $\rightarrow \pi^-$ + X interactions with -15.0 GeV/c beam momentum; the first error is statistical, the second systematic; p_T in GeV/c, polar angle θ in degrees.

	$20 < \theta < 30$					$30 < \theta < 40$				
p_T	$\langle p_\mathrm{T}\rangle$	$\langle\theta\rangle$	$\mathrm{d}^2\sigma/\mathrm{d}p\mathrm{d}\Omega$			$\langle p_\mathrm{T}\rangle$	$\langle\theta\rangle$	$\mathrm{d}^2\sigma/\mathrm{d}p\mathrm{d}\Omega$		
0.10–0.13	0.116	25.0	910.81 ± 37.32	±	77.52	0.116	34.9	803.67 ± 33.43	±	64.34
0.13–0.16	0.146	24.7	929.24 ± 32.94	±	60.13	0.145	35.0	760.36 ± 29.12	±	49.68
0.16–0.20	0.180	24.8	1064.19 ± 29.98	±	60.63	0.181	34.9	857.07 ± 26.72	±	48.46
0.20–0.24	0.220	24.9	1080.30 ± 29.54	±	53.41	0.220	34.5	812.54 ± 25.61	±	40.50
0.24–0.30	0.269	24.8	946.23 ± 22.51	±	40.89	0.270	34.8	720.86 ± 20.02	±	32.39
0.30–0.36	0.329	24.8	801.09 ± 20.81	±	32.29	0.329	34.8	604.12 ± 18.00	±	24.05
0.36–0.42	0.390	24.8	621.16 ± 17.87	±	25.08	0.389	34.9	491.06 ± 16.31	±	19.82
0.42–0.50	0.457	24.6	494.92 ± 14.18	±	23.04	0.458	34.7	370.65 ± 12.19	±	16.76
0.50–0.60	0.545	25.0	311.24 ± 9.80	±	18.05	0.547	34.7	219.35 ± 8.14	±	12.46
0.60–0.72	0.655	24.9	187.37 ± 7.17	±	14.50	0.656	34.7	131.94 ± 5.63	±	10.01
0.72–0.90						0.798	34.4	63.39 ± 3.31	±	6.51

	$40 < \theta < 50$					$50 < \theta < 60$				
p_T	$\langle p_\mathrm{T}\rangle$	$\langle\theta\rangle$	$\mathrm{d}^2\sigma/\mathrm{d}p\mathrm{d}\Omega$			$\langle p_\mathrm{T}\rangle$	$\langle\theta\rangle$	$\mathrm{d}^2\sigma/\mathrm{d}p\mathrm{d}\Omega$		
0.10–0.13	0.115	45.2	716.71 ± 34.02	±	60.79					
0.13–0.16	0.145	45.0	625.49 ± 26.84	±	41.44	0.144	55.2	572.16 ± 26.01	±	38.92
0.16–0.20	0.179	44.9	655.91 ± 23.02	±	37.43	0.179	54.7	512.85 ± 20.49	±	29.24
0.20–0.24	0.219	44.9	617.77 ± 22.34	±	31.22	0.219	54.9	468.70 ± 19.63	±	23.83
0.24–0.30	0.268	44.9	562.97 ± 17.81	±	25.96	0.267	55.0	451.26 ± 15.76	±	19.82
0.30–0.36	0.327	44.5	450.41 ± 15.59	±	18.09	0.328	55.0	368.21 ± 14.45	±	16.05
0.36–0.42	0.385	44.9	366.46 ± 13.94	±	15.17	0.386	54.6	282.35 ± 12.43	±	12.13
0.42–0.50	0.453	44.7	290.15 ± 10.72	±	13.65	0.454	54.6	199.52 ± 8.81	±	9.79
0.50–0.60	0.540	44.8	186.84 ± 7.58	±	11.17	0.541	54.6	133.63 ± 6.56	±	8.30
0.60–0.72	0.646	44.9	93.03 ± 4.83	±	7.39	0.646	54.7	78.05 ± 4.55	±	6.42
0.72–0.90	0.784	44.6	45.26 ± 2.66	±	4.99	0.783	54.6	26.60 ± 2.02	±	3.05
0.90–1.25						1.008	54.4	6.12 ± 0.62	±	1.10

	$60 < \theta < 75$					$75 < \theta < 90$				
p_T	$\langle p_\mathrm{T}\rangle$	$\langle\theta\rangle$	$\mathrm{d}^2\sigma/\mathrm{d}p\mathrm{d}\Omega$			$\langle p_\mathrm{T}\rangle$	$\langle\theta\rangle$	$\mathrm{d}^2\sigma/\mathrm{d}p\mathrm{d}\Omega$		
0.13–0.16	0.145	67.1	524.08 ± 23.17	±	35.32	0.148	80.3	343.39 ± 32.05	±	87.75
0.16–0.20	0.179	67.3	428.75 ± 15.34	±	23.23	0.181	81.4	392.86 ± 17.58	±	28.84
0.20–0.24	0.219	67.3	412.05 ± 15.17	±	20.04	0.219	82.1	304.43 ± 13.83	±	16.57
0.24–0.30	0.268	67.0	315.56 ± 11.08	±	15.05	0.268	81.9	250.20 ± 10.44	±	15.14
0.30–0.36	0.328	66.9	252.93 ± 9.99	±	12.20	0.330	81.5	159.30 ± 8.45	±	10.98
0.36–0.42	0.388	66.9	198.38 ± 8.69	±	9.38	0.390	81.7	127.32 ± 7.40	±	8.58
0.42–0.50	0.457	67.0	136.53 ± 6.10	±	7.35	0.456	82.2	87.55 ± 5.11	±	6.13
0.50–0.60	0.545	67.2	89.18 ± 4.37	±	6.18	0.545	81.5	51.08 ± 3.39	±	4.43
0.60–0.72	0.652	66.4	43.32 ± 2.63	±	4.03	0.650	81.5	18.11 ± 1.77	±	2.07
0.72–0.90	0.793	67.0	20.74 ± 1.50	±	2.58	0.793	81.7	6.66 ± 0.80	±	1.05
0.90–1.25	1.013	67.4	3.71 ± 0.40	±	0.72	1.009	81.6	1.76 ± 0.27	±	0.42

	$90 < \theta < 105$					$105 < \theta < 125$				
p_T	$\langle p_\mathrm{T}\rangle$	$\langle\theta\rangle$	$\mathrm{d}^2\sigma/\mathrm{d}p\mathrm{d}\Omega$			$\langle p_\mathrm{T}\rangle$	$\langle\theta\rangle$	$\mathrm{d}^2\sigma/\mathrm{d}p\mathrm{d}\Omega$		
0.13–0.16						0.144	114.2	321.92 ± 16.46	±	18.47
0.16–0.20	0.175	96.5	400.47 ± 131.87	±	28.51	0.178	113.7	211.87 ± 9.55	±	9.96
0.20–0.24	0.219	97.0	230.48 ± 12.28	±	12.96	0.218	114.0	139.09 ± 7.72	±	6.64
0.24–0.30	0.266	97.4	159.35 ± 8.37	±	9.58	0.268	113.7	85.33 ± 4.98	±	4.88
0.30–0.36	0.330	97.0	108.77 ± 6.88	±	7.45	0.326	113.8	54.50 ± 3.97	±	4.16
0.36–0.42	0.390	96.4	64.00 ± 5.05	±	4.70	0.387	113.5	32.76 ± 2.95	±	3.23
0.42–0.50	0.458	97.2	48.60 ± 3.75	±	4.45	0.456	112.7	21.05 ± 2.06	±	2.64
0.50–0.60	0.547	97.0	26.36 ± 2.43	±	3.17	0.538	111.9	8.96 ± 1.21	±	1.45
0.60–0.72	0.647	97.1	10.81 ± 1.35	±	1.72	0.646	110.7	2.64 ± 0.56	±	0.56
0.72–0.90	0.783	97.0	4.11 ± 0.67	±	0.88	0.784	110.6	1.43 ± 0.31	±	0.41
0.90–1.25	0.962	97.1	0.39 ± 0.10	±	0.13					